NMR SELF-DIFFUSION COEFFICIENTS, NMR RELAXATION AND VISCOSITY INVESTIGATION OF IONIC LIQUID MIXTURES AND CONFINED MEDIA

A THESIS SUBMITTED TO THE
SAVITRIBAI PHULE PUNE UNIVERSITY

FOR THE DEGREE OF
DOCTOR OF PHILOSOPHY
IN CHEMISTRY

SUBMITTED BY
RAJU NANDA

UNDER THE GUIDANCE OF
Dr. ANIL KUMAR
(RESEARCH GUIDE)

PHYSICAL AND MATERIALS CHEMISTRY DIVISION
CSIR-NATIONAL CHEMICAL LABORATORY
PUNE-411008
INDIA

MARCH 2015

CERTIFICATE

This is to certify that the work incorporated in this thesis entitled, "**NMR Self-Diffusion Coefficients, NMR Relaxation and Viscosity Investigation of Ionic Liquid Mixtures and Confined Media**" submitted by **Mr. Raju Nanda**, for the degree of **Doctor of Philosophy** to **Savitribai Phule Pune University**, was carried out by the candidate under my supervision in the Physical and Materials Chemistry Division, CSIR-National Chemical Laboratory, Pune-411008, India. Any material that has been obtained from other sources has been duly acknowledged in the thesis.

Date: **Dr. Anil Kumar**

Place: Pune **(Research Guide)**

DECLARATION

I, Mr. Raju Nanda, hereby declare that the work incorporated in the thesis entitled "**NMR Self-Diffusion Coefficients, NMR Relaxation and Viscosity Investigation of Ionic Liquid Mixtures and Confined Media**" submitted by me to the **Savitribai Phule Pune University** for the degree of **Doctor of Philosophy** is original and has not been submitted to this or other University or Institution for the award of Degree or Diploma. Such material, as has been obtained from other sources has been duly acknowledged.

Date:

Place: Pune **Raju Nanda**

TO

MY LOVING PARENTS

Dedicated to the Loving Memory of

My

Grandparents

CONTENTS

Acknowledgements

It is the most pleasant opportunity to express my sincere gratitude to all who have supported me in either professionally or personally during my doctoral studies. Certainly the numbers are uncountable, however, there are certain personalities without whom the journey is incomplete and I am fortunate to come across with such individuals during my past five year doctoral studies.

First, I would like to acknowledge my research supervisor Dr. Anil Kumar for giving me the opportunity to work under him. Both professionally and personally I learned a lot from him. I am really fortunate to work under such an excellent scientist who has been highly recognized by scientific community around the globe. He has been an excellent supervisor with great management skill and an exceptional team leader. He has constantly encouraged and motivated me during my difficult phases. He always advised me to keep patience when I was not able to get results. I thank him for showing trust in me. Though words are less to express still his leadership quality and his caring and motivating words have a deep impact in my life in both professionally and personally.

Secondly, I would like to express my sincere gratitude to Dr. P. R. Rajamohanan and Dr. K. Sreekumar, in helping me for the successful completion of my experimental work. I am really thankful to them for their unconditional support and timely help. I thank Dr. Gitanjali Rai (Dii) for helping me a lot to stand on my leg during my initial stages of the doctoral studies. I would also like to acknowledge Miss Snehal Dhokle for her support in successfully completion of all of my experimental work related to NMR spectroscopy. I would also like to acknowledge Mr. Bipin Lal for his unconditional support in the completion of all of my cyclic voltammetric experimental work.

I would like to sincerely acknowledge Dr. Sourav Pal, Director, CSIR-NCL for giving the infrastructure and facilities to carry out my research work. Invaluable suggestions from Dr. P. A. Joy, Dr. B. L. V. Prasad, Dr. C. S. Gopinath, Dr. T. G. Ajithkumar, Dr. S.

K. Bhat, Dr. Sudip Roy, Dr. Rahul Banerjee, and Dr. Ashish Lele are highly acknowledged.

I sincerely acknowledge all my teachers from my school level to the university level for their unconditional teaching and mentorship in building myself.

I thank to my lab senior Dr. Nagesh Khupse (Da) and special thanks to Dr. Gitanjali Rai (Dii) for their unconditional moral support during my difficult times. I have learnt a lot from them regarding both the experiments and theory in order to have a better understanding of the subjects. Special thanks to my seniors and friend Amit Da and Arpan Manna. I learned many things from them in terms of scientifically and personally. I would like to thank my other lab mates Shashi, Anshu, Sachin, Vijay, Preeti, Anirban, Puja, Seema, Jenofer, and Rosy for their all kind of support during my doctoral journey.

The doctoral studies have been incomplete without friends. Friends are the beautiful gift of life and they always made my life comfortable during my doctoral journey. During my stay on this campus I am fortunate to have a beautiful friend circle without whom it the journey was impossible. First, I would like to thank to all of my lab friends, specially Vijay, Sachin, Amit Da, Arpan, and Shashi for being with me in every phases of this journey. The moments we share are really memorable till the end of my life. Special thanks to Kshirodra, Chaka, Jitu, Puspa, Manoj, Bishnu, Laxmi, Prajnya, Pitambar Dada, Gokarneshwar Bhai, Ramakanta Bhai, Debashish Bhai, Siba Bhai, Mandakini Nani, Manaswini Nani, Rosy Nani, and Subash Bhai for having cheerful moments during our stay in the campus. Other friends are Achintya (my ex-room mate), Subrata, Anjan, Anup, Chini, Bala, Prabhu, Krishanu, Deepak, Partho, Sushanta, Arya, Himadri, Deva, Negi, Anjani, Kanak, Sumantra, Ravi, Mohan, Ramsundar, Lenin, Govind, Saikat, Prabhat, Soumen, Karthika, Manzoor, Wahid, Saleem, Brijesh, Kundan, Tiwari ji, Manoj Sharma, Deepak Chand, Hemendar, Innaiha, Shantivardhan, Krunal, Rambabu, Jankiram, Yadagiri, Ashok, Sunil, Chandrababu, Ramireddy, Chaitanya Krishana, Chaitanya Kiran, Atul, Tamboli, and Dnyaneswar with whom I had pleasant time.

I sincerely thank the staff members of Physical and Materials Chemistry Division for their kind help and support during my doctoral journey.

The journey will be incomplete without the unconditional support from the family and family friends. Words are less to express the scarification made by my parents and my late grandparents during my doctoral journey. On this occasion, I would also like to thank my sisters Minu, Puja, and Mukta; brothers Rahul, Ashish, Harish, Banti, Pramod, and Prashanta; 'Mausi', 'Mausa', 'Mamu', 'Maiin', 'Kaka', 'Khudi', 'Dada', and 'Mama' for their love and care, which made my life always comfortable during my stay in the laboratory.

Finally, I wish to conclude with a prayer to my Lord:

"Oh my Lord, thank you so much for giving me this beautiful life

Oh my Lord, thank you for giving me this path to travel

Oh my Lord, thank you for giving me this life to help others

Oh my Lord, thank you, thank you for everything."

Raju Nanda

ABSTRACT

In the present thesis we have focused our investigation on the NMR self-diffusion coefficients, NMR relaxation and viscosity study of different green mixtures. Green mixtures were prepared by taking water, salts, surfactant and ionic liquids (ILs). Basically we have concentrated on the two types of green mixtures; one is the aqueous salt solutions of IL mixtures and the other one is the aqueous IL microemulsions. Both of these mixtures were chosen because of their variety of applications in electrochemical, biological and synthetic processes. The viscosity of the mixtures plays a significant role for their potential applications. It is inversely related with the self-diffusion coefficients of the individual particles present inside the mixtures. However both are completely different in their molecular level due to the presence of microheterogeneity in the mixtures. Here we have investigated how the different types of microscopic molecular phenomenon are related with their macroscopic bulk property like viscosity of the mixtures. The high viscosity of these green mixtures is one of the important drawbacks for their uses in different synthetic and electrochemical applications. Salts are used to decrease the viscosity of these mixtures and studied the mechanism of salt effects. In addition to that we have studied the physicochemical properties of confined water molecules inside the reverse miceller media with the help of NMR relaxation approach. These water molecules resemble to that of confined water present inside the mitochondria and chloroplast of cellular system and can be used as a model system for the in-vitro study. In addition to that these aqueous confined media are used in the synthesis of nanoparticles, used as a solvent media for different organic and bioorganic reactions, and are also used in the separation processes. The physical properties of these aqueous confined media play a prominent role for their potential use in all of the above applications. We have confined the water molecules inside the reverse micelles by taking hydrophobic ionic liquid as the dispersion medium and studied the physicochemical properties like microviscosity, micropolarity and pH of these aqueous confined media.

The total research work is divided into the three main working chapters and a brief description of each chapter is given below.

Chapter 1

This chapter includes a detailed literature survey on ILs and green solvents. The industrial importance of ILs as a green component and the role of viscosity and self-diffusion coefficients on it have been discussed. The origin of the microscopic properties like self-diffusion coefficients, translational and rotational motion of particles and their relation to the macroscopic bulk properties have been discussed. The importance of Stokes-Einstein and Stokes-Einstein-Debye equation on the viscosity and self-diffusion coefficients has been discussed. The concept of activation energy for the flow of a fluid and the theory of hole formation has been discussed. Also a brief literature survey has been carried out on the salt effects especially focused on the effects of salts on the structure and properties of water. In addition to that a detailed literature survey has been carried out on the confined water molecules especially the water molecules confined inside the reverse micelles and microemulsions media. Emphasis has been given to the construction and morphology of the microemulsions. More importantly the physical properties like microviscosity, pH and micropolarity of the water molecules confined inside the reverse miceller media has been discussed.

Chapter 2

This chapter includes the important objectives of the present research work and the motivation behind choosing each section of the work has been discussed.

Chapter 3

This chapter deals with the different types of techniques used in the current research programme in order to complete the experiment. The techniques used are Diffusion Order Nuclear Magnetic Resonance Spectrometer (DOSY), Cyclic Voltammetric (CV) technique, Dynamic Light Scattering (DLS) technique, UV-Vis spectrophotometer, Viscometer, pH meter. A detailed description of the basic principles of each technique and the purpose for using it has been presented.

Chapter 4

This chapter is divided into two sections. The first section deals with the temperature dependent viscosity, self-diffusion coefficients, translational and rotational motions of individual particle present inside the aqueous salt solutions of ILs mixtures. Activation energy of viscous and diffusive flow has been calculated and discussed. Much importance has been given to the different types of molecular motion like translational and rotational motions of individual particles and correlated with the viscosity and self-diffusion coefficients. As the molecular structure and physical properties of water is substantially different from that of the ILs, it is expected that the self-diffusion coefficients and the translational and rotational motions of both of the species are different from each other. Also the average jump distance of both the IL and water molecules are calculated and discussed.

In the second section of the chapter we have discussed about the validity of Stokes-Einstein equation by taking the measured temperature dependent self-diffusion coefficients and viscosity data. As the self-diffusion coefficients of both the IL and water molecules are substantially different from each other, therefore in both the cases the Stokes-Einstein equation is valid up to different extent. Also the concept of hole formation, the boundary condition for the Stokes-Einstein equation and the concept of microviscosity experienced by the individual moving particles are calculated and discussed.

Chapter 5

This chapter deals with the study of water molecules present inside the confined media by especially focusing on the reverse micelles or microemulsions media. For this purpose the microemulsions are constructed and the different microheterogeneous regions are detected with the help of viscosity and cyclic voltammetric study. The morphology of the microemulsions are studied through the help of DLS measurements. NMR relaxation measurements have been carried out to understand the behavior of water molecules present inside the confined reverse miceller media. Also the micropolarity of the confined water media are measured through the UV-Vis spectrophotometer and discussed.

Chapter 6

This chapter is divided into two sections. The first section deals with the effects of salts on the viscosity of IL solutions. The effects of salts on the structure of water are a topic of considerable discussion. As the salt alters the structure of water, therefore it might effects the viscosity of its aqueous solutions of ILs and we have achieved what we thought. The effects of salts in its aqueous solutions of ILs are becomes prominent with the increase in the hydrophobicity of alkyl chain length attached to the cation of ILs. On the basis of salt effects we have given a possible mechanism of salting-in/salting-out effects of salts in its aqueous solutions of ILs. In the category of salting-in salts, different salt shows different mechanism of salt effects in the IL solutions. However the mechanism of salting-out salts is same in all the studied IL solution.

In the second section of the chapter we have focused on the effects of polar non-electrolyte, urea on the viscosity of its aqueous solutions of ILs. The motivation behind choosing this work is due to the controversial role of urea on the structure of water. As it affects the structure of water, it certainly affects the viscosity of its aqueous solutions of ILs. The role of urea in its aqueous solutions of ILs is changes with the change in the alkyl chain length of ILs. With the lower alkyl chain length based ILs the urea behaves as a mild salting-out species, however with the increase in the alkyl chain length of ILs the behavior of urea changes to salting-in.

Chapter 7

This chapter includes the important outcomes of the above research work and is summarized in the following points.

1. The translational and rotational motions of water molecules in its salt solutions of ILs are substantially different from the IL cations.
2. The validity of Stokes-Einstein equation is up to different extent for both the water molecules and IL cations.
3. The frictional coefficients obtained from the Stokes-Einstein equation is a measure of microviscosity experienced by individual particle inside the solution.

4. The NMR relaxation time is an alternative parameter for the measurement of microviscosity and pH of aqueous IL confined media.
5. The salting-out and salting-in effects of urea is being reversed with the change in the alkyl chain length of ILs.
6. The hydrophobicity of alkyl chain length of IL is one of the prominent factors in deciding the salting-in and salting-out effects of salts and the mechanism of salting effects are different for different salts.

List of Abbreviations

IL	Ionic Liquid
[BMIM]	1-butyl-3-methylimidazolium
[HMIM]	1-hexyl-3-methylimidazolium
[OMIM]	1-octyl-3-methylimidazolium
[BBIM]	1,3-dibutyl imidazolium
$[BF_4]$	tetrafluoroborate
$[NTf_2]$	bis(trifluoromethane sulfonyl)imide
η	Viscosity
D_t	Translational self-diffusion coefficient
D_r	Rotational self-diffusion coefficient
D_{app}	Apparent diffusion coefficient
τ_t	Translational correlation time
τ_2	Rotational correlation time
τ_c	Reorientational correlation time
T_1	Spin-lattice relaxation time
T_2	Spin-spin relaxation time
D_h	Hydrodynamic radii
I_p	Peak current
λ	Wavelength

CHAPTER 1

Introduction

The transport phenomena like diffusion, viscosity and microviscosity of ionic liquid (IL) mixtures plays a significant role for its potential applications. This chapter presents a comprehensive literature survey on these transport processes in the IL mixtures. The diffusion processes has been studied in correlation with the translational and rotational motions of ^{1}H NMR active nuclei. The discussion has been extended to the Stokes-Einstein and Stokes-Einstein-Debye equation. In order to understand these transport phenomena in biological system, water/IL microemulsion has been taken as a model system for the discussion. Finally, the potential role of salt effects has been studied in the IL mixtures in correlation with the Hofmeister phenomena.

1.1. GREEN CHEMISTRY:

To date, volatile organic solvents (VOC) have been extensively used in industrial scale in most of the chemical manufacturing processes.[1] It causes environmental pollutions and is hazardous to mankind. A detailed survey has been done by the European and American environmental agencies to estimate the release of different organic compounds to the environment by different chemical processes. According to the toxicity release index, (TRI) the estimated release of organic compounds from chemical industries are surprisingly highest as compared to other industries. The environmental accessibility of different chemical processes can be measured by the two processes that are the E-factor and the atom efficiency.[2,3] The E factor can be defined as the mass ratio of waste to desired products and the atom efficiency is the ratio of the molecular weight of all the desired products to the sum of the molecular weight of all the substances. The higher is the E-factor for a chemical process, higher is the production of waste materials and consequently has a greater negative environmental effect. The E-factor with respect to the product tonnage of various industry segments of the chemical industry is given in Table 1. The higher magnitude of E-factor from the pharmaceuticals and fine chemicals segments indicates that the pharmaceuticals and chemical manufacturing companies have greater negative environmental effect.

Table 1. The E-factor of Various Industrial Segments.[4]

Industry Segment	Product Tonnage	E-factor
Oil refining	10^6-10^8	< 0.1
Bulk chemicals	10^4-10^6	< 1-5
Fine chemicals	10^2-10^4	5- > 50
Pharmaceuticals	10-10^3	25- > 100

Therefore, in recent time, increasing demand of environmentally acceptable processes has been developed in chemical industry and is widely acknowledged by the scientific community. The chemistry practicising it, emerges a new branch of chemistry known as 'Green Chemistry' or 'Sustainable Technology'.[5-7] It generates a new paradigm shift

from process efficiency to focus on chemical yield of higher economic value by reducing the wastes and avoiding the use of hazardous and/or toxic materials. Green Chemistry is defined as the design and efficiently utilizes of chemical products and processes in the manufacture and potential applications of chemical products by avoiding the use of toxic and/or hazardous materials. For the better practice of Green Chemistry by different chemical and industrial processes, they have to follow its 12 principles which can be phrased as: 1) waste prevention instead of remediation, 2) follow atom economy processes, 3) less hazardous chemical synthetic procedures, 4) safer products by design, 5) used of safer solvents and auxiliaries, 6) design for energy efficiency, 7) use of renewable raw materials, 8) follow shorter synthetic procedure to avoid derivatives, 9) use of catalytic reagents as compared to the stoichiometric reagents, 10) design products for degradation, 11) follow analytical methodologies for lesser environmental pollution and 12) practice safer chemistry for the prevention of any accidents. Among all, there is an urgent need to practice chemistry in less hazardous media for reducing the environmental pollutions. A growing interest has been developed for that reason among the scientific community for the use of less hazardous media like water, supercritical fluids, deep eutectic mixtures, polyethylene glycols, ionic liquids (ILs) etc.

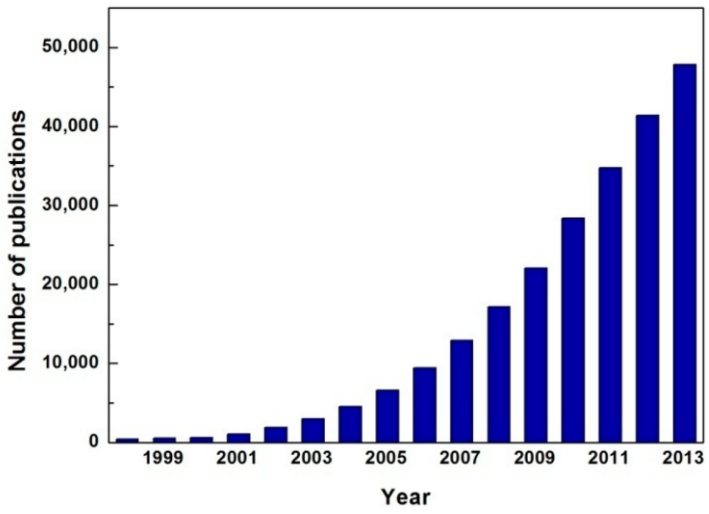

Figure 1. Bar diagram representing the increasing number of publications for ILs with respect to increasing year.[8]

Among all the unusual media, an increasing interest has been developed recently, among the scientific community for the use of ionic liquids. A bar diagram showing the increasing number of publications with respect to different years is presented in Figure 1 indicates that the potential use of ILs are increasing in recent times.[8] However, to make the best use of ILs, a much detailed knowledge of its physicochemical properties is necessary and in recent years it has been quite extensively studied by different research groups. However, lesser facts are known about the physicochemical properties of mixtures of ILs with different additives (like salts, surfactants, cosolvents etc.) as these mixtures are significantly used in different energy devices, a component in the microemulsion systems and used as a green media to carryout different organic, bioorganic and enzymatic reactions.

Among the physicochemical properties of IL mixtures, transport properties like viscosity, microviscosity and diffusion phenomenon are of much importantance for their wider applications in different fields of science and technology. Therefore, the present thesis is primarily emphasized on the detailed molecular level investigation of the above mentioned transport processes inside the IL mixtures. Before discussing about the transport phenomenon, a brief introduction to ILs has been discussed in the following paragraph.

Several definitions of ILs are available in the literature.[9] However, the most widely accepted definition of ILs is; "salts constitute of organic cation in combination with an inorganic and/or organic anion, having melting points below 100 ^{0}C". The first IL synthesized by Paul Walden to be ethyl ammonium nitrate (EAN) $[EtNH_3][NO_3]$ in 1914 having melting point of 12 ^{0}C. However, much less progress has been made in this filed for another two decades. In the late 1950s the growing interest of chloroalumino-based ILs has been developed and is known as the first generation ILs. However, they were very difficult to prepare because of their hygroscopic nature and therefore, limits their applications. Then the growing interest of easy prepared 1-alkyl-3-methylimidazolium cations ($[RMIM]^+$, R-alkyl, aryl groups) with tetrafluoroborate ($[BF_4]^-$) and hexafluorophophate ($[PF_6]^-$) anions-based ILs has been developed in late 1990s and are called as the second generation ILs. It fulfills most of the requirements which the former

generation ILs could not. However, anions of the second generation ILs are unstable towards moisture and hydrolyzed to form HF, which gives incorrect information about most of their physicochemical properties. For that reason, water stable trifluoromethanesulfonate $[CF_3SO_3]^-$ and bis((trifluoromethyl)sulfonyl)amide $[NTf_2]^-$ anion-based ILs (hydrophobic ILs) has been received considerable attentions in recent years and are known to be the third generation ILs. Nowadays researchers have focused on the task specific ILs designed for their specific application purposes. ILs possess special physicochemical properties for which these are potentially used in a variety of scientific and industrial purposes. It possess broad liquidus range up to 400 ^{0}C which are below the high temperature molten salts and above the boiling points of common molecular solvents.

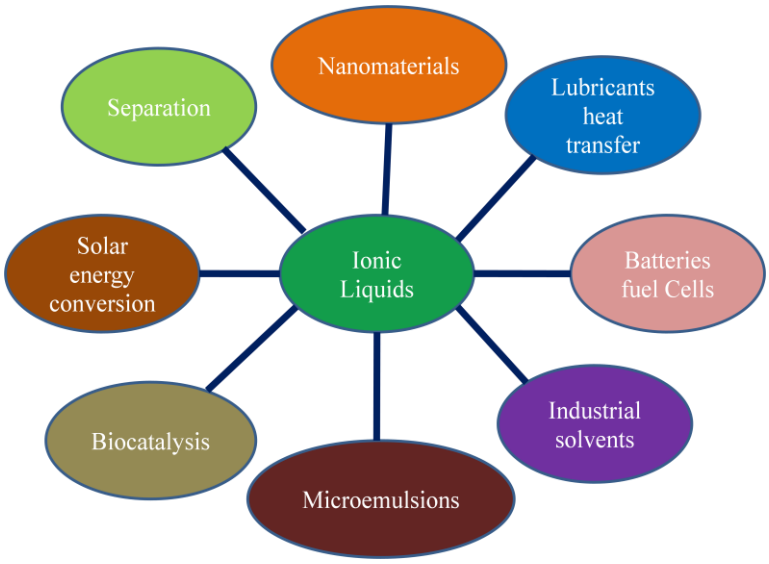

Figure 2. Schematic representation of applications of ionic liquids.

Therefore, it has been used as a medium to carry out different high temperature reactions. It also possess insignificant vapor pressure and have high thermal stability causing negligible environmental pollution which can be used as an alternative replaceable media to the volatile organic solvents. ILs are also known to be the designer solvents as it possesses tunable solvent properties. The physicochemical properties of ILs like self-diffusion coefficient, conductivity, viscosity, polarity can be tuned in order to apply it for

the specific application purpose. Another most important physical property of ILs is of its large electrochemical windows. It is defined as the difference between the anodic and cathodic potential limits at which the oxidation and reduction of the material takes place, respectively. ILs possesses a large electrochemical window of 2.5-8 V, because of which it can be used as an electrolyte in the Li-ion battery and supercapacitors.[10] Because of the above mentioned special physicochemical properties, ILs are used in a wide variety of application purposes which can be schematically represented in the Figure 2.

Among the discussed physicochemical properties of ILs and IL mixtures, the transport phenomenon like diffusion, viscosity and conductivity are the most important to understand for the better applications of ILs and its mixtures in different industrial processes. Among all the transport processes, we have mainly focused on the self-diffusion coefficients, viscosity and microviscosity of the IL mixtures in the present thesis. In addition to this, we have also advanced the knowledge of our discussion on these transport processes inside the aqueous hydrophobic microemulsion systems. The concept of salt effects and its relation to the transport processes also has been discussed. Therefore, in the present chapter of the thesis, an introduction to the above mentioned phenomenon and a detailed literature survey regarding it has been discussed.

1.2. DIFFUSION PHENOMENON IN ILS AND IL MIXTURES

The diffusion phenomenon is defined as the random Brownian motion of substances (atom, ion or molecule) from a higher concentration region towards the lower concentration region inside a system. Fundamentally, it is the net transfer of mass through a concentration gradient. However, the diffusion processes can still occur without any concentration gradient. Mathematically, the concept of diffusion phenomenon was first introduced by Joseph Fourier in 1822 and Adolf Fick in 1855. Later on it was Albert Einstein elaborated it in 1905. Adolf Fick proposed two laws for the diffusion phenomenon popularly known as Fick's first law and second law given in equation 1 and 2, respectively as:

$$J = -\frac{dc}{dx} \qquad (1)$$

$$-\frac{dJ}{dx} = D\frac{d^2c}{dx^2} \quad (2)$$

where, J (mol/cm^2/sec) is the diffusive flux , is the concentration of the diffusing particle. x is the position of the particle and D is the diffusion coefficient of the particle, respectively. Fick's first law applies to the steady state system where the concentration of the system remains constant. However, if the concentration of the diffusing particle changes with time then the Fick's second law is used to calculate the diffusion coefficient of the diffusing particle.

1.2.1. Types of Diffusion Phenomenon

After the discovery of diffusion phenomenon in early 1880s, later on many other types of diffusion processes were defined which are given below as:

a) Atomic Diffusion: It is the net transport of atoms in a solid material due to their random motion by thermal energy.

b) Momentum Diffusion: It is the diffusion of momentum between the particles in liquid state and also called as the viscosity.

c) Photonic Diffusion: It is the diffusion of photons in a material without being absorbed.

d) Surface Diffusion: It is the diffusive motion of adatoms (atom lies on a crystal surface) or molecules present at the surface of a solid material.

e) Reverse Diffusion: It is the diffusion of atoms of molecule from a region of lower concentration towards the high concentration region.

f) Chemical Diffusion: It is the process in which the diffusion of a chemical compound occurs inside a system due to the existence of chemical potential gradient. It is a non-equilibrium process, and approaches towards the equilibrium by increasing the entropy of the system.

g) Tracer Diffusion (Self-Diffusion): It is the random motion of the particle in the absence of any chemical potential gradient and always takes place under the equilibrium condition.

In the present thesis, we have focused our discussions primarily on the tracer or self-diffusion phenomenon obtained from the self-diffusion coefficient measurements through the pulsed-gradient-spin-echo NMR spectrometer (PGSE-NMR). This technique is widely used to measure the self-diffusion coefficients of ILs.[11-13] Besides this, other experimental techniques like cyclic Voltammetry, dynamic light scattering and fluorescence techniques also has been used to measure the diffusion coefficients in ILs media.[14-16] Many theoretical reports are also available in the literature in order to understand the diffusion phenomenon in different ILs media.[17,18] The introduction to the self-diffusion phenomenon in ILs media has been discussed in the present chapter in two separate sections; 1) Diffusion studies in ILs which only includes the literature survey regarding the self-diffusion coefficients in neat ILs and 2) Diffusion studies in IL mixtures which include the literatures regarding binary mixtures of ILs with salts and/or solvents.

1.2.2. Diffusional Behavior of ILs

The diffusional motion or translational motion of ILs is one of the vital phenomena to understand in order to apply the ILs in different application purposes like; as a fuel in solar cell devices and Li^+ ion battery, as a lubricants etc. Recently, Tokuda et al. reported that the summation of the self-diffusion coefficients of cation and anions for a series of ILs with $[BMIM]^+$ as the cation and with a series of anions; the order of their self diffusion coefficients follows the order as $[BMIM][(CF_3SO_2)_2N]$ > $[BMIM][CF_3CO_2]$ > $[BMIM][CF_3SO_3]$ > $[BMIM][BF_4]$ > $[BMIM][(C_2F_5SO_2)_2N]$ > $[BMIM][PF_6]$ at 30 ^{0}C.[19] They have shown that in spite of the higher van der Waals radii of $[BMIM]^+$ as compared to the studied anions, its self-diffusion coefficient values are more as compared to the anions. The variation of alkyl group substitution in the cation of ILs and its effect on the self-diffusion coefficients also has been studied.[20] The summation of the self-diffusion coefficients of cations and anions of ILs constitutes of different imidazolium cations with the $[(CF_3SO_2)_2N]$ anion follows the order as $[EMIM][(CF_3SO_2)_2N]$ >

[MMIM][$(CF_3SO_2)_2N$] > [BMIM][$(CF_3SO_2)_2N$] > [HMIM][$(CF_3SO_2)_2N$] > [OMIM][$(CF_3SO_2)_2N$] and the order is strictly showing the contrasting behavior as compared to the bulk dynamic viscosity of these ILs.[20] The self-diffusion coefficient for a series of imidazolium-based ILs with the variation in their alkyl chain length from ethyl (n = 2) to hexadodecyl (n = 12) with bis(trifluoromethanesulfonyl)imide (TFSI) as anion has been shown that their ionic diffusion coefficients are strongly depends upon the alkyl group attached to the imidazolium cations.[21] The self-diffusion coefficients of cations are faster as compared to the anion in shorter alkyl group substitution ILs with a crossover in octyl (n = 8) group substitution and anion diffuses faster as compared to the cations.[21] The higher self-diffusion coefficient values for imidazolium cations as compared to the anion in its TFSI anion-based ILs are showing the contrasting behavior to the ionic sizes. This variation in the self-diffusion coefficient values of ions is due to the presence of their nanoscale segregation into the polar and non-polar regions.[21] Noda et al. reported that the summation of the cationic and anionic self-diffusion coefficients of non-chloroaluminate-based room temperature ILs follows the order as [EMIM][$(CF_3SO_2)_2N$] > [EMIM][BF_4] > [BP][$(CF_3SO_2)_2N$] > [BP][BF_4]; also in contrast with the viscosities of these ILs.[22] The temperature dependent self-diffusion coefficients studies of these ILs follow the VFT equation rather than Arrhenius behavior.[22] The summation of self-diffusion coefficients of cations and anions of a series of ILs constitutes of [$(CF_3SO_2)_2N$] anion with different cationic structure are in the order of [BMIM][$(CF_3SO_2)_2N$] > [BPY][$(CF_3SO_2)_2N$] > [BMPRO][$(CF_3SO_2)_2N$] > [(n-C_4H_9)-$(CH_3)_3N$][$(CF_3SO_2)_2N$].[23] This order of the self-diffusion coefficient values is in inverse order to that of their bulk viscosity values.[23] Their study reveals that in addition to the ionic size of individual ions their geometrical shapes also effect significantly on the ionic self-diffusion coefficients of the ILs.[23] Beside this, PGSE NMR technique is used to study the self-diffusion coefficients of task specific ILs.[24] Recently, Filippov et al. reported the temperature dependent self-diffusion coefficients study of halogen free trihexyltetradecylphosphonium bis(mandelato)borate [$P_{6,6,6,14}$][BMB] IL.[24] Two phases coexist in the low temperature regions of the IL and the self-diffusion coefficients of [$P_{6,6,6,14}$] is 20 times slower as compared to the [BMB]. It is because of the existence of aggregated structural domains of cation in the IL which makes the cation hard to

diffuse.[24] However, both the ions diffuse as ion-pairs and have same diffusion coefficient values with the increase in the temperature above 60 ^{0}C.[24]

Generally, ^{1}H, ^{7}Li, ^{19}F, and ^{31}P nuclei are the best NMR probe to measure and understand the diffusional behavior of a material having these nuclei. However, it limits and handicaps the analysis of samples without these nuclei. Recently, Herriot et al. therefore demonstrated the use of ^{13}C-PGSE NMR method to measure and analyze the self-diffusion coefficients of nonfluorinated 4,5-dicarbonitrile-1,2,3-triazole ($DCTA^{-}$) anion-based ILs with imidazolium and pyrrolidinium as the cation.[25] It indicates that the ^{13}C nucleus which is a readily available nucleus in a diverse range of materials can also be used for the self-diffusion coefficient studies.

In addition to the PGSE-NMR technique, cyclic Voltammetry technique also has been used for the diffusion studies.[14,26] Theoretical studies are also available in the literature in order to understand the diffusional behavior of ILs.[18,27] Molecular dynamics simulation studies have been performed to understand the diffusional behavior of hydrophobic imidazolium and pyrrolidinium-based ILs.[28] The self-diffusion coefficients of [EMIM][FSI] and [PYR_{13}][TFSI] obtained from the MD simulation study shows an excellent agreement with the experimentally measured self-diffusion coefficients.[28]

1.2.3. Diffusional Behavior in IL Mixtures

In addition to the study of neat ILs, a growing demand for IL mixtures has been observed in recent years. The IL mixtures constitute of binary mixtures of ILs in molecular solvents, ILs in salt mixtures, ILs in IL mixtures etc. Among the IL mixtures, ILs in salt mixtures (especially Li^{+} salts) have been explored in much detailed recently, due to its applications in Li-ion battery and fuel cells. In this 21st century, the demand of batteries increases a lot due to the growing use of cellular phones, laptops, computers, cameras and automobiles. The ideal battery should be economical, lightweight, ecofreindly and stable in storage. Among different batteries, Li-battery has been chosen a lot because of its special properties. In the case of Li^{+}-ion battery the Li metal is used as an anode because of its two most important properties. First, Li^{+} has the lowest tendency to reduce to its metallic state because of its higher negative reduction potential (–3.04 V

for Li^+/Li). Secondly, it produces the greatest quantity of charge per unit weight because of its exceptionally low atomic weight and possesses greatest electrochemical capacity (3.86 A h g^{-1}). As the battery is an electrochemical cell, therefore it must contain an electrolytic solution of the same materials to that of anode. In case of Li^+ ion battery with Li-metal as anode, the electrolyte must contain a solution of Li^+ salts and a schematic representation of a Li^+ ion battery is shown in Figure 3.

Aqueous solutions of Li^+ salts cannot be used for this purpose because the water molecules may reacts with the Li^+ salts to produce hydrogen gas. This is one of the most fundamental limitations of using aqueous solutions of salts as electrolytes in Li^+-ion battery. However, Li^+ salt solutions of hydrophobic ILs can be a better replacement for the above limitation. For that reason, it is important to understand the self-diffusion coefficients of Li^+ salt solutions of ILs. Recently, Hayamizu et al. studied the temperature dependent diffusional motion of mixtures containing $^7Li^+$ salts doped of $[PYR_{13}][TFSA]$ and $[PYR_{13}][FSA]$ with Li-TFSA and Li-FSA.[12]

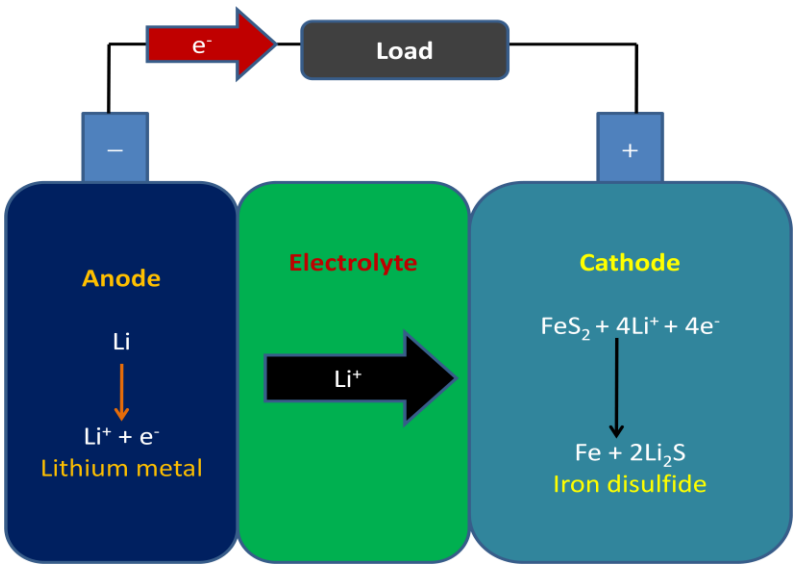

Figure 3. Li^+ ion battery with a solid cathode of iron disulfide.

In their study, the self-diffusion coefficient of different ions follows the order as $D_{[PYR13]+} > D_{[TFSA]-} > D_{Li+}$ in $[PYR_{13}]$-TFSA-Li mixture and $D_{[FSA]-} > D_{[PYR13]+} > D_{Li+}$ in its $[PYR_{13}]$-FSA-Li mixtures, respectively.[12] In an another report by the same research

group, the self-diffusion coefficient study of Li^+ salts doped in [EMIM][TFSA] and [EMIM][FSA] has been reported.[13] The relative self-diffusion coefficients are in the order of [EMIM][FSA] > [EMIM]-FSA-Li > [EMIM][TFSA] > [EMIM]-TFSA-Li for $[EMIM]^+$, anions and Li^+ ions. However, within the same IL the self-diffusion coefficients is in the order of $D_{[EMIM]+} > D_{anion} > D_{Li+}$.[13]

The room-temperature ionic liquid (RTIL) of a quaternary ammonium cation with an ether chain length, *N*,*N*-diethyl-*N*-methyl-*N*-(2-methoxyethyl)ammonium bis(trifluoromethylsulfonyl)amide (DEME-TFSA), is used as an electrolyte in Li^+-ion batteries.[29] The self-diffusion coefficients of different ions of Li-TFSA salt doped DEME-TFSA with the increasing compositions of Li^+ salts follows the order as $D_{Li} < D_{TFSA} < D_{DEME}$.[29] The MD simulation studies of Borodin et al. show that the mechanism of diffusional motion of Li^+ ion primarily occurred through the structural-diffusion mechanism.[30] However, a small contribution comes out from the vehicular mechanism where the diffusion of Li^+ ions takes place along with its whole coordination shell.[30]

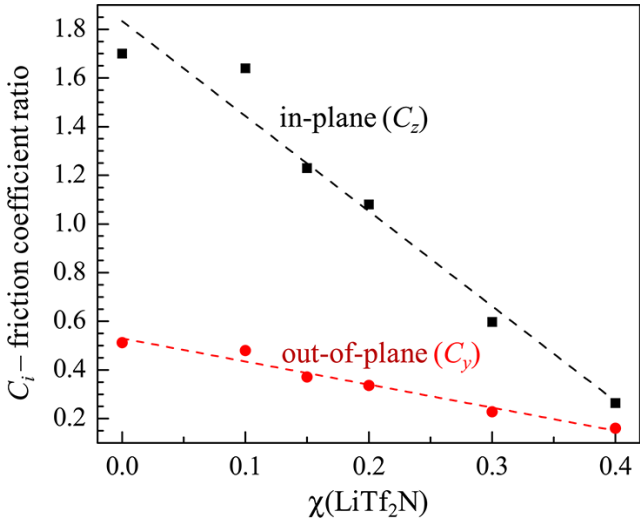

Figure 4. The ratios of the in-plane and out-of-pane frictional coefficients as a function of $LiNTf_2$.[16]

Generally, the self-diffusion coefficients of Li^+ ions in its LiX-IL mixtures depends mainly on the charge and size of the solvated Li^+ ions.[30] Recently, heteronuclear NOE experiments of [PYR_{14}]-TFSI-Li mixtures reveal that the molecular environment of Li^+

and $TFSI^-$ anions are similar in its 0.1 LiTFSI–0.9 $[PYR_{14}][TFSI]$ system indicating the existence of $[Li\text{-}(TFSI)_n]^{(n-1-)}$ structure.[30] The relaxation dynamics of a fluorescent hydrophobic probe, perylene has been studied in the $LiNTf_2$ salt mixtures of $[BMIM][NTf_2]$.[16] Both the in-plane and out-of-plane orientational relaxation dynamics of perylene becomes slower with the increase in the composition of $LiNTf_2$ in the system due to the increase in the viscosity of the mixtures. On the other hand, the frictional coefficient of the perylene molecule is decreased. The frictional coefficient coming out from the in-plane mode is decrease to a greater extent than the out-of-plane mode as illustrated in the Figure 4.[16] It indicates that solution viscosity is not only the solely factor responsible for the decrease in the orientational diffusion constant of the perylene probe. The reduction in the frictional coefficients also indicates the reduction in the packing of the alkyl chain length of $[BMIM]^+$ around the perylene molecule and the effect is more pronounced for the in-plane mode as compared to the out-of-plane mode.[16]

MD simulation studies of LiTFSI doped [MPPY][TFSI] and [MMPY][TFSI] ILs has been studied in the temperature range of 303-500 K.[31] The self-diffusion coefficients of different ions follows the order as $Li^+ < TFSI^- <$ $[MMPY]^+$ or $[MPPY]^+$.[31]

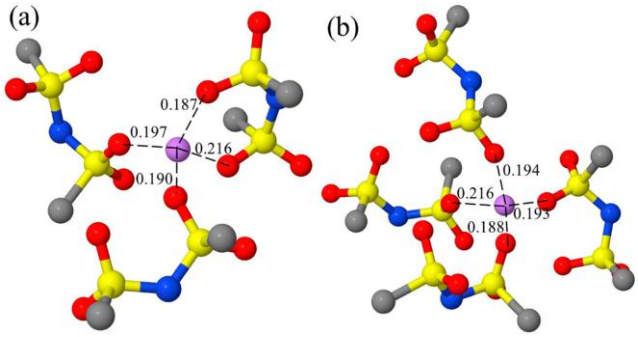

Figure 5. Solvation of Li^+ ions representing the bidentate (a) and monodentate (b) coordination of NTf_2^- ions in its $[PYR_{13}]$-Li-$[NTf_2]$ system.

The Li^+ coordination number and its aggregation behavior also have been studied through the MD simulation approach. Li^+ ions are mainly coordinated by the $TFSI^-$ anions with a coordination number of around < 4 and a fraction of Li^+ cations are adjacent to other Li^+ ions forming aggregated structures of $Li^+\cdots O{=}S{=}O\cdots Li^+$.[31] In another study of Li^+ salt doped mixtures in $[PYR_{13}]$-Li-$[NTf_2]$ system, the coordination number of Li^+ ion is found

to be around 4.1.[32] In this system both the monodentate and bidentate coordinated Li^+ ions with the $[NTf_2]^-$ anions are observed as represented in Figure 5.[32]

1.3. STOKES-EINSTEIN (SE) AND STOKES-EINSTEIN-DEBYE (SED) EQUATIONS

The relationship between the viscosity with the self-diffusion coefficient of the symmetrically spherical molecule can be obtained from the Stokes-Einstein (SE) equation 3 as:

$$D = \frac{k_B T}{c\pi\eta r} \tag{3}$$

where, k_B is the Boltzmann constant, T is the absolute temperature, r is the hydrodynamic radius (Stokes radius) of the diffusing molecule, D is the diffusion coefficient of the molecule, η is the viscosity of the medium and c is the coupling factor and theoretically its values ranges from 4 to 6 for 'slip' and 'stick' boundary conditions.[21] The denominator of the equation 3 (= $c\pi\eta r$) gives the information regarding the 'frictional coefficient' experienced by the diffusing molecule in the system. For the "perfect sticking" condition, the diffusing molecule experience a force due to the existence of pressure in front of it (= $4\pi\eta r$) and a frictional force acting parallel to the surface of the diffusing molecule (= $2\pi\eta r$).[33] Both the forces add up under the perfect sticking condition to give the value of coupling factor c = 6. However, there is no frictional force under the perfect sliding condition which gives the value of c = 4 and is known as Sutherland coefficient.[33]

Many reports are available in the literature to test the validity of this SE equation in ILs and IL mixtures. Recently, the diffusional behavior of FcMeOH has been studied in RTILs through the help of cyclic voltammetric measurements and observed that neither the SE (c = 6) nor the Sutherland coefficient (c = 4) holds good in the RTIL systems indicates that the coefficients lies in between the two limiting values.[33] The violation to SE equation in ILs is might be due to the existence of a balance between different attractive and repulsive forces in addition with the existence of equilibrium between the various associated and dissociated species present inside the ILs.[21] The ionic diffusivity

of ions in the imidazolium and pyridinium cation-based ILs follows the equation 3.[22] The coupling factor, *c* for the $[BMIM]^+$ based ILs are obtained as 3.3, 3.4, 3.4, 3.0, 3.8, and 3.3 for $[(C_2F_5SO_2)_2N]^-$, $[(CF_3SO_2)_2N]^-$, $[CF_3SO_3]^-$, $[PF_6]^-$, $[CF_3CO_2]^-$, and $[BF_4]^-$, respectively. On the other hand, for the anionic diffusivity with $[(C_2F_5SO_2)N]$, $[(CF_3SO_2)_2N]^-$, $[CF_3SO_3]^-$, $[PF_6]^-$, and $[BF_4]^-$ the coupling factor are obtained as 4.1, 4.3, 5.0, 4.6, and 4.6, respectively.[19] In another report of imidazolium-based ILs, the coupling factor of cation in $[RMIM][(CF_3SO_2)_2N]$ (R = alkyl groups) are 3.0, 2.9, 3.4, 3.4, and 3.6 for $[MMIM]^+$, $[EMIM]^+$, $[BMIM]^+$, $[HMIM]^+$, and $[OMIM]^+$, respectively.[20] On the other hand, the anionic diffusivity in same ILs for $[MMIM]^+$, $[EMIM]^+$, $[BMIM]^+$, $[HMIM]^+$, and $[OMIM]^+$ cations are 4.4, 4.3, 4.3, 4.1, and 4.2, respectively.[20]

The interaction between the diffusing molecule with the solvent molecules is negligible in the case of slip boundary condition (c = 4). However, it is strong in the case of stick boundary condition with SE coupling factor, c = 6.[12] The plot of the self-diffusion coefficients with the $kT/\pi\eta$ for different ions in the $[PYR_{13}]$-TFSA-Li and $[PYR_{13}]$-FSA-Li mixtures gives a straight line; and the coupling factor for individual diffusing ions obtained from the gradient of each line are given in the Table 2.

Table 2. SE Coupling Factor for each Ion in Different Mixtures.[12]

Ion	$c \times a$ / nm	c	Sample
$[PYR_{13}]^+$	$0.98_2 \pm 0.02_7$	2.9_8	$[PYR_{13}]$-TFSA
	$1.04_1 \pm 0.006$	3.1_6	$[PYR_{13}]$-FSA
	$0.98_5 \pm 0.01_4$	2.9_9	$[PYR_{13}]$-TFSA-Li
	$1.15_7 \pm 0.007$	3.5_1	$[PYR_{13}]$-FSA-Li
$TFSA^-$	$1.22_9 \pm 0.02_6$	3.7_3	$[PYR_{13}]$-TFSA
	$1.37_1 \pm 0.01_5$	3.9_1	$[PYR_{13}]$-TFSA-Li
FSA^-	$0.87_4 \pm 0.01_5$	3.0_7	$[PYR_{13}]$-FSA
	$1.04_6 \pm 0.007$	3.6_8	$[PYR_{13}]$-FSA-Li
Li^+	$1.86_6 \pm 0.020$	4.5_2	$[PYR_{13}]$-TFSA-Li
	$1.52_8 \pm 0.02_9$	3.7_5	$[PYR_{13}]$-FSA-Li

The validity of SE equation also has been studied for the diffusional motion of ions present inside the [EMIM]-TFSA-Li and [EMIM-FSA-Li] mixtures.[13] The value of coupling factor for $[EMIM]^+$ is higher in its Li-doped mixtures as compared to the neat IL system. The *c* value for $[EMIM]^+$ (c = 2.5) is smaller as compared to that of the $TFSA^-$ (c = 3.3) and FSA^- (c = 3.5) anions.[13]

Beside the translational diffusion coefficients, the diffusing molecule also possesses the rotational diffusion coefficient values which can be obtained from the Stokes-Einstein-Debye (SED) equation 4 as:

$$D_r = \frac{k_B T}{8\pi\eta r^3} \quad (4)$$

where, D_r is the rotational diffusion coefficient of the diffusing molecule and rest of the symbols have their usual meaning.

In addition to the SE equation, the use and validity of SED equation also has been tested in various ILs and IL mixtures. Recently, MD simulation studies has been performed in order to test the validity of SED equation in $[EMIM][NTf_2]$ and its binary mixtures in chloroform (50 wt% IL).[17] It was observed that the equation is not valid in the studied system due to the presence of dynamical heterogeneity in the IL and its mixtures with chloroform.[17] The SED equation is also deviates for the rotation of a spinning molecular probe (TEMPOL) in ILs media, when its alkyl chain length exceeds six carbon atom (hexyl).[34]

1.4. TRANSLATIONAL AND ROTATIONAL MOTIONS

Translations motion is defined as the motion of a molecule from one position to another with a change in their center of mass. However, in the case of rotational motion the molecule has to move along its axis of rotation and the center of mass of the molecule remains unchanged during its motion. The information regarding the translational motion of a molecule can be obtained from their translational correlation time values (τ_t) and similarly the rotational correlation time values (τ_2) gives the information regarding the rotational motion of the diffusing molecule inside the system. This τ_t and τ_2 values of

molecules are obtained from the experimentally measured self-diffusion coefficients and viscosity of the system, respectively which can be obtained from equation 5 and 6 as:

$$\tau_t = \frac{2r^2}{D} \quad (5)$$

and,

$$\tau_2 = \frac{V\eta}{kT} \quad (6)$$

where, V is the effective molecular volume of the diffusing molecule and rest of the symbols have their usual meaning as described in the above text.[13]

The molecular motions of $[PYR_{13}]^+$ has been calculated in its Li-doped salts and compared with the reorientational time obtained from the NMR-T_1 measurements and the molecular motions follows the order as τ_t (self-diffusion) > τ_2 (viscosity) > τ_c (T_1).[12] The same trend in the molecular motions are observed for the $[EMIM]^+$ in its Li-doped salt systems in between the temperature range of 283-353 K.[13] The temperature dependent translational and rotational motions of cations of [RMIM][BF_4]-based ILs (R = CH_3, C_2H_5) also has been studied and compared with the c values obtained from the NMR-T_1 measurements.[35] The same order has been observed in both the ILs, however, the correlation time of $[EMIM]^+$ is shorter as compared to that of $[BMIM]^+$.[35] Beside the experimental studies, theoretical reports are also available in order to understand the translational and rotational dynamics of IL and its mixtures. The MD simulation studies of translational motion of terminal carbon atom of alkyl side chain of imidazolium ILs is substantially faster than compared to the atoms present in the imidazolium ring and anions of ILs.[36] It indicates that the translational dynamics of atoms present in the polar domains of ILs is substantially different as compared to the nonpolar domains.[36]

1.5. ACTIVATION ENERGY

It was Arrhenius in 1889 first introduced the term activation energy in chemical kinetics. It is the minimum energy required for the reactant molecules to react among themselves to give the product and have the general form represented in equation 7 as:

$$k = Ae^{-\frac{E_a}{RT}} \quad (7)$$

where, k is the rate constant of a chemical reaction, R is the universal gas constant, T is the absolute temperature, E_a is the activation energy and A is the preexponential factor. Temperature dependent of a physical property can be fitted with an exponential equation proposed by Arrhenius in order to obtain the information regarding the activation energy of a physical property. A minimum amount of energy is also required for the molecules present inside a fluid mixture in order to diffuse and the amount of energy is known as the activation energy for diffusive flow and can be obtained from the Arrhenius type equation 8 as:

$$D_T = D_0 e^{\frac{E_D}{RT}} \tag{8}$$

where, D_T is the translational diffusion coefficient, D_0 is the preexponential factor for the diffusive flow, E_D is the activation energy of the diffusive flow and rest of the symbols have their usual meaning.[37] In similar way the activation energy of viscous flow can be obtained from the temperature dependent viscosity study of fluids and can be obtained from equation 9 as:

$$\eta = \eta_0 e^{\frac{E_\eta}{RT}} \tag{9}$$

where, η is the viscosity of the system, η_0 is the preexponential factor for the viscous flow, E_η is the activation energy of viscous flow and rest of the symbols have their usual meaning.[38,39] Recently, NMR spectroscopic studies has been performed to measured the T_1 relaxation time of different protons present in the Li-salt doped imidazolium-based ILs and calculated the reorientational correlation time of each proton.[13] The activation energy of the reorientational motion of individual protons has been obtained from the temperature dependent reorientational correlation time values and higher values are observed in case of Li-salt doped systems as compared to the neat ILs.[13] Similarly, the activation energy for rotational motion of the pyrrolidinium-based ILs also has been studied from its temperature dependent rotational motions.[40]

Beside the study of transport phenomena like diffusion, viscosity and microviscosity in IL mixtures, we have also studied these phenomenons in microheterogeneous regions of ILs called as the microemulsions. Different types of microheterogeneous regions are

water in IL microemulsions (W/IL), IL in water microemulsions (IL/W) and bicontinuous microemulsions. Our study is mainly concentrated on the W/IL microemulsion systems. A brief introduction to it with the literature work has been presented in the following sections.

1.6. AQUEOUS IL CONFINED MEDIA: MICROEMULSIONS

The confined media are the small nanometer volume of space present in a large continuous medium. These confined spaces contain different kind of solvents in a small phase depending upon their thermodynamic stability. It is called as the aqueous confined media when water is present in the smaller phase. Because of the presence of the water phase, it forms different geometries of confined media due to the interplay between the hydrophilic and hydrophobic interactions as shown in the Figure 6.[41] These confined media are the center of attraction in many nanometer sized electronic devices,[42] drug delivery system,[43] and molecular recognition.[44]

1.6.1. Microemulsions

Microemulsions are thermodynamically stable, optically transparent and isotropic mixtures of oil, water and surfactants frequently in combination with a cosurfactants.[45] In small scale it is called as a emulsion. However, there exists a significant difference between both of them. The size of emulsions increases continuously with time and after a certain period of time, phase separation occurs due to its thermodynamic instability. However, microemulsions can be stored over years and are thermodynamically stable in nature. The formation of microemulsions depends upon the types and structure of the surfactants used. For ionic and single chain surfactants (e.g., sodium dodecylsulphate, SDS) the formation of microemulsions are only possible when a cosurfactant is added into the system. However, there is no need of any cosurfactants in the preparation of microemulsions for double chain ionic (e.g., Aerosol-OT) and non-ionic surfactants (e.g., Triton X-100). The prime role of the surfactant is to reduce the interfacial tension between the oil and water phase, $\gamma_{O/W}$. This results in the increase in the surface area between the two phases by lowering its energy which leads to the spontaneous dispersion of oil/water droplets and the system becomes thermodynamically stable. The observation

of spontaneous emulsion of oil and water by the addition of a surface active agent into the system was first introduced by Schulman in 1943,[46] who named it microemulsion later in 1959.[47]

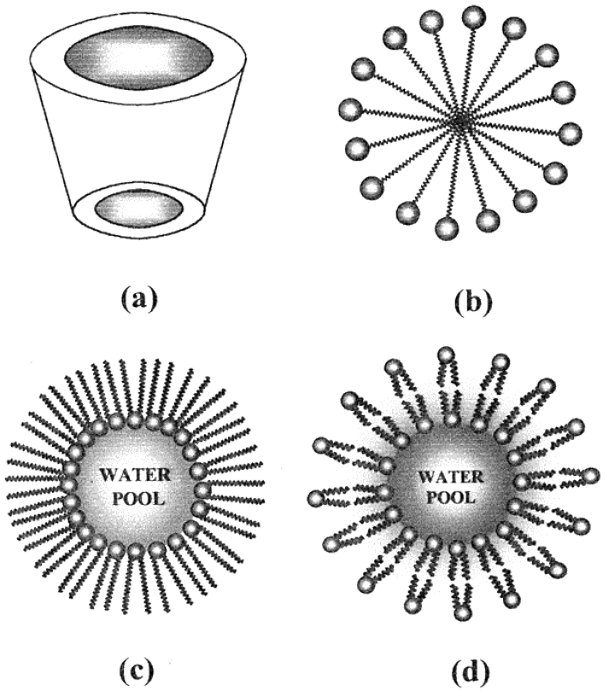

Figure 6. Different geometries of confined water are cyclodextrin (a), micelles (b), microemulsions (c), and lipid vesicles (d). The structure of micelle is given in order to distinguish it from the structure of microemulsions and vesicles.[41]

In the late 1970's and early 1980's, the demand of microemulsions are really stepped up due to its use in oil recovery processes.[48] In addition to this, nowadays it has been used in a variety of processes such as, solar energy conversion, catalysis, liquid-liquid extraction (proteins, minerals, etc.) and many more.

1.6.2. Types of Microemulsions

It was Winsor in 1948, who classified four general types of microemulsions and are known as Winsor I, II, III, and IV type microemulsions.[49]

a) Type I: It is known as the oil in water (O/W) microemulsion and here the surfactant is preferentially soluble in the water phase (Winsor I). Both the surfactant rich water phase coexist with the oil phase with small concentration of surfactants.

b) Type II: The surfactant is preferentially soluble in the oil phase forming water in oil (W/O) microemulsions (Winsor II). Both the surfactant rich oil phase and surfactant-poor water phase are coexisting with each other.

c) Type III: A surfactant rich middle phase that coexist with both the surfactant-poor oil and water phase (Winsor III).

d) Type IV: An isotropic, single phase miceller solutions forms by the addition of sufficient quantity of surfactants (Winsor IV).

1.6.3. Terminology

1.6.3.1. Bancroft's Rule

In 1913 the first concept of Bancroft as Bancroft's rule came which state that the O/W emulsion forms if the surfactant is preferentially soluble in the water phase, however, the W/O emulsion forms when the surfactant is preferentially soluble in the oil rich phase.[50]

1.6.3.2. Packing Parameter

Israelachivili et al.[51] in 1976 proposed a quantitative relationship popularly known as the critical packing parameter (CPP) in order to know about the preferred curvature of the interface of an emulsion and is governed by the area of the head group (a_0) of surfactants and the effective area of the tail (v/l_c) of surfactants; where v is the volume and l_c is the effective area of the hydrocarbon chain of the surfactants. The CPP is described by the equation 10 as:

$$CPP = \frac{v}{l_c a_0} \qquad (10)$$

where the symbols have their usual meaning as described in the text. The equation 10 is very informative to predict the type of microemulsions.

- O/W microemulsion forms if $a_0 > v/l_c$
- W/O microemulsion forms, if $a_0 < v/l_c$
- Middle phase microemulsion forms if $a_0 \approx v/l_c$

The value of CPP is also used in order to know the information regarding the morphology of the micelles. Theoretically, CPP value of between 1/2 and 1 corresponds to the planar structure, between 4/3 and 1/2 corresponds to rod like micelles, and values less than 1/3 corresponds to the spherical micelles, respectively.

1.6.3.3. Hydrophilic-Lipophilic Balance (HLB)

It is an empirical equation based on the relative percentage of lipophilic and hydrophilic groups present in a surfactant molecule. It was first introduced by Griffin[52] for non-ionic alkyl polyglycols ethers and later on Davis et al.[53] extended it and proposed an empirical equation given in equation 11 as:

$$\text{HLB} = [(n_H \times H) - (n_L \times L)] + 7 \qquad (11)$$

where L and H are the constants assigned to hydrophobic and hydrophilic groups, respectively and, n_L and n_H are the numbers of these groups per surfactant molecule. The HLB value for bicontinuous structure is ≈ 10 with zero curvature. O/W and W/O microemulsion forms when HLB > 10 and HLB < 10, respectively.

These microemulsions are of great importance in a wide variety of processes such as in catalysis.[54-59] material synthesis,[60] enzymatic reactions.[61-65] electron-transfer[66,67] and biochemical reactions[61-65]. In the late 1970's and early 1980's there is an increasing interest in the field of aqueous microemulsions because of the above mentioned reasons. Therefore, many research groups around the globe have done extensive work in order to understand the water confined inside the microemulsions. Recently, a series of paper published from the group of Levinger and Crans[68-70] to study the properties of water confined inside the reverse micelles. Beside this, different spectroscopic studies like fluorescence spectroscopy,[41,67] NMR spectroscopy,[69] IR spectroscopy,[71] UV-vis spectroscopic studies[72,73] also have been performed in order to understand the physical properties of aqueous miceller core. These aqueous microemulsions are thermally unstable and therefore it is necessary to prepare new type of microemulsions with the

increased range of their thermal stability. In order to increase the thermal stability of microemulsions, ILs are the suitable materials for it. ILs are selected for this purpose because of their special physicochemical properties like negligible vapor pressure, high thermal stability and having wide electrochemical range as discussed in the initial section of the chapter. The IL microemulsions came into its use because of two reasons: 1) the increase demand of high thermal stability microemulsions and, 2) it can be used as an alternative better replacement for the volatile organic solvents because of their special physicochemical properties. Therefore, the IL microemulsions are of two types; one is the microemulsion where the IL is replaced the water phase and in the other case the volatile organic components are replaced by the ILs. A brief literature survey regarding this has been presented in the following sections.

1.6.4. IL Microemulsions

1.6.4.1. Non-Aqueous IL Microemulsions

As discussed above, when one component of the microemulsion is IL, it is called as the IL microemulsion. Extensive research has been carried out in order to prepare high thermal stability microemulsions. Gao et al. reported the formation and stability of [BMIM][BF_4]/TX-100/cyclohexane microemulsions for their potential applications in chemical, biological and enzymatic reactions; organic, inorganic and material synthesis.[74] The study of IL in oil (IL/O) microemulsion also has been explored by Eastoe et al. with the cyclohexane as the oil phase.[75] The IL/O microemulsions are also formed with the [BMIM][BF_4] as the polar phase by taking *p*-xylene as the oil phase.[76] Herein the interactions between the oxyethylene units of nonionic TX-100 surfactants with the polar imidazolium ring of $[BMIM]^+$ are the driving force for the formation of microemulsions. The nonionic TX-100 surfactant is also used for the formation of [BMIM][BF_4]-in-toluene microemulsions.[77] Here, the initial reverse micelles are swollen with the increase in the compositions of [BMIM][BF_4] confirmed from the DLS measurements.[77]

Beside its structure and formation, other physicochemical properties like micropolarity, microviscosities etc. also have been studied for these nonaqueous IL microemulsions because of their wider applications in different field of science and

technology. The micropolarity of the polar IL core of the [BMIM][BF_4]/TX-100/toluene has been studied by the help of methyl orange (MO) and methylene blue (MB) as the UV-vis spectroscopic probe.[78] The polarity of the polar core of IL is increases with the initial addition of [BMIM][BF_4] into the system. However, it remains constant when the IL pool begins to form in the microemulsion system.[78] Different metal salts and biological molecule like riboflavin is also solubilized inside the polar [BMIM][BF_4] core of [BMIM][BF_4]/TX-100/toluene microemulsion systems indicating its potential use as a media in the preparation of nanomaterials, semiconductor and different enzymatic reactions.[78] The microviscosity of the polar core ([N_{3111}][NTf_2]) of the [N_{3111}][NTf_2]/TX-100/cyclohexane microemulsion system has been studied by the help of steady state and time resolved fluorescence spectroscopic study of coumarin 480 (C-480) as a fluorescence molecular probe.[79] The rotational relaxation time of C-480 increases with the increase in the [N_{3111}][NTf_2] into the microemulsion systems indicating the increase in the microviscosity of the polar IL core of the microemulsion system.[79] In an another report, the rotational relaxation time of the coumarin-153 (C-153) inside the polar core of the [PY][NTf_2]/[BMIM][AOT]/benzene microemulsion system increases from 0.32 to 0.39 ns with the increase in the *R* ([PY][NTf_2]/[BMIM][AOT] molar ratio) value from 0.14 to 0.20 indicating an increase in the microviscosity of the polar IL region of microemulsion.[80]

1.6.4.1.1. Effect of Solubilized Water on Non-Aqueous IL Microemulsions

The non-aqueous IL microemulsions can solubilize a significant amount of water. It affects the properties of these non-aqueous IL microemulsions to greater extent. Recently, the effect of solubilized water on the properties of [BMIM][BF_4]/TX-100/benzene microemulsions has been studied by the help of FTIR and ^{1}H-NMR spectroscopy.[81] Here the polarity of the IL pool of the microemulsions remains constant after the addition of water into the system indicating the absence of water molecules inside the IL pool. However, the water molecules are present in the interstitial sites of the polar part of the TX-100 molecules through the strong H-bonding interactions with the oxyethylene (EO) units of surfactant molecules. The stability of [BMIM][BF_4]/TX-100/benzene microemulsions has been increased with the addition of small amount of

water into the system and the water molecules are mainly present as in the state of trapped and bound state.[82] However, the droplet size and its morphology have been changed with the addition of water into the [BMIM][BF_4]/TX-100/cyclohexane microemulsion systems.[83] Increase in the water content decreases the droplet size and consequently increases the number of microemulsion droplets of the [BMIM][BF_4]/TX-100/cyclohexane system and the schematic representation of the change in its morphology is presented in the Figure 7.

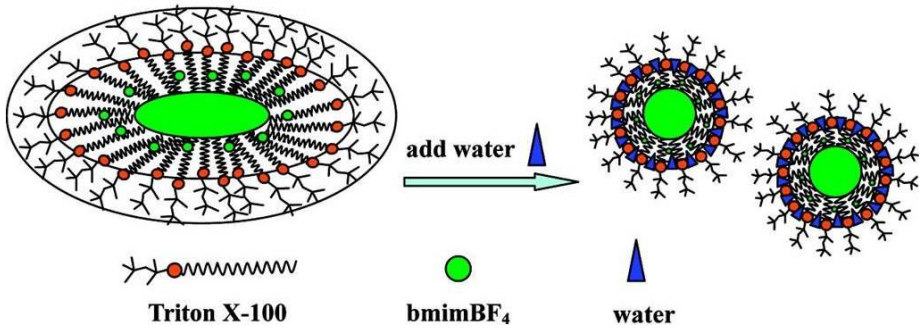

Figure 7. Schematic representation of the change in the morphology of the [BMIM][BF_4]/TX-100/cyclohexane microemulsion system from elliptical to spherical with the addition of water.[83]

The steady state and time resolved fluorescence spectroscopic study of C-480 in the [BMIM][BF_4]/TX-100/cyclohexane microemulsion system indicates an increase in the solvent relaxation time which confirms the decrease in the size of the microemulsion droplets.[84] The rotational relaxation time of the C-480 of the IL pool is unchanged, indicating that the microviscosity of the pool remains unaltered with the addition of water into the microemulsion system.[84]

1.6.4.2. Aqueous IL Microemulsions

The microemulsion in which its one component is water and the other component is the IL is known as the aqueous IL microemulsion. The IL must be hydrophobic in nature in order to form the biphasic system with water without the addition of any surface active agents. There is a growing interest in its use in past decade as the IL can be used as a better alternative replaceable media to the volatile organic solvents for the preparation of microemulsions. Recently, the [BMIM][PF_6] is used to prepare the aqueous

microemulsion with water, and TX-100 as the surfactant.[72] Time resolved fluorescence spectroscopy has been used to study the interaction between the water and IL molecules inside the [BMIM][PF_6]/TX-100/H_2O microemulsion systems.[85] The solvent and rotational relaxation of coumarin 153 (C-153) and coumarin 490 (C-490) has been studied in the above mentioned microemulsion system.[86] It was observed that the probe molecules experienced a bulk water like environment with the increase in the composition of water.[86]

One of the most important applications of these aqueous IL microemulsions is its use as a medium to carryout different organic and enzymatic reactions. Recently, Moniruzzaman et al. reported about the formation of aqueous microemulsion by taking hydrophobic [OMIM][NTf_2] with AOT and 1-hexanol as the surfactant and cosurfactant, respectively.[87] The catalytic activity of the lipase PS on the hydrolysis reaction of *p*-nitophenyl butyrate (*p*-PNB) has been studied in this microemulsion system and a higher activity has been observed in this system as compared to AOT in isooctane microemulsion system.[88]

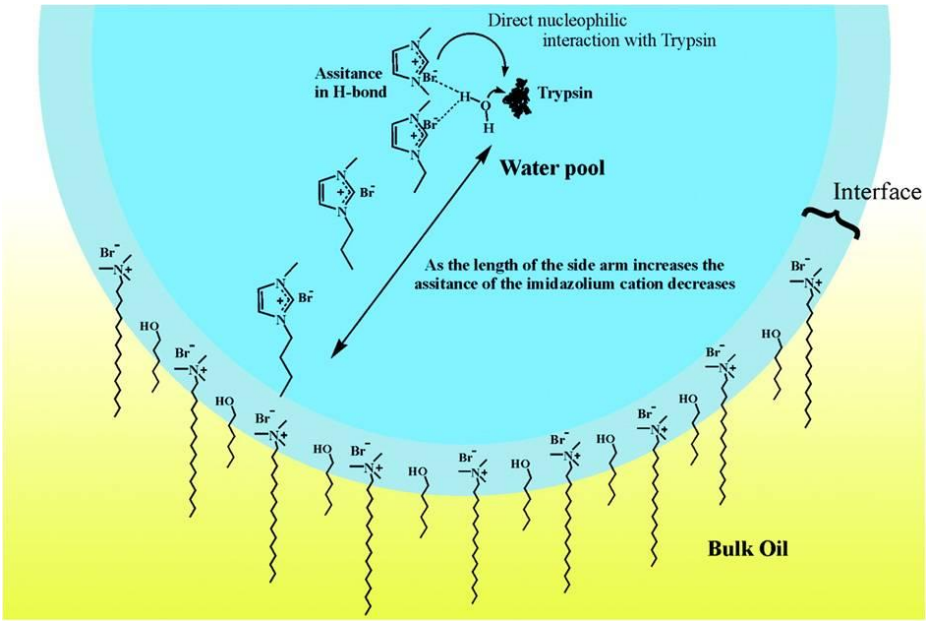

Figure 8. Schematic representation of the effect of lower alkyl chain length imidazolium bromide-based IL on the activity of trypsin.[91]

In an another report, the catalytic activity of horseradish peroxidase (HRP) on the oxidation of pyrogallol has been studied in this microemulsion system.[89] A significant enhancement in its activity has been observed in the aqueous IL microemulsion system as compared to the traditional water/oil microemulsions. Therefore, the aqueous IL microemulsions can be selected over the water/oil microemulsions for the catalytic oxidation of different organic compounds like phenols, anilines, biphenols, and many heteroaromatic compounds.[89] In an another type of aqueous IL microemulsion, the 1-tetradecyl-3-methylimidazolium bromide [C_{14}MIM]Br has been used as a surfactant with *p*-xylene as the oil phase and the microemulsion formed with water can be used as a reaction media for the photocyclization reaction of substituted anthracene derivatives.[90] Other reports suggests the enhanced activity of enzymes by the addition of ILs into the aqueous microemulsions. The lower alkyl chain length imidazolium bromide-based IL increases the enzyme activity of trypsin in the case of CTAB aqueous microemulsions system as represented in the Figure 8.[91]

As discussed in the previous sections, the aqueous IL microemulsion plays a significant role in different industrial applications especially in the improved enzyme activity of various enzymes. Therefore, it is of great interest to understand the fundamental physical properties like microviscosity, micropolarity and pH of these aqueous pools confined in the IL dispersion medium for its better industrial application purposes which has been discussed in the chapter V of the thesis.

These aqueous confined media are ubiquitous in biological systems like in mitochondria and chloroplast of cellular organelles. In addition to water, other salts and minerals are also present inside these confined biological systems which greatly affect most of its physiological functions. In addition to this, salts also effects the stability of proteins, amphiphiles, and other hydrophobic molecules present inside the system. As it affects the stability of the amphiphilic molecules, therefore its properties are significantly altered in their aqueous solutions containing various salts.

There are ILs which contain hydrophobic alkyl groups attached to its cation and because of which they shows amphiphilic character in their aqueous solutions.[92] The addition of salts, therefore, effects most of its physical properties in their aqueous solutions and the following sections of the chapter present a brief introduction to the effects of salts on the ILs in its aqueous solutions.

1.7. SALT EFFECTS

The salt effects were noted after the observation of Hofmeister on the precipitation of some proteins and colloids in the 1870's.[93] He observed that the precipitation of proteins and colloids depends upon the charge density of ions. On the basis of his observations he arranged the ions in a series popularly known as the Hofmeister series as given below.[94]

$CO_3^{2-} > SO_4^{2-} > S_2O_3^{2-} > H_2PO_4^- > F^- > Cl^- > Br^- \approx NO_3^- > I^- > ClO_4^- > SCN^-$

$Zn^{+2} > Mg^{+2} > Ca^{+2} > Li^+ > Na^+ > K^+ > NH_4^+ > Rb^+ > Cs^+$

The ions present in the left side of the series precipitate the proteins and hydrophobic molecules in their aqueous solutions and are known as "water structure-makers" or salting-out agents and the ions on the right sides of the series destabilizes the proteins and are called as "water structure-breakers" or salting-in agents.[95] The salting-in and salting-out salts are also popularly known as the chaotropic and kosmotropic agents, respectively.

In addition to the spectroscopic tools, bulk physical properties of solutions can be also used in order to explain about the salting phenomenon in solutions. Solubility of a solution can be used to estimate the salting phenomena of a salt. It was Setschenow proposed an equation based on the solubility phenomena $\log (s_0/s) = kc_s$, in which s and s_0 are the solubility of nonelectrolyte in the aqueous electrolytes and in aqueous solutions, respectively. c_s is the composition of salts used and k is the salting constant which tells about the salting nature of the salt in the solutions.[96] If the value of salting coefficient is positive, then the salt is characterized as the salting-out salt, however, negative value of salting coefficient tells about the salting-in nature of salts.[96] Similarly, the surface tension

measurements of solutions and the cavitation phenomena can be also used to define the salting-out/salting-in nature of salts.[97]

The measurement of bulk viscosity of solutions is also used by many workers in order to classify the nature of salt as salting-in/salting-out.[96] Generally, the viscosity *B*-coefficients, also known as the Jones-Dole *B*-coefficient obtained from the viscosity measurements can be used to characterize the salting-in/salting-out nature of salts.[96] Positive and negative values of *B*-coefficient show the salting-out and salting-in nature of salts, respectively.

To the best of our knowledge a few reports are available in the literature to understand the salting-in/salting-out phenomenon of salts in its aqueous solutions of ILs. Recently, the mechanism of salting effect has been analyzed on the solubility of [BMIM][NTf_2] in its aqueous solutions.[98] The mechanism of salting-out effect of salts is mainly cause by the entropic effect with the formation of ion-water complexes leading to the dehydration of the [BMIM][NTf_2]. However, the mechanism of salting-in effect is mainly caused by the low charge density ions by the direct binding of ions to the hydrophobic groups of IL.[99]

Considering the above development in the field of IL and its mixtures, it is of great interest to extend the study especially in the bulk and microscopic transport processes for their potential applications.

1.8. REFERENCES

(1) Reichardt, C. *Solvent Effects in Organic Chemistry*; Verlag Chemie, **1979**.

(2) Sheldon, R. A. *Industrial Environmental Chemistry*; Springer: **1992**, 99-119.

(3) Sheldon, R. A. *Precision Process Technology*; Springer: **1993**, 125-138.

(4) Carson, R. *Silent Spring, Houghton Mifflin*, Boston, **1962.**

(5) Anastas, P. T.; Farris, C. T. *ACS Symposium Series (USA)*; American Chemical Society: **1994**.

(6) Anastas, P. T.; Kirchhoff, M. M. *Acc. Chem. Res.* **2002**, *35*, 686-694.

(7) Matlack, A. S. *Introduction to Green Chemistry, Marcel Dekker*, New York **2001**.

(8) Park, J.; Jung, Y.; Kusumah, P.; Lee, J.; Kwon, K.; Lee, C. K. *Int. J. Mol. Sci.* **2014**, *15*, 15320-15343.

(9) Welton, T. *Chem. Rev.* **1999**, *99*, 2071-2084.

(10) Ong, S. P.; Andreussi, O.; Wu, Y.; Marzari, N.; Ceder, G. *Chem. Mat.* **2011**, *23*, 2979-2986.

(11) Stejskal, E. O.; Tanner, J. E. *J. Chem. Phys.* **1965**, *42*, 288-292.

(12) Hayamizu, K.; Tsuzuki, S.; Seki, S.; Fujii, K.; Suenaga, M.; Umebayashi, Y. *J. Chem. Phys.* **2010**, *133*, 194505-194518.

(13) Hayamizu, K.; Tsuzuki, S.; Seki, S.; Umebayashi, Y. *J. Chem. Phys.* **2011**, *135*, 84505-84516.

(14) Lovelock, K. R. J.; Ejigu, A.; Loh, S. F.; Men, S.; Licence, P.; Walsh, D. A. *Phys. Chem. Chem. Phys.* **2011**, *13*, 10155-10164.

(15) Rausch, M. H.; Hopf, L.; Heller, A.; Leipertz, A.; Froba, A. P. *J. Phys. Chem. B* **2013**, *117*, 2429-2437.

(16) Lawler, C.; Fayer, M. D. *J. Phys. Chem. B* **2013**, *117*, 9768-9774.

(17) Koddermann, T.; Ludwig, R.; Paschek, D. *ChemPhysChem* **2008**, *9*, 1851-1858.

(18) Kashyap, H. K.; Annapureddy, H. V. R.; Raineri, F. O.; Margulis, C. J. *J. Phys. Chem. B* **2011**, *115*, 13212-13221.

(19) Tokuda, H.; Hayamizu, K.; Ishii, K.; Susan, M. A. B. H.; Watanabe, M. *J. Phys. Chem. B* **2004**, *108*, 16593-16600.

(20) Tokuda, H.; Hayamizu, K.; Ishii, K.; Susan, M. A. B. H.; Watanabe, M. *J. Phys. Chem. B* **2005**, *109*, 6103-6110.

(21) Martinelli, A.; Marechal, M.; Ostlund, A., Cambedouzou, J. *Phys. Chem. Chem. Phys.* **2013**, *15*, 5510-5517.

(22) Noda, A.; Hayamizu, K.; Watanabe, M. *J. Phys. Chem. B* **2001**, *105*, 4603-4610.

(23) Tokuda, H.; Ishii, K.; Susan, M. A. B. H.; Tsuzuki, S.; Hayamizu, K.; Watanabe, M. *J. Phys. Chem. B* **2006**, *110*, 2833-2839.

(24) Filippov, A.; Shah, F. U.; Taher, M.; Glavatskih, S.; Antzutkin, O. N. *Phys. Chem. Chem. Phys.* **2013**, *15*, 9281-9287.

(25) Herriot, C.; Khatun, S.; Fox, E. T.; Judeinstein, P.; Armand, M.; Henderson, W. A.; Greenbaum, S. *J. Phys. Chem. Lett.* **2012**, *3*, 441-444.

(26) Taylor, A. W.; Licence, P.; Abbott, A. P. *Phys. Chem. Chem. Phys.* **2011**, *13*, 10147-10154.

(27) Rey-Castro, C.; Vega, L. F. *J. Phys. Chem. B* **2006**, *110*, 14426-14435.

(28) Borodin, O.; Gorecki, W.; Smith, G. D.; Armand, M. *J. Phys. Chem. B* **2010**, *114*, 6786-6798.

(29) Hayamizu, K.; Tsuzuki, S.; Seki, S.; Ohno, Y.; Miyashiro, H.; Kobayashi, Y. *J. Phys. Chem. B* **2008**, *112*, 1189-1197.

(30) Castiglione, F.; Ragg, E.; Mele, A.; Appetecchi, G. B.; Montanino, M.; Passerini, S. *J. Phys. Chem. Lett.* **2011**, *2*, 153-157.

(31) Borodin, O.; Smith, G. D.; Henderson, W. *J. Phys. Chem. B* **2006**, *110*, 16879-16886.

(32) Li, Z.; Smith, G. D.; Bedrov, D. *J. Phys. Chem. B* **2012**, *116*, 12801-12809.

(33) Edward, J. T. *J. Chem. Educ.* **1970**, *47*, 261-270.

(34) Strehmel, V.; Rexhausen, H.; Strauch, P. *Phys. Chem. Chem. Phys.* **2010**, *12*, 1933-1940.

(35) Hayamizu, K.; Tsuzuki, S.; Seki, S.; Umebayashi, Y. *J. Phys. Chem. B* **2012**, *116*, 11284-11291.

(36) Tsuzuki, S.; Shinoda, W.; Saito, H.; Mikami, M.; Tokuda, H.; Watanabe, M. *J. Phys. Chem. B* **2009**, *113*, 10641-10649.

(37) Alam, T. M.; Dreyer, D. R.; Bielawski, C. W.; Ruoff, R. S. *J. Phys. Chem. B* **2013**, *117*, 1967-1977.

(38) Evans, R. G.; Klymenko, O. V.; Price, P. D.; Davies, S. G.; Hardacre, C.; Compton, R. G. *ChemPhysChem* **2005**, *6*, 526-533.

(39) Abbott, A. P.; Capper, G.; Davies, D. L.; Rasheed, R. K. *Chem.-A Eur. J.* **2004**, *10*, 3769-3774.

(40) Alam, T. M.; Dreyer, D. R.; Bielwaski, C. W.; Ruoff, R. S. *J. Phys. Chem. A* **2011**, *115*, 4307-4316.

(41) Bhattacharyya, K. *Acc. Chem. Res.* **2003**, *36*, 95-101.

(42) Xia, Y.; Rogers, J. A.; Paul, K. E.; Whitesides, G. M. *Chem. Rev.* **1999**, *99*, 1823-1848.

(43) Mueller, A.; O'Brien, D. F. *Chem. Rev.* **2002**, *102*, 727-758.

(44) Selinger, J. V.; Spector, M. S.; Schnur, J. M. *J. Phys. Chem. B* **2001**, *105*, 7157-7169.

(45) Lindman, B.; Danielson, I. *Colloid Surf.* **1981**, *3*, 391-392.

(46) Sjoblom, J.; Lindberg, R.; Friberg, S. E. *Advan. Colloid Interface Sci.* **1996**, *65*, 125-287.

(47) Schulman, J. H.; Stoeckenius, W.; Prince, L. M. *J. Phys. Chem.* **1959**, *63*, 1677-1680.

(48) Friberg, S.; Mandell, L.; Larsson, M. *J. Colloid Interface Sci.* **1969**, *29*, 155-156.

(49) Winsor, P. A. *Trans. Faraday Soc.* **1948**, *44*, 376-398.

(50) Bancroft, W. D. *J. Phys. Chem.* **1912**, *17*, 501-519.

(51) Israelachvili, J. N.; Mitchell, D. J.; Ninham, B. W. *J. Chem. Soc., Faraday Trans. 2*, **1976**, *72*, 1525-1568.

(52) Griffin, W. C. *J. Soc. Cosmetic Chemists* **1946**, *1*, 311-326.

(53) Davies, J. T.; Haydon, F. *Proc. 2nd Int. Congr. Surface Activity*. Butterworths, London: **1959**.

(54) Correa, N. M.; Durantini, E. N.; Silber, J. J. *J. Org. Chem.* **1999**, *64*, 5757-5763.

(55) Correa, N. M.; Durantini, E. N.; Silber, J. J. *J. Org. Chem.* **2000**, *65*, 6427-6433.

(56) Correa, N. M.; Zorzan, D. H.; Chiarini, M.; Cerichelli, G. *J. Org. Chem.* **2004**, *69*, 8224-8230.

(57) Correa, N. M.; Zorzan, D. H.; D'Anteo, L.; Lasta, E.; Chiarini, M.; Cerichelli, G. *J. Org. Chem.* **2004**, *69*, 8231-8238.

(58) Fernandes, M. L. M.; Krieger, N.; Baron, A. M.; Zamora, P. P.; Ramos, L. P.; Mitchell, D. A. *J. Mol. Catal. B: Enzymatic* **2004**, *30*, 43-49.

(59) Pal, T.; De; Jana, N. R.; Pradhan, N.; Mandal, R.; Pal, A.; Beezer, A. E.; Mitchell, J. C. *Langmuir* **1998**, *14*, 4724-4730.

(60) Sharma, S.; Pal, N.; Chowdhury, P. K.; Sen, S.; Ganguli, A. K. *J. Am. Chem. Soc.* **2012**, *134*, 19677-19684.

(61) Falcone, R. D. o.; Biasutti, M. A.; Correa, N. M.; Silber, J. J.; Lissi, E.; Abuin, E. *Langmuir* **2004**, *20*, 5732-5737.

(62) Martinek, K.; Levashov, A. V.; Klyachko, N.; Khmelnitski, Y. L.; Berezin, I. V. *Eur. J. Biochem.* **1986**, *155*, 453-468.

(63) Gebicka, L.; Jurgas-Grudzinska, M. *Z. Naturforsch. C.* **2004**, 887-891.

(64) Durfor, C. N.; Bolin, R. J.; Sugasawara, R. J.; Massey, R. J.; Jacobs, J.; Schultz, P. G. *J. Am. Chem. Soc.* **1988**, *110*, 8713-8714.

(65) Menger, F. M.; Yamada, K. *J. Am. Chem. Soc.* **1979**, *101*, 6731-6734.

(66) Borsarelli, C. D.; Cosa, J. J.; Previtali, C. M. *Photochem. Photobiol.* **1998**, *68*, 438-446.

(67) Nandi, N.; Bhattacharyya, K.; Bagchi, B. *Chem. Rev.* **2000**, *100*, 2013-2046.

(68) Crans, D. C.; Rithner, C. D.; Baruah, B.; Gourley, B. L.; Levinger, N. E. *J. Am. Chem. Soc.* **2006**, *128*, 4437-4445.

(69) Baruah, B.; Roden, J. M.; Sedgwick, M.; Correa, N. M.; Crans, D. C.; Levinger, N. E. *J. Am. Chem. Soc.* **2006**, *128*, 12758-12765.

(70) Sedgwick, M.; Cole, R. L.; Rithner, C. D.; Crans, D. C.; Levinger, N. E. *J. Am. Chem. Soc.* **2012**, *134*, 11904-11907.

(71) Piletic, I. R.; Moilanen, D. E.; Levinger, N. E.; Fayer, M. D. *J. Am. Chem. Soc.* **2006**, *128*, 10366-10367.

(72) Gao, Y.; Han, S.; Han, B.; Li, G.; Shen, D.; Li, Z.; Du, J.; Hou, W.; Zhang, G. *Langmuir* **2005**, *21*, 5681-5684.

(73) Gao, Y. a.; Li, N.; Zheng, L.; Zhao, X.; Zhang, S.; Han, B.; Hou, W.; Li, G. *Green Chem.* **2006**, *8*, 43-49.

(74) Gao, H.; Li, J.; Han, B.; Chen, W.; Zhang, J.; Zhang, R.; Yan, D. *Phys. Chem. Chem. Phys.* **2004**, *6*, 2914-2916.

(75) Eastoe, J.; Gold, S.; Rogers, S. E.; Paul, A.; Welton, T.; Heenan, R. K.; Grillo, I. *J. Am. Chem. Soc.* **2005**, *127*, 7302-7303.

(76) Gao, Y. a.; Zhang, J.; Xu, H.; Zhao, X.; Zheng, L.; Li, X.; Yu, L. *ChemPhysChem* **2006**, *7*, 1554-1561.

(77) Gao, Y.; Voigt, A.; Hilfert, L.; Sundmacher, K. *ChemPhysChem* **2008**, *9*, 1603-1609.

(78) Li, N.; Zhang, S.; Ma, H.; Zheng, L. *Langmuir* **2010**, *26*, 9315-9320.

(79) Pramanik, R.; Sarkar, S.; Ghatak, C.; Rao, V. G.; Setua, P.; Sarkar, N. *J. Phys. Chem. B* **2010**, *114*, 7579-7586.

(80) Rao, V. G.; Mandal, S.; Ghosh, S.; Banerjee, C.; Sarkar, N. *J. Phys. Chem. B* **2012**, *116*, 8210-8221.

(81) Gao, Y. a.; Li, N.; Zheng, L.; Zhao, X.; Zhang, J.; Cao, Q.; Zhao, M.; Li, Z.; Zhang, G. *Chem. – A Eur. J.* **2007**, *13*, 2661-2670.

(82) Gao, Y. a.; Li, N.; Zheng, L.; Bai, X.; Yu, L.; Zhao, X.; Zhang, J.; Zhao, M.; Li, Z. *J. Phys. Chem. B* **2007**, *111*, 2506-2513.

(83) Gao, Y.; Hilfert, L.; Voigt, A.; Sundmacher, K. *J. Phys. Chem. B* **2008**, *112*, 3711-3719.

(84) Pramanik, R.; Sarkar, S.; Ghatak, C.; Setua, P.; Rao, V. G.; Sarkar, N. *Chem. Phys. Lett.* **2010**, *490*, 154-158.

(85) Seth, D.; Chakraborty, A.; Setua, P.; Sarkar, N. *Langmuir* **2006**, *22*, 7768-7775.

(86) Seth, D.; Chakraborty, A.; Setua, P.; Sarkar, N. *J. Chem. Phys.* **2007**, *126*, 224512-224524.

(87) Moniruzzaman, M.; Kamiya, N.; Nakashima, K.; Goto, M. *ChemPhysChem* **2008**, *9*, 689-692.

(88) Moniruzzaman, M.; Kamiya, N.; Nakashima, K.; Goto, M. *Green Chem.* **2008**, *10*, 497-500.

(89) Moniruzzaman, M.; Kamiya, N.; Goto, M. *Langmuir* **2008**, *25*, 977-982.

(90) Li, X.-W.; Zhang, J.; Zheng, L.-Q.; Chen, B.; Wu, L.-Z.; Lv, F.-F.; Dong, B.; Tung, C.-H. *Langmuir* **2009**, *25*, 5484-5490.

(91) Debnath, S.; Das, D.; Dutta, S.; Das, P. K. *Langmuir* **2010**, *26*, 4080-4086.

(92) Jiang, W.; Wang, Y.; Voth, G. A. *J. Phys. Chem. B* **2007**, *111*, 4812-4818.

(93) Hofmeister, F. *Arch Exp Pathol Pharmakol* **1888**, *24*, 247-260.

(94) Lo Nostro, P.; Ninham, B. W. *Chem. Rev.* **2012**, *112*, 2286-2322.

(95) Kumar, A. *Chem. Rev.* **2001**, *101*, 1-20.

(96) Jenkins, H. D. B.; Marcus, Y. *Chem. Rev.* **1995**, *95*, 2695-2724.

(97) Breslow, R.; Guo, T. *Proc. Natl. Acad. Sci.* **1990**, *87*, 167-169.

(98) Freire, M. G.; Carvalho, P. J.; Silva, A. M. S.; Santos, L. M.; Rebelo, L. P. N.; Marrucho, I. M.; Coutinho, J. o. A. P. *J. Phys. Chem. B* **2008**, *113*, 202-211.

(99) Freire, M. G.; Neves, C. M. S. S.; Silva, A. M. S.; Santos, L. s. M.; Marrucho, I. M.; Rebelo, L. P. N.; Shah, J. K.; Maginn, E. J.; Coutinho, J. A. P. *J. Phys. Chem. B* **2010**, *114*, 2004-2014.

CHAPTER 2

Aims and Objectives

This Chapter presents a brief outlines of the aims and objectives of the research work carried out during the PhD programme. Our prime objective is to understand the microscopic transport processes such as translational and rotational diffusion, microviscosity, and viscosity in the ionic liquid (IL) mixtures. The aim of the research work carried out in the present thesis is three fold; however, our objectives are interconnected with each other. Our first aim is to understand the diffusional motion in the aqueous Li^+ containing mixtures of ILs as these mixtures are of wider applications in different energy devices, as a solvent medium for different organic and enzymatic reactions. Secondly, these microscopic transport processes are studied in the model biological confined water by taking microemulsion as an example. Our third aim is to study the effects of different denaturating agents on the hydrophobic alkyl group substitution in ILs.

In view of the aforementioned aims and to give broad overview of our research work, different objectives are presented below as:

- The first objective of our research work is to understand the diffusional behavior of ^1H NMR active nuclei in the aqueous Li^+ containing mixtures of ILs. Translational and rotational motions of molecules present inside the mixtures give more insight into the transport phenomenon. As these Li^+ containing mixtures are applied in different energy devices, therefore understanding of the diffusional behavior and their translational and rotational motions helps the researchers in selecting a better Li^+ containing IL mixtures. The understanding of other physical phenomenon like activation energy of diffusional motion, translational and rotational motions add more insight into the existing knowledge in the field of Li^+ containing mixtures of ILs.

- In addition to this, the validity of Stokes-Einstein equation has been discussed in order to understand the microviscosity phenomenon. The concept of hole formation and the average jump distance of ^1H NMR active nuclei significantly improve the understanding of these Li^+ containing mixtures of ILs.

- The second objective of our research work is to understand the behavior of biological water present in a confined state inside the microemulsion system. For this purpose we have selected the water in hydrophobic IL confined media as an example. As these confined media are used as a medium for the preparation of nanomaterials and as a solvent media for different enzymatic reactions, therefore understanding of its physicochemical properties helps the researcher working in these area. Understanding of microviscosity, micropolarity, pH and the state of water present inside the aqueous IL microemulsion system has been studied.

- The third objective is to understand the effect of various denaturants on the hydrophobic alkyl group substitution on the cationic part of imidazolium-based ILs. As these denaturants are hydrophobic bond breaker and also known as water structure breakers, their effects must therefore, be reflected in the aqueous solutions of ILs with hydrophobic alkyl group substitution. By considering this assumption we have studied the effect of different denaturants on the behavior of ILs in their aqueous solutions and showed that the denaturants have substantial effects on the IL solutions containing higher alkyl group.

CHAPTER 3

Instrumentation Techniques

In the present chapter are discussed the working principles of different experimental techniques used in order to obtain the experimental data for the successful completion of the research work. The principles of NMR spectroscopy, NMR relaxations and diffusion order NMR spectroscopy have been discussed. In addition to this, the basic principles of UV-vis spectrophotometer, dynamic light scattering, viscometer and cyclic voltammetric technique have been described.

3.1. INTRODUCTION

This chapter deals with the discussion regarding the basic principles of the experimental techniques used in successful completion of all the experimental work. Diffusion order NMR spectroscopy has been used to measure the self-diffusion coefficients of the ^{1}H NMR active nuclei in the aqueous Li^{+} containing mixtures of ionic liquids (ILs). The spin-lattice relaxation time (T_1) and spin-spin relaxation time (T_2) data has been obtained from the inversion recovery method and Carr-Purcell-Meiboom-Gill (CPMG) method, respectively. Viscosity of the system has been measured by the help of viscometer. In order to obtain the particle size of the microemulsion droplets, dynamic light scattering (DLS) has been used. The electrochemical behavior of the electro-active probe inside the microemulsion system has been analyzed through the help of cyclic voltammetric technique. UV-vis spectrophotometer is used to study the micropolarity by the absorption of methyl orange.

3.2. NMR Spectroscopy

It is the interaction of electromagnetic radiation in the radio-wave regions with the matter. This spectroscopy mainly deals with the nuclear transition in the radio frequency regions and a schematic representation of NMR spectrometer is given in Figure 1.[1]

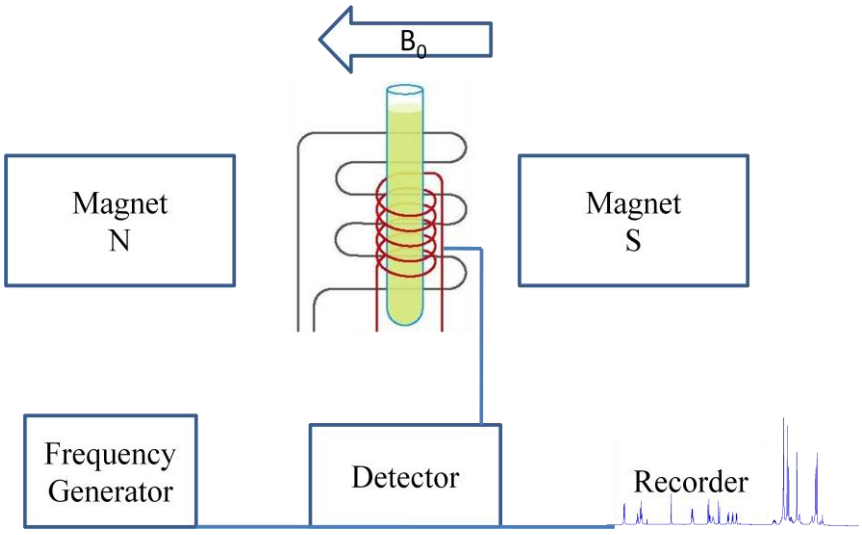

Figure 1. Schematic representation of the NMR spectrometer.[1]

The material must contain a NMR active nucleus in order to get a signal in the NMR spectrometer.

A nucleus is NMR active, if its total spins quantum number (I) has an integral or half-integral value. It means nuclei with spin quantum number value of $I \neq 0$ can only absorb/emit electromagnetic radiations in the radio frequency regions. Hydrogen atom has the I value of 1/2 and the NMR spectroscopy deals with it is popularly known as the ^{1}H NMR spectroscopy. It means the magnitude of their magnetic moments ($\mu = \gamma I\, h/2\pi$, where γ is the gyromagnetic radius of the nuclei) has only two possibility that is +1/2 (α spin state) and -1/2 (β spin state) which are same in magnitude but opposite in their directions in presence of external magnetic field B_0 as represented in Figure 2.[2]

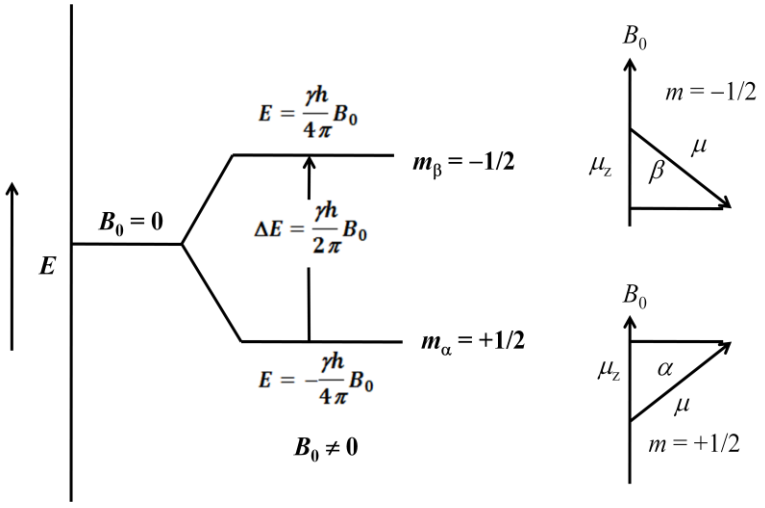

Figure 2. Splitting of a nuclear spin with a spin 1/2 in a magnetic field of B_0.[2]

In the presence of an external magnetic field of B_0 the nuclear spin is split into two energy levels as represented in the Figure 2. The lower energy with α spin state where the nucleus is spinning in the direction of external magnetic field and the higher energy β spin state where the nucleus is spinning in an opposite direction to that of the applied field as shown in the right side of the Figure 2. To observe a signal in the NMR spectrum, we have to provide energy that is equal to the difference between the energy of the two nuclear spin states. It can be achieved either by varying the radiofrequency ($\nu = \Delta E/h$) or by varying the external magnetic field. Generally, in modern NMR spectrometer the

spectra are recorded by varying the external magnetic field, keeping the frequency of the electromagnetic radiation constant. Once the magnitude of the external magnetic field is matched with the energy difference between the two spinning state, resonance occurs giving a signal in the detector. For multinuclear system where each nucleus has different precessional frequency, then in that condition Fourier transformation of the signal is necessary to convert the frequency domain signal into the time domain. However, as the NMR spectra is in the PPM scale therefore, the time domain signal is again converted into the frequency domain by the inverse Fourier equation and the chemical shift is calculated from the observed resonating frequency as represented in equation 1.[3,4]

$$\delta = \frac{\nu_0(\mathrm{H}) - \nu_0(\text{reference})}{\text{Spectrometer frequency in MHz}} \qquad (1)$$

where, ν_0 (H) and ν_0 (TMS) are the resonating frequency of the observed proton and the reference compound, respectively.

3.2.1. NMR Relaxation

It is the phenomenon in which the magnetically excited nuclei return to the equilibrium. In the equilibrium state (a) the population of the magnetic nuclei in both the sates (α and β) are in accordance with the Boltzmann distribution and (b) there is zero transverse magnetization.

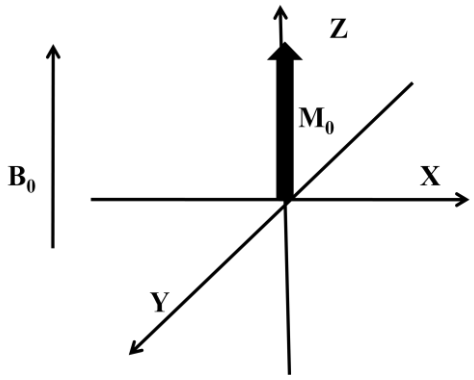

Figure 3. The net bulk magnetization M_0 along the *z*-axis in presence of applied magnetic field B_0.[5]

Let us assume that a system consist of many smaller nuclear magnets and has a net bulk magnetic moment of *M*. In the presence of an external magnetic field B_0, applied in the *z*-direction, the net magnetic moment has only *z*-component with a magnetic moment of M_z (M_0) whereas the transverse *xy*-component has zero magnetization ($M_{xy} = 0$) and is the condition of equilibrium as represented in the Figure 3.[5] This equilibrium is perturbed by the presence of radio frequency pulse and the time it takes to again coming back into the equilibrium condition is known as the relaxation time.

Two types of relaxation phenomenon are observed in NMR spectroscopy. The first one is the relaxation of the transverse magnetization (M_{xy}) and is known as the transverse relaxation or spin-spin relaxation and the time required for it is known as the transverse relaxation time, T_2.[6] The second one is the relaxation of the *z*-component of the magnetization (M_z) and is known as the longitudinal relaxation or spin-lattice relaxation and the time it takes to coming back to the equilibrium condition is known as the longitudinal relaxation time, T_1.[5] Though there are several methods are available for the determination of relaxation phenomenon, we have applied the inverse recovery method[5] for the determination of T_1 relaxation time and Car-Purcell-Meiboom-Gill (CPMG) method for the measurement of T_2 relaxation time.[6]

3.2.1.1. Longitudinal Relaxation Time (T_1)

The longitudinal relaxation is the relaxation of the z-component of the magnetization into the equilibrium and the time required for it is known as the longitudinal relaxation time or spin-lattice relaxation time T_1. We have used the inversion recovery method to measure the T_1 relaxation time of the ^{1}H NMR active nuclei present in our samples and the pulse sequence for the method is represented in the Figure 4.[5] Initially a recycle delay time (t_{1d}) has to be given to the sample which is sufficiently long enough to attain a net z-magnetization followed by an 180^0 pulse (p1) to invert the magnetization into the $-z$ direction. Then a recovery delay time (vd) has been given in order to relax the magnetization. Finally a 90^0 pulse is given to convert the *z*-magnetization vector into the *xy*-magnetic coordinate and is detected in the acquisition period. Therefore, the pulse sequence of the inversion recovery experiment can be represented as

t_{rd}–180^0–vd–90^0–acq. If the recovery delay time (vd) is very short then the pulse sequence is equivalent to t_{rd}–270^0–vd–acq which gives the signals of negative intensity.

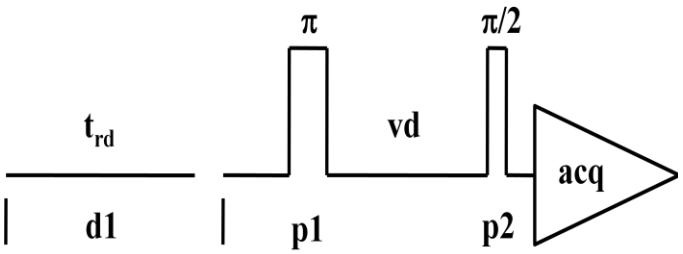

Figure 4. The pulse sequence for the measurement of T_1 relaxation time of ^{1}H NMR active nuclei through the inversion recovery method.[5]

However, the signal has positive intensity if the delay time applied is very long and in that case the pulse sequence is equivalent to t_{rd}–180^0–vd–90^0–acq. The spin-lattice relaxation time (T_1) can be obtained by collecting the data of varying delay time (vd). Finally the plot of the peak intensity with respect to the recovery delay time gives the curve of an exponential nature with rate $1/T_1$ as given in equation 2 as:

$$M_z(t) \propto I(t) = I_0(1-2e^{-t/T_1}) \qquad (2)$$

where, I_0 and I(t) are the equilibrium peak intensity and intensity at time t, respectively.[5] M_z(t) is the z-magnetization vector at time t. t and T_1 are the delay time and spin-lattice relaxation time relaxation time, respectively.

3.2.1.2. Transverse Relaxation Time (T_2)

The spin-spin relaxation time (T_2) is the time required for the decaying of the transverse magnetization vector and is also known as the transverse relaxation time. It can be measured through the Car-Purcell-Meiboom-Gill (CPMG) method and the pulse sequence for it is represented in the Figure 5.[6] Both the T_1 and T_2 relaxation occurs simultaneously for a ^{1}H NMR active proton, however, the pulse sequence used for their determinations are completely different as represented in the Figure 4 and 5 for the T_1 and T_2 relaxation time, respectively. In non-viscous fluids both the relaxation times are

nearly equal to each other, however the $T_2 << T_1$ in case of viscous and solid materials due to the presence of strong local magnetic field inhomogeneity.

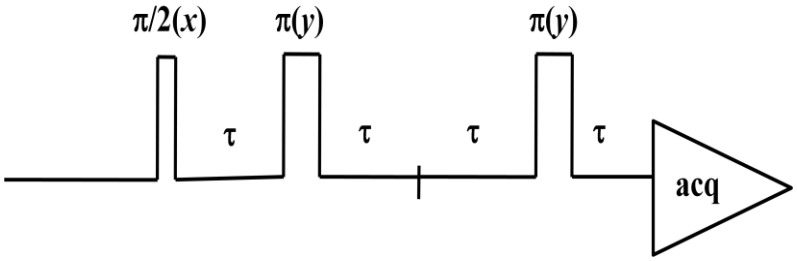

Figure 5. The pulse sequence used for the measurement of T_2 relaxation time through the CPMG method.[6]

Therefore, a spin-echo pulse sequence is used as represented in the Figure 5 in order to eliminate the magnetic field inhomogeneity for the determination of true relaxation time. And, the equation 3 is used for the determination of T_2 relaxation time which is given by:

$$M_y \propto I_t = I_0 e^{-\tau/T_2} \tag{3}$$

where, the symbols have their usual meanings.[6] The T_2 relaxation time can be found out from the exponential plot of the I_t versus τ. This transverse relaxation time is also related with the line width of the NMR signal according to the equation 4 as:

$$T_2 \sim \frac{1}{\Delta \nu_{1/2}} \tag{4}$$

in which $\Delta \nu_{1/2}$ is the line width at half height.

3.2.2. Diffusion Order NMR Spectroscopy (DOSY)

Diffusion order NMR spectroscopy is used to measure the self-diffusion coefficient of the NMR active nuclei present in the sample.[7-9] Here in case of DOSY experiment, pulse field gradient (PFG) is produced by putting a small three dimensional coil around the NMR probe to generate the PFG in addition to the large super conducting magnet (SCM) to produce the static magnetic field. In the case of anisotropic condition it is possible to measure the self-diffusion coefficients along the *x*, *y*, and *z*-directions. We have applied the modified spin echo pulse sequence in order to measure the self-diffusion coefficient

of the molecule and its pulse sequence is given in the Figure 6. The Stejskal-Tanner equation given in equation 5 is used in order to get the self-diffusion coefficient of molecule.[10]

$$E = \exp(-\gamma^2 \delta^2 g^2 D(\Delta - \frac{\delta}{3})) \quad (5)$$

where, γ is the gyromagnetic ratio of the ^{1}H nucleus, δ and g are the signal width and strength, respectively. Δ, is the time interval between the two applied pulse.

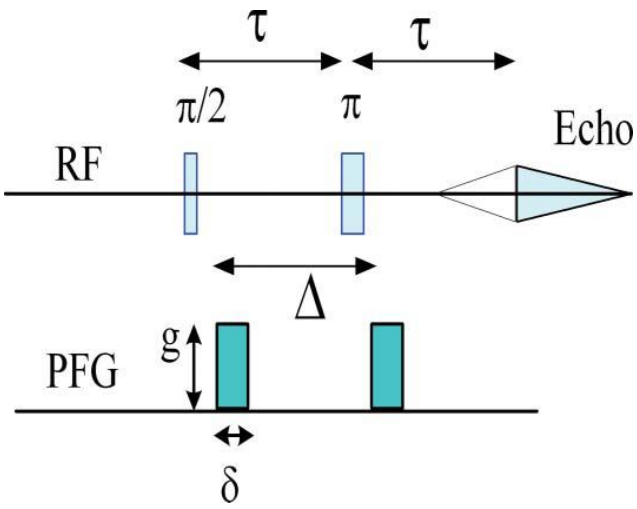

Figure 6. The modified Hahn echo pulse sequence for the measurement of self-diffusion coefficient of ^{1}H NMR active nuclei.[11]

3.3. UV-vis Spectroscopy

This spectroscopy is deals with the electronic transition between the highest occupied molecular orbital (HOMO) of a molecule or compound into the lowest unoccupied molecular orbital (LUMO) and can be observed in between the 200-800 nm range in the electromagnetic spectrum.[12] As it absorbs the UV-vis light to excite the electron therefore, this branch of spectroscopy is also known as the absorption spectroscopy or electronic spectroscopy. A molecule is said to be active in the UV-vis region, if it contains a pair of non-bonding electrons or have an unsaturated group. There are six possibilities of transitions in the UV-vis spectroscopy and are describe below.[13]

a) $n \rightarrow \pi^*$: Electronic transition from the non-bonding orbital to the anti-bonding π orbital.

b) $\pi \rightarrow \pi^*$: Electronic transition from the bonding π orbital to the anti-bonding π^* orbital.

c) $n \rightarrow \sigma^*$: Electronic transition from the non-bonding orbital to the anti-bonding σ^* orbital.

d) $\pi \rightarrow \sigma^*$: Transition from the bonding π orbital to the anti-bonding σ^* orbital.

e) $\sigma \rightarrow \pi^*$: Transition from the bonding σ orbital to the anti-bonding π^* orbital.

f) $\sigma \rightarrow \sigma^*$: Transition from the bonding σ orbital to the anti-bonding σ^* orbital.

From the above six types of electronic transitions only the first two that are the $n \rightarrow \pi^*$ and $\pi \rightarrow \pi^*$ transitions can be seen in the UV-vis region. When a sample having an UV-vis active compound is placed in the spectrophotometer, then it absorbs the light in the UV-vis region and the spectrometer records the wavelength at which absorption of the sample occurs. And, the UV-vis spectrum is a plot of this absorbance with the wavelength.

3.4. Viscometer

The viscosity of the samples is measured with the help of a Brookfield cone-plate viscometer.[14-16] Basically it is a torque measuring system. It consist of a beryllium-copper spring connecting to the rotating cone which senses the frictional force experienced by the rotating cone inside the stationary plate containing the fluid. This frictional force or resistance experienced by the rotating cone produces torque inside the system which is proportional to the shear stress experienced by the fluid. The viscometer displays this torque and shear stress produced experienced by the fluid which is converted into the absolute centipoises (mPa.s) unit from the known geometric constants of the viscometer.

3.5. Dynamic Light Scattering (DLS)

The dynamic light scattering gives us the information regarding the hydrodynamic radii of the diffusing particle by measuring its Brownian motion.[17-19] It is also known as the quasi-elastic light scattering or photon correlation spectroscopy and measures the size

of particles in the sub-micron regions. The Brownian motion is the random motion of the particles by the collision with the solvent molecules suspended in a solution. The translational diffusion coefficient (D) of the particles gives the information regarding the velocity of the Brownian motion which helps in estimating the size of the particle from the Stokes-Einstein equation as $D = kT/c\pi\eta a$, in which a is the hydrodynamic radii of the particle, D and η are the translational diffusion coefficient and viscosity of the medium; k is the Boltzmann constant and T is the absolute temperature of the medium, respectively.[19]

The dynamic light scattering measures the velocity of the diffusing particle by measuring the rate of the intensity of the scattered light by an optical arrangement. The rate of fluctuation in the intensity with respect to time is more for smaller particle as compared to the larger particle and therefore, smaller particle diffuse faster as compared to larger particle. The DLS instrument convert this scattering intensity into the correlation function $G(\tau)$ in which the τ is the correlator time delay. For a large monodispersed particle this correlation function follows a single exponential form as given in equation 6.[18]

$$G(\tau) = A + (1 + Be^{-2\Gamma\tau}) \qquad (6)$$

Here, A and B are the baseline and intercept of the correlation function, $\Gamma = Dq^2$ in which $q = (4\pi n/\lambda_0)\sin(\theta/2)$, where, n is the refractive index of the medium, λ_0 is the wavelength of the laser light used and θ is the scattering angle.

A typical plot of the correlation coefficient as a function of time obtained from our experimental results is given in the Figure 7 for 70 wt% of H_2O.

3.6. Cyclic Voltammetry (CV)

This technique gives us information regarding the qualitative and quantitative information of an electrochemically active species present in an electrolytic solution.[20,21] We have used a three electrode system with glassy carbon as the working electrode and platinum as both the reference and counter electrode, respectively. The current produced is measured between the counter and the working electrode and the reference Pt electrode

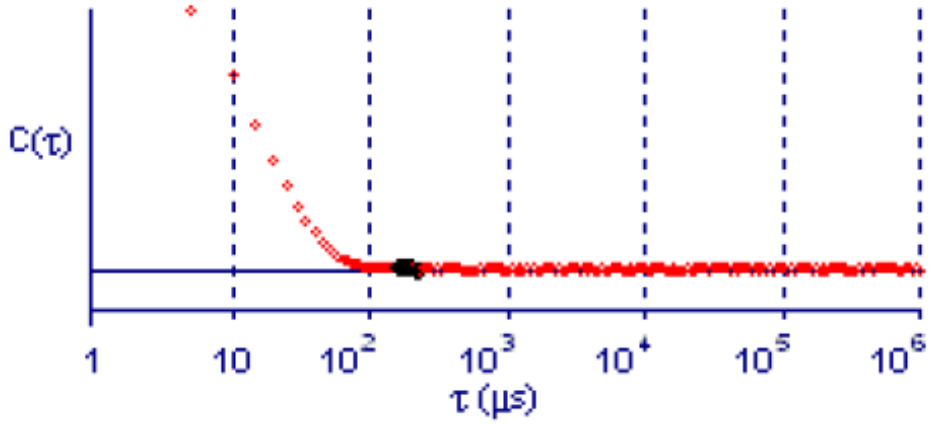

Figure 7. The plot of the correlation coefficient (C(τ)) as a function of time (τ) for 70 wt% of H_2O in H_2O/[BBIM][NTf_2]/TX-100 microemulsion system.

maintain the potential constant between the working electrode and itself. The potential of the working electrode has to be scanned from an initial value to a limiting value and a voltammogram is obtained by plotting the current produced in the working electrode during the total potential scan. A typical voltammogram from our experimental data for 70 wt% of water inside the H_2O/[BBIM][NTf_2]/TX-100 microemulsion system is presented in the Figure 8.

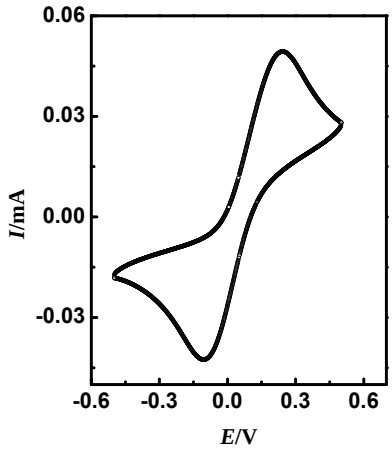

Figure 8. A typical voltammogram of the Fe^{+2}/Fe^{+3} redox system present inside the 70 wt% H_2O of H_2O in [BBIM][NTf_2] microemulsion system.

3.7. References

(1) Eisner, L. *J. Chem. Educ.* **1964**, *41*, A607-A624

(2) Roberts, J. D. *J. Chem. Educ.* **1961**, *38*, 581-584.

(3) Jackman, L. M.; Sternhell, S. *Application of Nuclear Magnetic Resonance Spectroscopy in Organic Chemistry: International Series in Organic Chemistry*; Elsevier, **2013**.

(4) Gunther, H. *NMR Spectroscopy: Basic Principles, Concepts and Applications in Chemistry*; John Wiley & Sons, **2013**.

(5) Wink, D. J. *J. Chem. Educ.* **1989**, *66*, 810-813.

(6) Carr, H. Y.; Purcell, E. M. *Phys. Rev.* **1954**, *94*, 630-638.

(7) Harmon, J.; Coffman, C.; Villarrial, S.; Chabolla, S.; Heisel, K. A.; Krishnan, V. V. *J. Chem. Educ.* **2012**, *89*, 780-783.

(8) Pelta, M. D.; Morris, G. A.; Stchedroff, M. J.; Hammond, S. J. *Magn. Reson. Chem.* **2002**, *40*, S147-S152.

(9) Atkins, P.; De Paula, J.; Friedman, R. *Quanta, Matter, and Change: A Molecular Approach to Physical Chemistry*; Oxford University Press, **2009**.

(10) Stejskal, E. O.; Tanner, J. E. *J. Chem. Phys.* **1965**, *42*, 288-292.

(11) Hayamizu, K.; Tsuzuki, S.; Seki, S.; Umebayashi, Y. *J. Chem. Phys.* **2011**, *135*, 084505.

(12) MacAdam, D. L. *Color Measurement, Theme and Variations*; Springer-Verlag, **1981**; Vol. *27*.

(13) Perkampus, H.-H.; Grinter, H.-C.; Threlfall, T. L. *UV-Vis Spectroscopy and its Applications*; Springer, **1992**.

(14) McKennell, R. *Anal. Chem.* **1956**, *28*, 1710-1714.

(15) Nanda, R.; Kumar, A. *Ind. J. Chem.* **2013**, *52*, 1377-1382.

(16) Nanda, R.; Kumar, A. *J. Phys. Chem. B* **2015,** *119*, 1641-1653.

(17) Pecora, R. *Dynamic Light Scattering: Applications of Photon Correlation Spectroscopy*; Springer Science & Business Media, **1985**.

(18) Brown, W. *Light Scattering: Principles and Development*; Clarendon Press Oxford, **1996**.

(19) Berne, B. J.; Pecora, R. *Dynamic Light Scattering: with Applications to Chemistry, Biology, and Physics*; Courier Corporation, **2000**.

(20) Van Benschoten, J. J.; Lewis, J. Y.; Heineman, W. R.; Roston, D. A.; Kissinger, P. T. *J. Chem. Educ.* **1983**, *60*, 772-776.

(21) Compton, R. G.; Banks, C. E. *Understanding Voltammetry*; World Scientific, **2007**.

CHAPTER 4

^{1}H NMR, Self-diffusion Coefficients, Translational and Rotational Motions of Ionic Liquids and Water Molecules in the Aqueous Li^{+} Containing Mixtures of Ionic Liquids

Diffusion-order NMR spectroscopy (DOSY-NMR) has been used to study the temperature dependent self-diffusion coefficients of ionic liquids and water molecules in the aqueous Li^+ mixtures of ionic liquids. The self-diffusion coefficients of individual protons of ionic liquid molecules has been measured and discussed. Temperature and compositions dependent ^1H NMR spectra of proton signals shows interesting behavior. Translational and rotational motions of ionic liquids and water molecules obtained from their correlation time values has been calculated and discussed. The activation energy of viscous and diffusive flow, activation energy of translational and rotational motions is discussed. The validity of Stokes-Einstein equation and the concept of hole formation are analyzed for the diffusional motion of both the ionic liquids and water molecules. Finally, qualitative information regarding the microviscosity is obtained from the frictional coefficient, f factor calculated from the Stokes-Einstein equation.

4.1. INTRODUCTION

Recently, imidazolium-based ILs has been studied extensively because of their spatial heterogeneity as these ILs possesses both the non-polar alkyl chain length and polar imidazolium ring.[1-16] Molecular dynamics simulation studies of pure 1-alkyl-3-methylimidazolium-based ILs shows the presence of nanostructural organization of ILs in the system.[1,3] Strong electrostatic interactions between the polar imidazolium ring with the anions forms the polar domains and short-range Van der Waals interactions between the non-polar alkyl groups forms the non-polar domains in the pure 1-alkyl -3-methyl imidazolium-based ILs and also in their aqueous solutions. In addition to this, in the case of IL/vacuum interface, the non-polar alkyl groups point towards the vacuum with polar groups attracted more towards the bulk phase.[7,17-22]

It has been reported that these ILs are hygroscopic in nature and absorb significant amount of water from the environment and therefore, the original ionic networks present in the ILs are broken by the interactions of ILs with the water molecules.[6,23-25] In dilute aqueous solutions, the imidazolium based ILs with alkyl chain length > 4 shows significant aggregation behavior and are therefore considered to be surfactant like in nature.[10] Because of the presence of the nanostructural organization of polar/non-polar part of imidazolium-based ILs in their aqueous solutions, it has a potential application in the field of catalysis and synthetic chemistry[7] and therefore, attracts many researchers to understand the behavior of ILs in water.[11,12,16]

The addition of salts into the aqueous solutions of ILs have interesting effect as it can lead to the precipitation of proteins and different organic compounds in its aqueous solutions.[26-29] Depending upon the precipitation of organic compounds and proteins in their aqueous salt solutions, two types of salt are defined, salting-out salts increase the precipitation of proteins and hydrophobic compounds and are also known as kosmotropic salts. The other type increases the solubility of proteins and hydrophobic compounds in their aqueous salt solutions and is known as salting-in or chaotropic salts. The salting-out salts are also known as water structure-makers whereas the salting-in salts are known as water structure-breaker.[29,30] To make the potential use of these aqueous salt solutions of

ILs in different industrial and biomedical applications, it is important to understand the behavior of ILs and water molecules in presence of different salts. A very few reports are available in the literature regarding the effects of salts on the aqueous solutions of ILs. Recently Freire et al. reported the presence of unexpected interactions between the polarizable salting-in salts with the hydrophobic alkyl chain length of ILs through the ^{1}H NMR study.[31] However, to the best of our knowledge there has not been a single report is available in the literature regarding the dynamical behavior of ILs and water molecules in the aqueous salt solutions of ILs. Therefore, in this Chapter we have focused on the dynamics of the aqueous salt solutions of ILs.

In the current chapter two alkylimidazolium bromide-based ILs with the variation in their alkyl chain length have been selected and the name of the ILs are 1-Butyl-3-methylimidazolium bromide ([BMIM]Br) and 1-Octyl-3-methylimidazolium bromide ([OMIM]Br). The purpose of choosing these ILs is due to their formation of nanostructure or micellization behavior in their aqueous solutions because of possessing the hydrophobic alkyl groups in the IL cation. Two salts have been selected that are LiCl and $LiClO_4$ with their opposite effects on the hydrophobic interactions and miceller behavior.

This chapter is divided into two sections. The first section deals with the temperature dependent self-diffusion coefficients and viscosity study of aqueous salt solutions of IL mixtures. The individual self-diffusion coefficients of each of the protons present on the cation of IL are also discussed. Activation energy of diffusive flow (E_D) and viscous flow (E_η) has been calculated and discussed. Translational (τ_t) and rotational motion (τ_2) of ILs and water molecules are calculated from the experimentally measured self-diffusion coefficients and viscosity of the mixtures and discussed. Finally, the average one jump distance (<*R*>) for both the IL and water molecules are estimated and analyzed.

In the second section of the chapter the validity of Stokes-Einstein equation has been discussed. For the diffusion of individual particle inside the IL mixtures the fluid must contains hole inside it and therefore, the formation of hole and its sizes were calculated

and has been analyzed. In the final section of the chapter the frictional coefficients experienced by the individual diffusing particles inside the fluid mixtures has been discussed and correlated with the microviscosity phenomenon.

4.2. EXPERIMENTAL PROCEDURE

4.2.1. Materials

1-Methylimidazole (purity, > 99%), 1-Bromobutane (purity, > 98%) and 1-Bromooctane (purity, > 99%) were obtained from Sigma Aldrich and used after distillation. Both the LiCl (purity, > 99%) and $LiClO_4$ (purity, > 99.99%) were obtained from Fluka Analytical. Before its use for the experimental purpose, these salts were dried overnight at 140 ^{0}C to remove any absorbed moisture. Deuterium oxide, D_2O used for the internal standard in the NMR experiments was obtained from the Sigma Aldrich with 99.9 atom % D.

4.2.2. Synthesis of Ionic Liquids

Both the ILs that are the 1-Butyl-3-methylimidazolium bromide ([BMIM]Br) and 1-Octyl-3-methylimidazolium bromide ([OMIM]Br) were synthesized according to the reported procedure and their structures and numbering scheme of protons are given in Figure 1.[32-36]

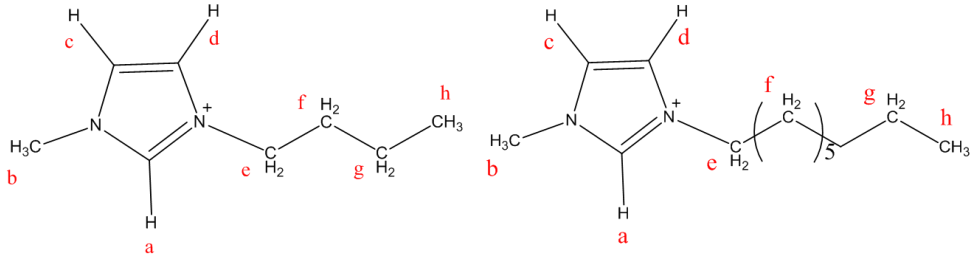

Figure 1. Structure and numbering scheme of protons of $[BMIM]^+$ (left) and $[OMIM]^+$ (right) for the [BMIM]Br and [OMIM]Br, respectively.

After the synthesis of ILs, it were dried under high vacuum for 10-12 h with a constant heating of 60 ^{0}C. The Karl-Fischer titrator was used to check the amount of absorbed water from the atmosphere and was found to be > 150 ppm in each of the ILs. The ^{1}H NMR spectra of these ILs are in good agreement with that reported in the literature.[34-36]

The aqueous salt solutions were prepared in deionized water (specific conductance < 0.55 $\times 10^{-6}$ S cm^{-1}) on the basis of molality with an accuracy of ± 0.0002 mol kg^{-1} and all the ternary mixtures were prepared by adding the ILs (*w/w*) into the aqueous salt solutions (*w/w*).

4.2.3. NMR Measurements

All the PGSE-NMR experiments were performed on a Bruker-400 spectrometer with a 9.4 T superconducting magnet (Larmor frequencies ν_0 = 400 MHz).[37] Neat samples were used in this study and were placed in a 5 mm (outside diameter) NMR tube and D_2O in a capillary tube was used as external lock. All the measurements were carried out at four different temperatures ranging from 300-315 K with an increment of 5±0.1 K. The temperature of the experiment was controlled by a Bruker BVT-3200 temperature controller unit. The samples were thermally equilibrated for 15 min before the start of each experiment. Self-diffusion coefficient of ionic liquid cations and H_2O molecules were measured for each of the studied composition of ILs and salts by using a standard Bruker pulse field gradient spin echo (PFGSE) experiment with longitudinal eddy current delay.[38] The spectral data were acquired with 70 ms diffusion delay (Δ) and 3.5 ms bipolar gradient pulse (δ) by varying the gradient strength (g). The diffusion coefficients were calculated from the experimental data using an online Bruker T_1/T_2 utility program by fitting the signal intensity (area) to the following equation.[39]

$$I = I_0 \exp [- \gamma^2 g^2 \delta^2 D (\Delta - \delta/3)] \qquad (1)$$

where I and I_0 are the echo intensities measured with and without the field gradient g, respectively. δ is the duration of the magnetic field gradient g, γ is the gyromagnetic ratio of the nuclei, Δ is the diffusion time that is the interval between the two gradient pulses and D is the self-diffusion coefficient.

4.2.4. Viscosity Measurements

Brookfield-ultra rheometer with a cone plate arrangement was used for the measurement of viscosity of IL solutions. The sample required for each measurements are 0.5 ml. All

the experiments were carried out with a temperature range from 300-315 K within an interval of 5±0.1 K. The temperature of the experimental set up was monitored by using a julabo temperature thermostat bath. The viscosity (η) values of the solutions were obtained through the equation as:

$$\eta = (100/RPM)\ (TK)\ (\text{Torque})\ (SMC) \qquad (2)$$

where *RPM*, *TK* (0.09373) and *SMC* (0.327) are the speed, viscometer torque constant and spindle multiplier constant, respectively. The calibration of the instrument was performed by taking the reported viscosity data of aqueous solutions of $CaCl_2$, $MgCl_2$ and [BMIM][BF_4] in different concentration.[40,41] The accuracy of the instrument was obtained as ±1%. The reported experimental viscosity data are the average of triplicate measurements with a precision of 0.25%.

4.3. Self-Diffusion Coefficients, Translational and Rotational Motion of Ionic Liquids and Water Molecules: A Temperature Dependent Study

4.3.1. RESULTS AND DISCUSSION

4.3.1.1 Diffusional Behavior of $[IL]^+$ and H_2O Molecules

This section primarily deals with the temperature dependent self-diffusion coefficients, translational and rotational motion of the individual ^1H NMR active particles present inside the aqueous salt solutions of ILs. The study has been carried out in the temperature range of 300-315 K with an increment of 5±0.1 K. In this study we have come across an unusual diffusion behavior of $[OMIM]^+$ and H_2O molecules in the aqueous $LiClO_4$ solutions of [OMIM]Br. Figure 2(a) and (b) represent the variation of temperature dependent self-diffusion coefficients of $[OMIM]^+$ and H_2O molecules with the increase in the compositions of $LiClO_4$. It can be seen from Figure 2 that the diffusion coefficients of H_2O molecules are much higher as compared to that of $[OMIM]^+$. The relative diffusion coefficients (D_{H2O} / $D_{[OMIM]+}$) of diffusing particles with the increase in the composition of $LiClO_4$ are also represented in Table 1. An increase in the temperature increases the diffusion coefficients of each of the diffusing particles present in the

mixtures. However, the relative values decrease with the increase in the temperature. It indicates that the magnitude of diffusion coefficients of $[OMIM]^+$ is approaching towards the H_2O molecules with the increase in the temperature of the mixtures.

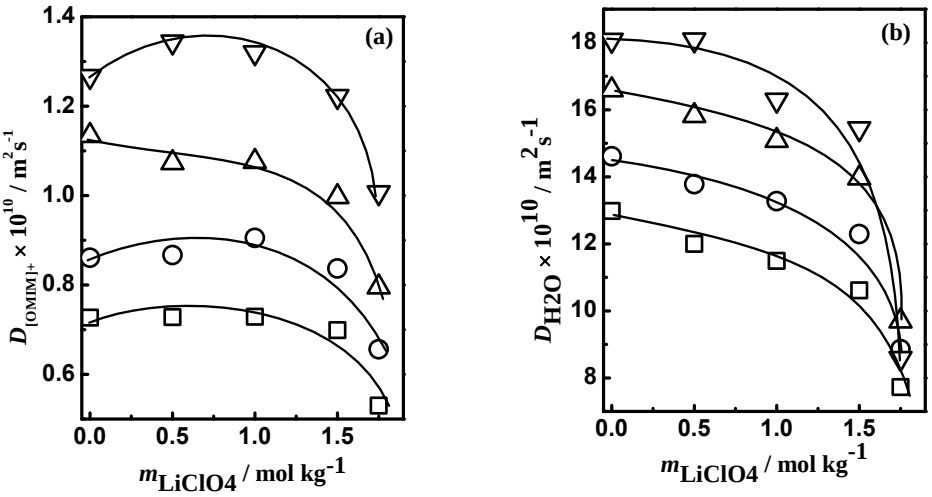

Figure 2. The variation of NMR self-diffusion coefficients with the m_{LiClO4} for $[OMIM]^+$ (a) and H_2O (b) molecules at 300 K (□), 305 K (○), 310 K (△) and 315 K (▽), respectively. The composition of [OMIM]Br in all the cases is fixed as 50% (*w/w*).

In Figure 2(b), it has been shown that the diffusion coefficient of the H_2O molecules decreases with the increase in the compositions of $LiClO_4$. This might be due to the high charge density of Li^+ ion which orients the water molecules strongly around itself through the electrostatic interactions, resulting into the decrease in the diffusive motion of the water molecules. However, the diffusion coefficients of $[OMIM]^+$ shows a maximum value with the increase in the composition of $LiClO_4$ as cleared from the values given in the Table 1. It was reported that the $[OMIM]^+$ cation-based ILs forms 3-D nanostructural aggregates in their aqueous solutions.[7] The imidazolium ring of the ILs forms a 3-D polar network facing towards the bulk water molecules whereas the $–C_8H_{17}$ group of the [OMIM]Br forms the inner core of the 3-D structures through the nonpolar van der Waals interaction between them.[7] As the imidazolium ring of the $[OMIM]^+$ cation have different H-bonding sites, therefore these protons are engaged in the H-bonding interactions with the Br^- and water molecules surrounding them. Due to the

presence of the 3-D nanostructured organization of [OMIM]Br in its aqueous solutions of $LiClO_4$, its diffusion coefficients values are < 10 order of in magnitude as compared to that of H_2O molecules.

Table 1. Translational Diffusion Coefficients, *D* of $[OMIM]^+$ and H_2O Molecules in both the Aqueous $LiClO_4$ Solutions of [OMIM]Br with their Relative Values at Different Temperatures. (The Composition of [OMIM]Br in all the Mixtures is Fixed as = 50% (w/w))

m_{LiClO4} / mol kg^{-1}	$D_{[OMIM]+} \times 10^{10}$ / m^2 s^{-1} (300 K)	$D_{H2O} \times 10^{10}$ / m^2 s^{-1} (300 K)	D_{H2O} / $D_{[OMIM]+}$ (300 K)
0	0.727	12.980	17.854
0.50	0.728	12.000	16.484
1.00	0.729	11.490	15.761
1.50	0.699	10.610	15.179
1.75	0.530	7.724	14.574
	$D_{[OMIM]+} \times 10^{10}$ / m^2 s^{-1} (305 K)	$D_{H2O} \times 10^{10}$ / m^2 s^{-1} (305 K)	D_{H2O} / $D_{[OMIM]+}$ (305 K)
0	0.861	14.610	16.969
0.50	0.867	13.780	15.894
1.00	0.905	13.270	14.663
1.50	0.837	12.290	14.683
1.75	0.656	8.854	13.497
	$D_{[OMIM]+} \times 10^{10}$ / m^2 s^{-1} (310 K)	$D_{H2O} \times 10^{10}$ / m^2 s^{-1} (310 K)	D_{H2O} / $D_{[OMIM]+}$ (310 K)
0	1.134	16.590	14.630
0.50	1.073	15.820	14.744
1.00	1.076	15.080	14.015
1.50	0.997	13.960	14.002
1.75	0.795	9.692	12.191
	$D_{[OMIM]+} \times 10^{10}$ / m^2 s^{-1}	$D_{H2O} \times 10^{10}$ / m^2 s^{-1}	D_{H2O} / $D_{[OMIM]+}$

	(315 K)	(315 K)	(315 K)
0	1.267	18.080	14.270
0.50	1.344	18.090	13.460
1.00	1.320	16.290	12.341
1.50	1.222	15.440	12.635
1.75	1.007	8.582	8.522

However, the self-diffusion coefficients of $[OMIM]^+$ is show a maximum value with the increase in the compositions of $LiClO_4$ and the maxima is retained at higher temperature of 315 K. On the other hand, such behavior is not observed in the case of H_2O molecules.

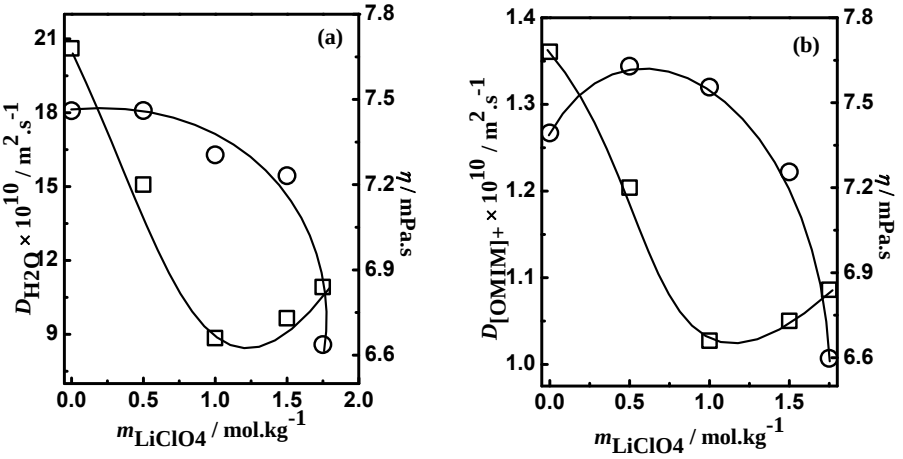

Figure 3. The plots of self-diffusion coefficients of H_2O, D_{H2O} (○, (a)) and $[OMIM]^+$, $D_{[OMIM]+}$ (○, (b)), respectively with the increasing composition of $LiClO_4$ in comparison with the bulk viscosity, η (□) of the mixtures at 315 K. The composition of [OMIM]Br in all the cases is fixed as 50% (*w/w*).

It indicates that there might be the possibility of weakening of the nanostructure of [OMIM]Br with the addition of $LiClO_4$ into the system. To confirm this observation we have also measured the bulk viscosity, η of the mixtures and compared with the experimentally observed NMR self-diffusion coefficient values. Figure 3(a) and (b)

represents the comparative plot for the diffusion coefficients of the H_2O and $[OMIM]^+$, respectively with the η of the 50 % (w/w) composition of [OMIM]Br with the increasing compositions of $LiClO_4$ at 315 K. The η of the mixtures is showing a minimum value with the increase in the compositions of $LiClO_4$. It indicates that the maximum observed in the diffusion coefficient values of $[OMIM]^+$ is due to the lower viscosity values of the mixtures. It was reported that the high polarizable anions interact with the hydrophobic alkyl chain length of ILs through the weak ion-induced dipole interactions.[31] Therefore, with the initial addition of $LiClO_4$ into the mixtures, the high polarizable ClO_4^- ions interact with the hydrophobic $-C_8H_{17}$ group of $[OMIM]^+$. In addition to this the ClO_4^- ions are involved in the H-bonding interactions with the ring protons of imidazolium ring. Here both the electrostatic and H-bonding interactions between the $[OMIM]^+$ and Br^- are broken by the water molecules due to the strong hydration of Br^- ions. Therefore, the Br^- ions present around the polar 3-D surface of imidazolium ring comes into the bulk water and forms solvated LiBr. To maintain the electro-neutrality of the 3-D charged polar surface of $[OMIM]^+$, the ClO_4^- ions comes from the bulk and starts interacting with the imidazolium ring of $[OMIM]^+$ forming the $[OMIM][ClO_4]$ kind of species. Thus the positive electronic charge cloud of $[OMIM]^+$ is now more concentrated on the imidazolium ring as it was before with Br^- as the counter anion. This increase the repulsion between the imidazolium ring of $[OMIM]^+$ of 3-D nanostructure. In addition to this the ClO_4^- ions forms strong ion-water complexes around the hydrophobic $-C_8H_{17}$ group of $[OMIM]^+$ near to the imidazolium ring.[42] Consequently, it increases the repulsion between the nonpolar $-C_8H_{17}$ group of $[OMIM]^+$ and weakens the van der Waals interactions between the $-C_8H_{17}$ group of $[OMIM]^+$. As a result of which, the initial 3-D nanostructure is being weakens with the increase in the compositions of $LiClO_4$ resulting into the increase in the self-diffusion coefficient values of $[OMIM]^+$ and is reflected in the decrease in the bulk viscosity values of the mixtures. After the maxima has reached, the self-diffusion coefficient of the $[OMIM]^+$ again decrease with the rise in the composition of $LiClO_4$, possibly due to the increase in the number of particles in the mixtures causing hindrance in the diffusivity of $[OMIM]^+$ and is reflected from the increased viscosity of the mixtures. The same trend is also observed at 300 K indicates that the 3-D nanostructure of $[OMIM]^+$ also exists at lower temperature and thermal

energy is not sufficient enough to break it. On the other hand, the self-diffusion coefficients of H_2O molecules are decrease with the increase in the composition of $LiClO_4$.

However, no such kind of trends in the self-diffusion coefficients of $[OMIM]^+$ are observed in the case of aqueous LiCl mixtures of [OMIM]Br as is represented in the Figure 4. The self-diffusion coefficients of H_2O molecules and $[OMIM]^+$ cations with the increasing compositions of LiCl are represented in Figure 4(a) and (b), respectively in comparison with the bulk viscosity, η of the mixtures. The mixtures were prepared in a 50% (w/w) composition of [OMIM]Br in aqueous solutions of LiCl at 315 K. Both the $D_{[OMIM]+}$ and D_{H2O} molecules are decrease with the increase in the viscosity of the mixtures.

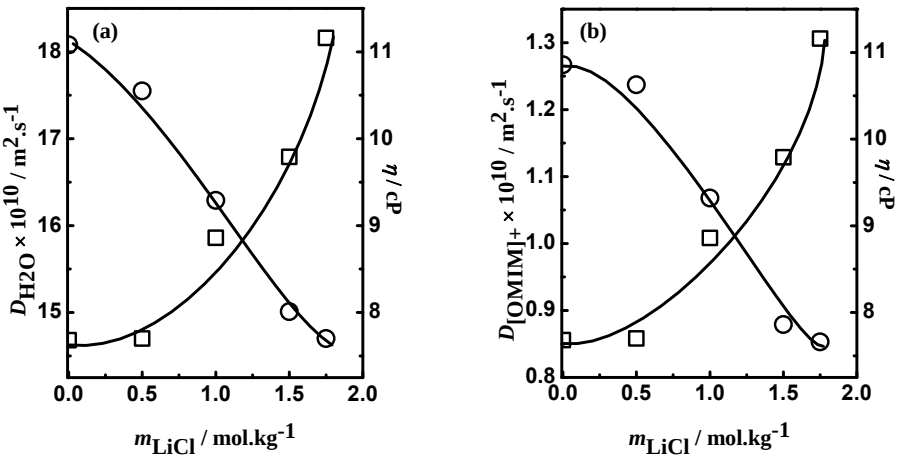

Figure 4. The plots of self-diffusion coefficients of H_2O, D_{H2O} (○, a) and $[OMIM]^+$, $D_{[OMIM]+}$ (○, b), respectively with the increasing composition of LiCl in comparison with the bulk viscosity, η (□) of the mixtures at 315 K. In all the cases the composition of [OMIM]Br is fixed as 50% (*w/w*).

We have also measured the self-diffusion coefficients of ^1H NMR active nuclei in the aqueous Li^+ mixtures of [BMIM]Br. Here both the $D_{[BMIM]+}$ and D_{H2O} molecules are increases with the increase in the thermal energy of the system. On the other hand, increase in the compositions of Li^+ salts decrease the diffusivity of each of the ^1H NMR

active nuclei that are $[BMIM]^+$ and H_2O. However, the relative diffusion coefficient values for the $[IL]^+$ and H_2O molecules presented in Table 2 shows interesting behavior.

Table 2. Temperature Dependent Relative Diffusivity of $[IL]^+$ and H_2O Molecules in the Aqueous Li^+ Salt Solutions ILs. (The $D_{[IL]+}$ is the Diffusion Coefficients of $[OMIM]^+$ and $[BMIM]^+$ in 1.75 mol kg^{-1} and 2.0 mol kg^{-1} of Aqueous Li^+ Salts, Respectively. $D^0_{[IL]+}$ and D^0_{H2O} are the Diffusion Coefficients of $[IL]^+$ and H_2O Molecules in the Aqueous Solutions of ILs, Respectively. D_{H2O} is the Diffusion Coefficients of H_2O Molecules in the 1.75 mol kg^{-1} ([OMIM]Br) and 2.0 mol kg^{-1} ([BMIM]Br) of Li^+ Salts, Respectively.)

System	T / K	$D_{[IL]+} / D^0_{[IL]+}$	D_{H2O} / D^0_{H2O}
[OMIM]Br (50% w/w)+ Aq. $LiClO_4$			
	300	0.729	0.595
	305	0.762	0.606
	310	0.701	0.584
	315	0.795	0.475
[OMIM]Br (50% w/w)+ Aq. LiCl			
	300	0.601	0.741
	305	0.655	0.757
	310	0.624	0.781
	315	0.673	0.813
[BMIM]Br (50% w/w)+ Aq. $LiClO_4$			
	300	0.731	0.792
	305	0.670	0.785
	310	0.728	0.780
	315	0.785	0.880
[BMIM]Br (50% w/w)+ Aq. LiCl			

	300	0.752	0.778
	305	0.750	0.775
	310	0.725	0.782
	315	0.777	0.786

Table 2 represents the temperature dependent relative diffusion coefficients of $[IL]^+$ and H_2O molecules. The Li^+ salt compositions are 1.75 mol kg^{-1} and 2.0 mol kg^{-1} for the [OMIM]Br and [BMIM]Br mixtures, respectively. In the case of aqueous Li^+ mixtures of [BMIM]Br, the addition of 2.0 mol kg^{-1} of Li^+ salts decrease the diffusivity of both the $[BMIM]^+$ and H_2O molecules compared to that in the system without any Li^+ salts at each temperature. However, with the rise in the temperature by 15 K from 300-315 K, the relative diffusivity of both the ^1H active nuclei increases. It means that the effect of Li^+ salts are more in lower temperature and at higher temperature the compensating effect of thermal energy decrease the effects of salts on the diffusional dynamics of ^1H NMR active nuclei. The relative diffusivity of $[BMIM]^+$ is less as compared to that of H_2O molecules at each temperature in both the Li^+ salt mixtures. It suggests Li^+ salts decrease the dynamics of $[BMIM]^+$ more as compared to that of H_2O molecules at each temperature.

On the other hand, in case of aqueous Li^+ salt solutions of [OMIM]Br, LiCl decreases the diffusivity of $[OMIM]^+$ significantly as compared to that of $LiClO_4$ at each temperature. However, the diffusional motion of H_2O molecules shows interesting behavior in the aqueous Li^+ solutions of [OMIM]Br. The diffusional motion of H_2O molecules are significantly faster in the case of aqueous LiCl solutions of [OMIM]Br as compared to that of $LiClO_4$ mixtures. This behavior of H_2O molecules is completely opposite to that of the diffusivity of $[OMIM]^+$ in the Li^+ salt mixtures. The $LiClO_4$ slower the diffusivity of H_2O molecules more as compared to that of $[OMIM]^+$, whereas the diffusional motion of H_2O molecules are faster than that of $[OMIM]^+$ in its aqueous LiCl solutions of [OMIM]Br. It is well known that LiCl is a salting-out (S-O) or structure-making salt whereas $LiClO_4$ is a salting-in (S-I) or structure-breaking salt.[29,43] Therefore, according to the classical concept of S-O/S-I phenomenon, $LiClO_4$ should accelerate the

dynamics of the water molecules more as compared to that of LiCl. However, by considering the diffusional motion of water molecules, the $LiClO_4$ is more S-O as compared to that of LiCl whereas, in view of the diffusivity of $[OMIM]^+$ the opposite is true in its aqueous Li^+ salt solutions of [OMIM]Br.

Temperature of the medium has also shows significant effect on the diffusional behavior of each of the ^1H NMR active nuclei in its aqueous Li^+ solutions of [OMIM]Br. The relative diffusivity of $[OMIM]^+$ in each of the Li^+ mixtures is more at higher temperature. It means both the Li^+ salts decrease the diffusional motion of $[OMIM]^+$ more at lower temperature and with the rise in temperature, the effect of thermal energy reduce the effect of Li^+ salt and the diffusional motion of $[OMIM]^+$ are faster. On the other hand, rise in temperature shows opposing behavior in the diffusional motion of H_2O molecules in case of Li^+ salt solutions of [OMIM]Br. The diffusional motion of H_2O molecules in 1.75 mol kg^{-1} of LiCl mixtures are 0.813 times faster as compared to the system without any LiCl (aqueous [OMIM]Br) at higher temperature of 315 K. However, decrease in temperature to 300 K, the diffusional motion of H_2O molecules decrease and is 0.741 times faster in aqueous LiCl mixture of [OMIM]Br as compared to that of aqueous solutions of [OMIM]Br. On the other hand, at higher temperature of 315 K the diffusional motion of H_2O molecules are 0.475 times faster in 1.75 mol kg^{-1} of aqueous $LiClO_4$ solution of [OMIM]Br than compare to the aqueous solution of [OMIM]Br. However, decrease in temperature to 300 K, the diffusivity of H_2O molecules increase and is 0.595 times faster in its ternary mixture of $LiClO_4$ in [OMIM]Br as compare to the aqueous solution of [OMIM]Br. It means the addition of 1.75 mol kg^{-1} of Li^+ salts shows faster mobility of water molecules at lower temperature in the aqueous $LiClO_4$ solutions of [OMIM]Br, whereas higher temperature shows faster mobility of water molecules in its aqueous LiCl solutions of [OMIM]Br.

4.3.1.2. Diffusional Motion of Individual Proton of ILs

Both the alkyl group substituted imidazolium-based ILs has different types of protons as represented in the Figure 1. The environment experienced by each of the protons is different from each other and therefore, has its own diffusivity as represented in Table 3. In the case of aqueous solutions of [OMIM]Br the diffusional motion of $–N-CH_2-$ proton

is more as compared to that of the –N-CH_3 proton. However, the addition of Li^+ salts into the system shows interesting effect in the diffusivity of the protons adjacent to the N-atom. In the case of aqueous $LiClO_4$ solutions of [OMIM]Br, the diffusional motion of –N-CH_2- protons are more as compared to that of –N-CH_3 protons showing similar in behavior to that of its aqueous solutions of [OMIM]Br. However, the addition of LiCl alters the trend in the diffusivity of the above mentioned protons and diffusional motion of –N-CH_3 protons are faster than compared to the –N-CH_2- protons. On the other hand, the diffusional motion of the protons present on the $–C_8H_{17}$ side chain of the [OMIM]Br increases on moving towards the end of the alkyl chain and the diffusivity of the individual protons are of the order of $D_f < D_g < D_h$. Similar behavior in the diffusivity are observed with the increase in the temperature and composition of Li^+ salts.

Table 3. Temperature Dependent Self-Diffusion Coefficient ($D\times10^{10}/m^2\ s^{-1}$) of Individual Proton of ILs in its Aqueous Li^+ Salt Mixtures. The Numbering of the Protons is in Accordance with the Numbering Scheme of Protons given in Figure 1. (SC – Alkyl Side Chain)

IL	System (50% (w/w))	e (-N-CH_2-)	b (-N-CH_3)	f (SC)	g (SC)	h (SC)
[OMIM]Br (50% w/w)						
	H_2O (300K)	0.759	0.718	0.707	0.716	0.727
	H_2O (315K)	1.523	1.243	1.212	1.247	1.267
	0.5 mol kg^{-1} LiCl (300K)	0.381	0.530	0.577	0.614	0.617
	0.5 mol kg^{-1} LiCl (315 K)	1.790	1.318	1.860	1.201	1.237
	1.5mol kg^{-1} LiCl (300K)	0.436	0.476	0.481	0.499	0.490
	1.5 mol kg^{-1} LiCl (315K)	0.598	0.762	0.825	0.906	0.879
	0.5mol kg^{-1} $LiClO_4$ (300K)	0.718	0.716	0.720	0.720	0.728
	0.5mol kg^{-1} $LiClO_4$ (315K)	2.872	1.517	1.290	1.289	1.344
	1.5mol kg^{-1} $LiClO_4$ (300K)	0.766	0.707	0.685	0.693	0.699
	1.5mol kg^{-1} $LiClO_4$ (315K)	1.443	1.215	1.182	1.204	1.222
[BMIM]Br (50% w/w)						
	H_2O (300K)	3.693	3.557	3.599	3.573	3.535

H_2O (315K)	6.372	5.696	5.211	5.431	5.273
0.5 mol kg^{-1} LiCl (300K)	2.047	2.987	3.167	3.229	3.327
0.5 mol kg^{-1} LiCl (315K)	4.756	4.968	5.083	5.165	5.181
1.5 mol kg^{-1} LiCl (300K)	3.105	2.920	2.867	2.912	2.872
1.5 mol kg^{-1} LiCl (315K)	5.035	4.549	4.480	4.552	4.561
0.5mol kg^{-1} $LiClO_4$ (300K)	2.678	3.056	3.311	3.289	3.268
0.5mol kg^{-1} $LiClO_4$ (315K)	6.091	5.418	5.093	5.241	5.128
1.5mol kg^{-1} $LiClO_4$ (300K)	2.613	2.724	2.841	2.822	2.847
1.5mol kg^{-1} $LiClO_4$ (315K)	6.019	4.876	4.483	4.597	4.430

However, both the temperature and composition of Li^+ salts shows unusual behavior on the diffusional motion of individual proton of lower alkyl group substituted [BMIM]Br. The diffusional motion of –N-CH_2- protons are more as compared to that of –N-CH_3 protons in its aqueous solutions of [BMIM]Br showing similar in behavior to that of the higher alkyl group substituted [OMIM]Br. On comparing with the diffusional motion of the terminal –CH_3 proton (h proton) of the –C_4H_9 group of [BMIM]Br, the order of their diffusivity follows the trend as $D_h < D_{\text{-N-CH3}} < D_{\text{-N-CH2-}}$. It means in the case of aqueous solutions of [BMIM]Br, the –N-CH_3 and –N-CH_2- protons which are closer to the imidazolium ring are moving faster than compared to the terminal –CH_3 proton of –C_4H_9 group. This might be due to the weak π-π interactions between the imidazolium rings due to the stronger H-bonding interactions with the water molecules. The addition of 0.5 mol kg^{-1} of aqueous solutions of LiCl into the [BMIM]Br resulting into the faster diffusivity of terminal –CH_3 proton as compared to that of the –N-CH_2- and –N-CH_3 proton and the order of their diffusivity follows the trend as $D_h > D_{\text{-N-CH3}} > D_{\text{-N-CH2-}}$. However, increase in the composition of LiCl to 1.5 mol kg^{-1}, the trend is being reversed as $D_h < D_{\text{-N-CH3}} < D_{\text{-N-CH2-}}$. The initial addition of LiCl (0.5 mol kg^{-1}) withdraws the water molecules surrounding the imidazolium ring due to the strong electrostatic influence of high charge density Li^+ ion. This increase the π-π interactions between the imidazolium rings resulting in the decreased diffusivity of its –NCH= protons compared to the terminal –CH_3 protons of –C_4H_9 group. However, increase in the composition of LiCl to

1.5 mol kg^{-1} decreases the diffusivity of terminal $–CH_3$ group of alkyl group as compared to the neighboring –NCH= protons of the imidazolium ring due to the stronger van der Waals interactions between the $–C_4H_9$ groups. Here in the case of LiCl mixtures, the trend in the diffusivity of individual protons of $[BMIM]^+$ are same at both the temperature. On the other hand, temperature has a significant effect on the diffusional motion of individual proton of $[BMIM]^+$ in the case of aqueous $LiClO_4$ solutions of [BMIM]Br. At lower temperature of 300 K the diffusivity follows the trend as $D_h > D_{\text{-N-CH3}} > D_{\text{-N-CH2-}}$ and at higher temperature of 315 K the trend in the diffusional motion of individual proton of $[BMIM]^+$ is being reversed as $D_h < D_{\text{-N-CH3}} < D_{\text{-N-CH2-}}$. At lower temperature of 300 K, the thermal energy is sufficient enough to break the weak attractive component of the van der Waals interactions present between the $–C_4H_9$ group of the $[BMIM]^+$. This makes the side chain of the $[BMIM]^+$ far apart from each other causing the faster diffusional motion of the terminal $–CH_3$ protons of the alkyl side chain as compared to the neighboring –NCH= protons of the imidazolium ring. However, the H-bonding interactions between the water molecules with the ring protons are broken at higher temperature of 315 K. Therefore, the π-π interactions between the imidazolium rings increase resulting in the slower diffusional motion of the neighboring –NCH= protons of the imidazolium ring as compared to the terminal $–CH_3$ protons of the alkyl side chain.

4.3.1.3. ^{1}H NMR Chemical Shifts

The ^{1}H NMR data of IL molecules show interesting behavior in its aqueous Li^+ salt solutions. Figure 5 represents the deviation in the ^{1}H NMR chemical shift for the C2 proton of imidazolium ring with the increase in the composition of Li^+ salts. The deviation in the ^{1}H NMR chemical shift is defined by the equation 3 as

$$\Delta\delta_H = \delta_{H(IL+Aq.\ salt)} - \delta_{H(Aq.\ IL)} \qquad (3)$$

where $\delta_{H(IL+Aq.\ salt)}$ and $\delta_{H(Aq.\ IL)}$ represents the ^{1}H NMR chemical shift of the C2 proton of imidazolium ring in its aqueous Li^+ salt solutions of ILs and in aqueous ILs, respectively. The purpose of selecting the C2 proton is because of its highest deviation observed in the ^{1}H NMR chemical shift values among all the imidazolium protons. The C2 proton of

imidazolium ring of ILs is concentration dependent and is more acidic in nature compared to other imidazolium protons.[32] It has been observed that the C2 proton is capable of forming H-bond with the water molecules and the counter anion of ILs in its aqueous solutions.[44] The deviation observed in the chemical shift values for the LiCl is positive whereas $LiClO_4$ shows negative deviation as illustrated in the Figure 5. The positive values of chemical shift deviation indicates that $\delta_{H(IL+Aq.\ salt)} > \delta_{H(Aq.\ IL)}$. It means the C2 proton experience a more deshielding environment in its aqueous LiCl solutions of ILs as compared to the aqueous solutions of ILs and is therefore considered to be as more acidic in nature in the LiCl system. This can be explained on the basis of H-bonding and π-π interactions.

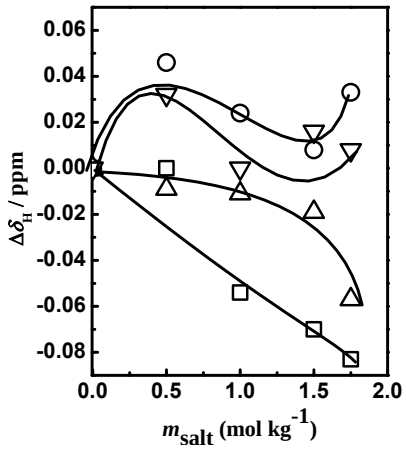

Figure 5. The plot of ^{1}H NMR chemical shift deviation ($\Delta\delta_H$) for C2 proton of imidazolium ring of ILs (50 wt%) as a function of salt compositions at 300 K. The symbols are representing for the [BMIM]Br in LiCl (▽) and $LiClO_4$ (△), and [OMIM]Br in LiCl (○) and $LiClO_4$ (□), respectively.

The addition of LiCl withdraws the water molecules surrounding the imidazolium ring leading to the enhancement in the π-π interactions between the imidazolium ring of ILs. Consequently, each π-electron cloud is sandwich between the two other π-electron cloud of imidazolium ring system. It increase the strength of the induced magnetic field caused by the circulating π-electronic systems and therefore, the C2 proton experience a higher magnetic field leading to the deshielded NMR signal with higher value of chemical shift. The higher positive values for [OMIM]Br as compared to that of [BMIM]Br in their

aqueous solutions of LiCl are because of its stronger π-π interactions between the imidazolium ring in case of former IL as compared to the later one. However, $LiClO_4$ shows the negative deviation in the chemical shift of their C2 proton. It means $\delta_{H(IL+Aq.\ salt)} < \delta_{H(Aq.\ IL)}$, which indicates that the imidazolium C2 proton experience a shielding environment in the aqueous $LiClO_4$ solutions as compared to the aqueous solutions of ILs and are therefore, considered to be less acidic in nature. It is because of the decreased π-π interactions between the imidazolium ring of ILs. $LiClO_4$ is known to be a well known structure-breaker and are considered as a salting-out agent.[26] It breaks the H-bonding network of water with the addition of aqueous solutions of $LiClO_4$ into the IL systems. Therefore, more number of free water molecules is available for the solvation of polar imidazolium ring of ILs. This minimizes the π-π interactions between the imidazolium rings and is therefore, the induced magnetic field experienced by the C2 proton is less in the aqueous $LiClO_4$ solutions of ILs as compared to the aqueous solutions of ILs. Therefore, the C2 proton experienced a shielded environment with lower chemical shift value in their aqueous $LiClO_4$ solutions of ILs as compared to that of the aqueous solutions of ILs. The effect being more pronounced with the increase in the compositions of $LiClO_4$. However, the more negative deviation in the chemical shift values of the C2 proton for [OMIM]Br as compared to that of the [BMIM]Br suggests the more weakening of the π-π interactions in the case of former IL as compared to the later one. This statement is in support of the weakening of the nanostructural organization of [OMIM]Br in aqueous $LiClO_4$ solutions as compared to the [BMIM]Br. Thus, the C2 proton is more acidic in case of [BMIM]Br as compared to that of [OMIM]Br in their aqueous solutions of LiCl. In general the order of acidity of C2 proton of alkyl group substituted imidazolium bromide based ILs in their aqueous Li^+ salt solutions is $C2_{[OMIM]Br + Aq.\ LiCl} > C2_{[BMIM]Br + Aq.\ LiCl} > C2_{[BMIM]Br + Aq.\ LiClO4} > C2_{[OMIM]Br + Aq.\ LiClO4}$. It means the addition of LiCl increases the acidic nature of C2 proton more as compared to the $LiClO_4$.

The chemical shifts of C2 proton (a) and $-CH_3$ protons (h) shows interesting behavior with the increase in the wt% of ILs as represented in the Figure 6a and 6b, respectively. Increase in the composition of ILs increase the chemical shift of the C2 proton and

experiencing a deshielding effect whereas it decrease the chemical shift values for the 'h' protons with a shielding environment. It means the electronic environment around the C2 proton decrease with the increase in the wt% of IL and therefore the acidity of C2 proton is increase. This is because of the increased π-π interactions between the imidazolium rings as explained previously. The higher chemical shift value of C2 proton for [OMIM]Br as compared to that of [BMIM]Br indicates the more acidic nature of C2 proton for [OMIM]Br as compared to that of the [BMIM]Br at each compositions of ILs.

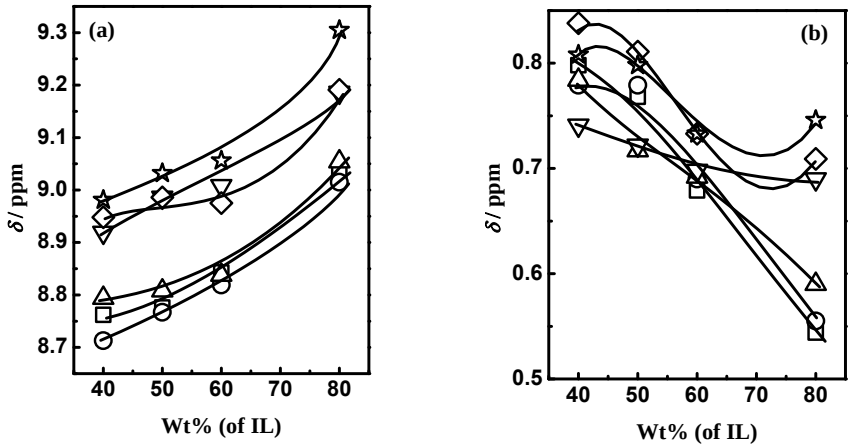

Figure 6. The chemical shift for C2 (a) proton (a) and $-CH_3$ (h) protons (b) with the increase in the wt% of water at 300 K. The symbols are representing for the aq. [BMIM]Br (□), [BMIM]Br in 0.5 mol kg^{-1} of aq. $LiClO_4$ (○), [BMIM]Br in 0.5 mol kg^{-1} of aq. LiCl (△), aq. [OMIM]Br (▽), [OMIM]Br in 0.5 mol kg^{-1} aq. $LiClO_4$ (◇) and [OMIM]Br in 0.5 mol kg^{-1} of aq. LiCl (☆), respectively.

This is because of the more π-π interactions in the case of [OMIM]Br due to the presence of the long $-C_8H_{17}$ group as compared to the short $-C_4H_9$ group of [BMIM]Br. It was reported that, increase in the compositions of alkylimidazolium bromide-based ILs leads to the micelle formation in their aqueous solutions.[10] A continuous decrease in the chemical shift values of the H12 proton of the [OMIM]Br is observed with the increase in the composition of IL.[45] Here in our studies, the chemical shift value of 'h' proton of ILs is decrease with the increase in the wt% of ILs suggesting the more favorable interactions between the alkyl groups of ILs. The 'h' protons of ILs are experiencing a less electronic environment in lower compositions of ILs due to the presence of icebergs of water

molecules. However, water molecules are expelled from the surface of alkyl groups with the increase in the compositions of ILs due to the increase in the van der Waals interactions between the alkyl groups of ILs. Consequently, it increases the electron density around the 'h' protons and therefore, experiences a shielding effect.

Increase in the temperature of the medium shows significant behavior on the chemical shift of the C2 proton as illustrated in the Figure 7a. The acidity of C2 proton for both the alkyl group substituted ILs increase with the increase in the temperature of the medium. Here the H-bonding plays the prominent role on the deviation observed in the case of C2 proton.

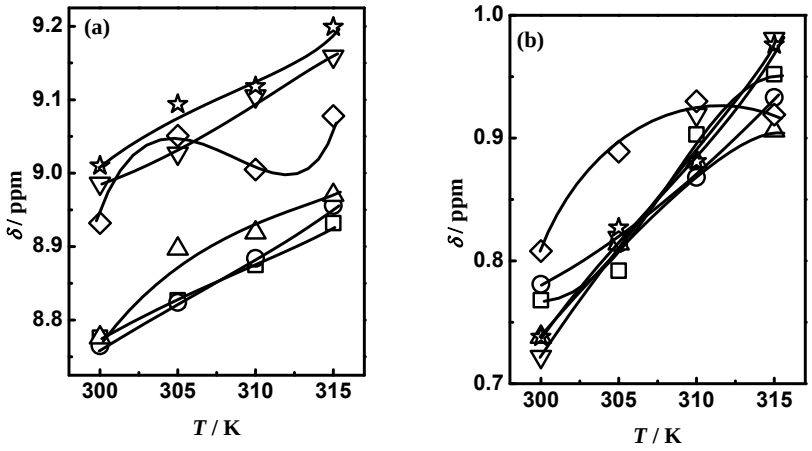

Figure 7. The chemical shift for C2 (a) proton (a) and $-CH_3$ (h) protons (b) with the increase in the temperature of the system at 50% (w/w) of ILs. The symbols represents the aq. [BMIM]Br (□), [BMIM]Br in 1.0 mol kg^{-1} of aq. $LiClO_4$ (○), [BMIM]Br in 1.0 mol kg^{-1} of aq. LiCl (△), aq. [OMIM]Br (▽), [OMIM]Br in 1.0 mol kg^{-1} aq. $LiClO_4$ (◇) and [OMIM]Br in 1.0 mol kg^{-1} of aq. LiCl (☆), respectively.

An increase in the temperature decreases the chemical shift of the =N-H proton of the 1,8-diazabicyclo-[5,4,0]-undec-7-ene (DBU) indicating the shortening of the =N-H bond due to the decreased strength of the H-bonding between the protonated 1,8-diazabicyclo-[5,4,0]-undec-7-ene (DBU) with different anions through the =N-H bond.[46] The increase in the chemical shift values of the C2 proton of alkyl group substituted imidazolium bromide based ILs as represented in Figure 7a indicates the weakening of the =N-H bond and consequently, it increase the acidic nature of C2 proton. Increase in the thermal

energy of the medium breaks the intermolecular H-bonding interactions between the water molecules as confirm from its (H_2O) increased NMR self-diffusion coefficient values discussed above. Also, the increased self-diffusion coefficient values of the $[IL]^+$ indicates the weakening of the aggregated structures of ILs in its solutions. However, increase in the C2 proton chemical shift of the =N-H proton indicates the increase in its bond length and therefore, experiencing a deshielding effect with a less electronic environment. It is due to the increase in the strength of the H-bonding interaction between the C2 proton with the water molecules. The higher chemical shift values of the C2 proton for [OMIM]Br as compared to that of the [BMIM]Br indicates that the strength of H-bonding interactions between the C2 proton with the water molecules is more in the case of former IL as compared to the later. The higher hydration number of [OMIM]Br as compared to that of the [BMIM]Br is one of the important finding in support of the above statement.[47] In each of the ILs the chemical shift of the C2 proton in their aqueous solutions of LiCl is more as compared to that of the $LiClO_4$. This might be due to the change in the H-bonded nature of the water molecules. As LiCl enhance the H-bonded structure of water and $LiClO_4$ disrupt it therefore, LiCl strengthen the H-bonding interactions between the water molecules with the C2 proton of ILs more as compared to the $LiClO_4$.[48] As a result of which the =N-H bond length is more in the case of aqueous LiCl solutions of ILs as compared to the $LiClO_4$ system and is reflected from the higher chemical shift value in the case of former system as compared to the later. Therefore, the acidic nature of C2 proton is more in case of aqueous LiCl solutions of ILs as compared to the $LiClO_4$.

The acidic nature of 'h' protons of ILs is also increase with the increase in the temperature of the medium; indicated from the increase in the chemical shift values shown in Figure 7b. It can be explained on the basis of the model proposed by N. S. Golubev *et al*.[49] According to them the dipole moment of a H-bonded H-X (X, heteroatom) bond is increase with the rise in the temperature of the medium. The 'h' protons attached to the C-atom possess a small dipole moment, directed C^-H^+. The electric dipoles of water molecules create an effective electric field around this C^-H^+ bond as illustrated in the Figure 8. The water dipoles around the C^-H^+ bond are highly ordered in lower temperature creating a higher electric field and at higher temperature the

ordering of the water dipoles decrease creating a lesser electric field. Therefore, due to the enthalpy-entropy compensation phenomenon of electric dipoles of water molecules around the $C^{-}H^{+}$ bond of 'h' protons, the electric field around it decrease with the increase in the temperature. For that reason, the partial electron cloud experienced by both the atom of $C^{-}H^{+}$ bond are less at lower temperature as compared to the higher temperature. As a consequence, the dipole moment of the $C^{-}H^{+}$ bond increase with the increase in the temperature in its aqueous Li^{+} salt solutions of imidazolium bromide-based ILs. Therefore, the 'h' protons are experiencing a less electronic environment at higher temperature with a higher chemical shift value.

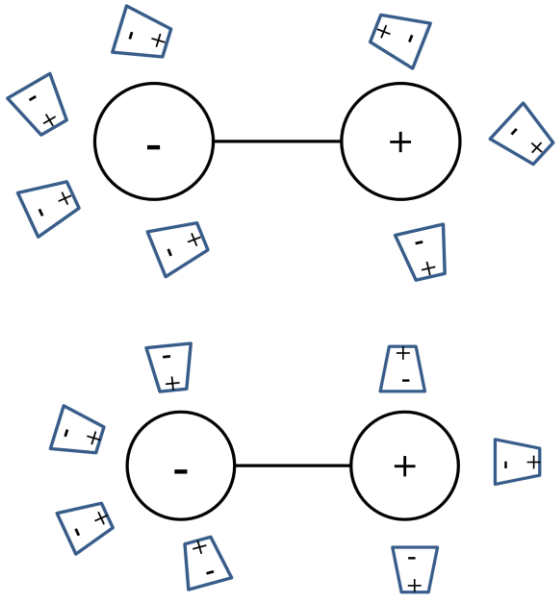

Figure 8. The arrangement of electric dipoles of water molecules around the $C^{-}H^{+}$ bond at higher (top) and lower (bottom) temperatures. The negative and positive circle represents the C and H atom, respectively.

4.3.1.4. Translational and Rotational Motion of ^{1}H NMR Active Nuclei

An attempt has been made to study the translational and rotational motion of ^{1}H NMR active nuclei in its aqueous Li^{+} salt solutions of ILs. The translational motion is defined as the motion of a molecule from one position to another in a fluid. However, in

rotational motion the molecular motion is only through its axis of rotation and during its motion there is no change in the position of the molecule. The time required for the translational and rotational motions are known as translational and rotational correlation time, respectively. There is a possibility that the molecule may exhibit both the motion simultaneously. These two kinds of molecular motions are schematically represented in the Figure 9. The translational and rotational correlation time of the diffusing particle inside its solution can be calculated from their translational and rotational diffusion coefficients, D_t and D_r respectively, which are obtained from the Stokes-Einstein (SE) and Stokes-Einstein-Debye relationships as represented in equation 4 and 5, respectively.

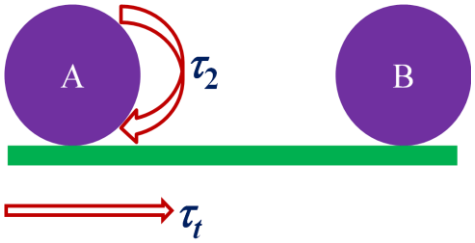

Figure 9. Schematic representation of the translational (τ_t) and rotational (τ_2) motion of a moving particle from position A to B.

According to the Stokes-Einstein (SE) relationship the translational diffusion coefficient, D_t is related with the viscosity of the medium as[50,51]

$$D_t = \frac{k_B\, T}{6\pi\eta a} \tag{4}$$

and the relationship between the rotational diffusion coefficient, D_r with the viscosity of the medium can be obtained from the Stokes-Einstein-Debye equation as[50]

$$D_r = \frac{k_B\, T}{8\pi\eta a^3} \tag{5}$$

where T is the absolute temperature, η is the bulk viscosity of the medium, k_B is the Boltzmann constant and a is the radius of the diffusing particle inside the IL mixtures.

The translational correlation time (τ_t) of the diffusing molecule inside the aqueous Li^+ salt solutions of IL mixtures can be obtained from the equation 4 as

$$\tau_t = \frac{2a^2}{D_t} \tag{6}$$

and the rotational correlation time (τ_2) can be obtained from the equation 5 as

$$\tau_2 = \frac{\eta V}{k_B T} \tag{7}$$

where *V* is the molecular volume of the diffusing particle. In the current research work, we have taken *a* and *V* as the van der Waals radius and volume of the diffusing molecule, respectively.

The translational and rotational correlation time τ_t and τ_2, of $[IL]^+$ in the aqueous 1.0 mol kg^{-1} of Li^+ salt solutions of ILs are represented in the Figure 10(a) and (b), respectively. The τ_t and τ_2 values are obtained from the experimentally measured self-diffusion coefficients and the viscosity of the mixtures as explained in the equation 6 and 7, respectively.

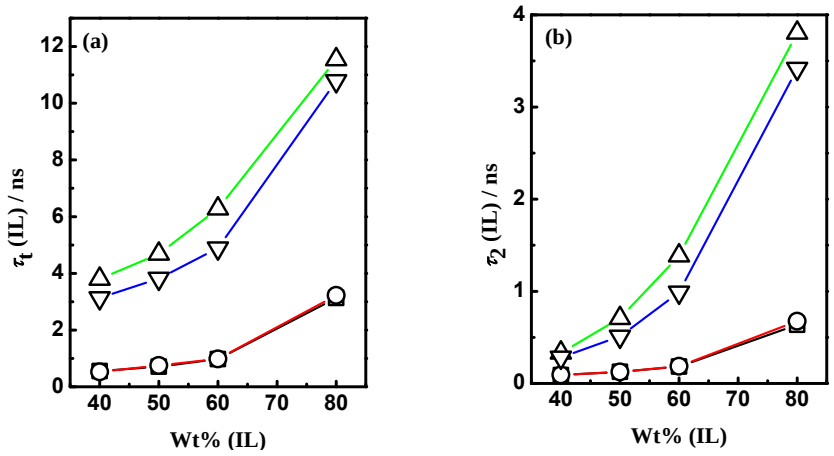

Figure 10. The plots of translational correlation time, τ_t (a) and rotational correlation time, τ_2 (b) of $[IL]^+$ with the increasing wt% of ILs. The symbols are representing as the [BMIM]Br in 1.0 mol kg^{-1} of aqueous LiCl (□) and $LiClO_4$ (○), and [OMIM]Br in 1.0 mol kg^{-1} of aqueous LiCl (△) and $LiClO_4$ (▽), respectively. The temperature of the medium in all the cases is kept constant as 300 K.

The τ_t and τ_2 values of $[IL]^+$ are increase with the increase in the wt% of ILs as illustrated in the Figure 10. It indicates that the cationic motion of ILs is being slowed down with the increase in its compositions. The $[BMIM]^+$ cation move faster as compared to the $[OMIM]^+$ in its aqueous Li^+ salt solutions indicated from their higher correlation time values for $[OMIM]^+$ as compared to the $[BMIM]^+$. This might be due to the possibility of higher van der Waals radii of $[OMIM]^+$ as compared to the $[BMIM]^+$. The τ_t values of $[IL]^+$ in its aqueous Li^+ salt solutions (1.0 mol kg^{-1}) are nearly three order of magnitude more as compared to the τ_2 values. This indicates that the rotational motion of $[IL]^+$ are faster as compared to the translational motion. It is because of the fact that the translating $[IL]^+$ has to come across more number of bond breaking/making phenomenon as compared to that of the rotating $[IL]^+$; as the former requires a change in the position of the molecule from one position to other while in the later case the position of the molecule remains as fixed, however, it has to rotate around its axis of rotation.

It is well established that both the LiCl and $LiClO_4$ have significant effect on the structure of water.[29] The former makes the H-bonded network of water whereas the later breaks it and are therefore known as water structure-maker and breaker, respectively. The former one increase the hydrophobic bonding between the hydrophobic molecules and are called as pro-hydrophobic agents whereas the later one decrease the hydrophobic bonding and are known as anti-hydrophobic agents.[52] It is also known that the LiCl enhance the rate of organic reactions more in its aqueous solutions as compared to that of the $LiClO_4$.[52] However, in this study the addition of Li^+ salts shows insignificant effect on both the τ_t and τ_2 values of $[BMIM]^+$ in its aqueous Li^+ salts. It means the τ_t values of $[BMIM]^+$ are same for both the Li^+ salts like that of τ_2 values. However, a substantial change in the behavior of τ_t and τ_2 values for $[OMIM]^+$ are observed with the addition of Li^+ salts into the system. At each compositions of [OMIM]Br the τ_t and τ_2 values of $[OMIM]^+$ are higher in its aqueous LiCl solution as compared to that of the $LiClO_4$ mixtures. It indicates that, both the translational and rotational motion of $[OMIM]^+$ is faster in its aqueous $LiClO_4$ solutions as compared to the LiCl. It is due to the fact that LiCl strengthen the hydrophobic interactions between the long alkyl chain length $–C_8H_{17}$ group of [OMIM]Br causing the slower mobility for $[OMIM]^+$. However, $LiClO_4$

weakens the hydrophobic interactions between the $-C_8H_{17}$ group of [OMIM]Br and leads to the faster mobility of its $[OMIM]^+$ group.

An attempt has been made to study the translational and rotational motion of water molecules in its aqueous Li^+ salt mixtures of ILs. The information regarding the translational and rotational motion of water molecules can be obtained from their translational and rotational correlation time, τ_t and τ_2 values, respectively. These τ_t and τ_2 values of water molecules are obtained from the measured NMR self-diffusion coefficient values of water molecules and the measured bulk viscosity of the system, respectively. Figure 11a and b represents the τ_t and τ_2 values of water molecules with the increase in the wt% of ILs in its aqueous Li^+ salt solutions of ILs, respectively.

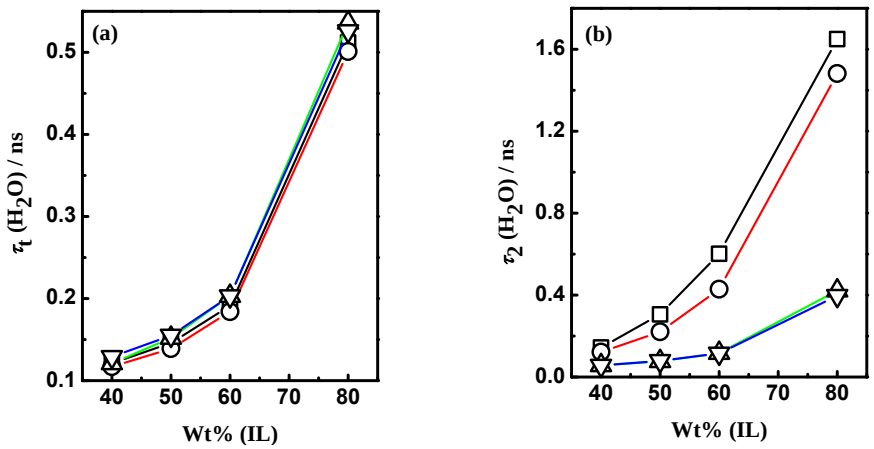

Figure 11. The plot of translational correlation time, τ_t (a) and rotational correlation time, τ_2 (b) of water molecules with the increasing wt% of IL. The symbols represents the [BMIM]Br in 1.0 mol kg^{-1} of aqueous LiCl (▽) and $LiClO_4$ (△), and [OMIM]Br in 1.0 mol kg^{-1} of aqueous LiCl (□) and $LiClO_4$ (○), respectively. The temperature of the medium in all the systems is kept constant as 300 K.

Increase in the wt% of ILs increase the τ_t and τ_2 values of water molecules indicating the slower translational and rotational motions. The magnitude of τ_t values of water molecules in both the ILs mixtures is nearly same with the increase in its wt%. It indicates that the magnitude of translational motion of water molecules is invariant with the increase in the wt% of ILs. It confirms that the size of IL cations have insignificant

effect on the translational motion of water molecules. At a fixed wt% of ILs, the addition of Li^+ salts also shows invariant effect on the translational motion of water molecules. It means the time required for the water molecules to change its position from one point to another is same in both the Li^+ salts mixtures of ILs.

On the other hand, the rotational motion of water molecules shows interesting behavior in the aqueous Li^+ salt solutions of ILs as represented in the Figure 11b. It decrease with the increase in the wt% of [BMIM]Br in the aqueous Li^+ salt solutions of [BMIM]Br. However, its magnitude is less than that of τ_t in the [BMIM]Br mixtures. This indicates that the rotational motion of water molecules is faster than that of the translational motion in the [BMIM]Br mixtures of Li^+ salts. On the other hand, the magnitude of rotational correlation time of water molecules is substantially higher than that of the translational correlation time in the aqueous Li^+ salt solutions of [OMIM]Br indicates the faster translational motion of water molecules as compared to that of the rotational motion. The magnitude of τ_2 of water molecules in the LiCl solutions of [OMIM]Br is higher as compared to that of the $LiClO_4$ systems. It means the rotational motion of water molecules is faster in the $LiClO_4$ mixtures of [OMIM]Br as compared to that of the LiCl which is according to the classical salting phenomenon. This leads to one of the most important finding that the rotational behavior of water molecules in the aqueous Li^+ salt solutions of [OMIM]Br is in accordance with the classical salting phenomenon of structure-maker/breaker. However, no such kind of behavior is observed in the case of [BMIM]Br mixtures.

4.3.1.5. Activation Energy of Viscosity, Self-Diffusion, Translational and Rotational Motions

The activation energy of viscous flow (E_η) can be calculated from the temperature dependent variation of the viscosity by applying the Arrhenius equation as:

$$\eta = \eta_0 exp^{E_\eta/RT} \qquad (8)$$

where η is the bulk viscosity of the medium, R is the gas constant, T is the absolute temperature in Kelvin, and η_0 is the preexponential factor.

Similarly, the activation energy of diffusive flow of $[IL]^+$ ($E_{D,IL}$) and water molecules ($E_{D,H2O}$) are calculated from the temperature dependent measurement of self-diffusion coefficients of $[IL]^+$ and water molecules, respectively by applying the Arrhenius equation as:

$$D_{[IL]+} = D_{0,[IL]+}\, exp^{E_{D,[IL]+}/RT} \quad (9)$$

and $$D_{H2O} = D_{0,H2O}\, exp^{E_{D,H2O}/RT} \quad (10)$$

where D_{IL+} and D_{H2O} are the measured self-diffusion coefficients of $[IL]^+$ and water molecules; $D_{0,[IL]+}$ and $D_{0,H2O}$ are the preexponential factors; and $E_{D,[IL]+}$ and $E_{D,H2O}$ are the activation energy of diffusive flow for $[IL]^+$ and water molecules, respectively. The calculated values of E_η, $E_{D,[IL]+}$ and $E_{D,H2O}$ are given in the Table 4.

Table 4. Temperature Dependent (300-315 K) Activation Energy of Viscous Flow (E_η), Diffusive Flow of $[IL]^+$ ($E_{D,[IL]+}$) and Water Molecules ($E_{D,H2O}$) in the Aqueous Li^+ Salt Solutions of ILs. The Values of Correlation Coefficient, r^2 are given in the Parenthesis.

IL	System	E_η/kJ mol^{-1} (r^2)	$E_{D,[IL]+}$/kJ mol^{-1} (r^2)	$E_{D,H2O}$/kJ mol^{-1} (r^2)
[BMIM]Br (50% w/w)	Aqueous Salt(mol kg^{-1}) (50% w/w)			
	H_2O	19.8±1.0 (0.993)	20.2±3.1 (0.942)	15.9±2.7 (0.926)
	1.0 (LiCl)	21.0±0.9 (0.996)	23.7±1.2 (0.993)	21.0±0.6 (0.998)
	1.5 (LiCl)	20.0±0.4 (0.999)	23.7±1.8 (0.985)	21.3±1.8 (0.982)
	1.0 ($LiClO_4$)	19.4±1.3 (0.988)	24.1±3.2 (0.958)	20.6±0.2 (0.999)
	1.5 ($LiClO_4$)	20.1±0.7 (0.996)	22.3±1.9 (0.981)	19.1±0.8 (0.995)
[BMIM]Br (80% w/w)	Aqueous Salt(mol kg^{-1}) (20% w/w)			

	H_2O	28.8±0.9 (0.998)	29.4±1.0 (0.997)	24.4±0.5 (0.999)
	1.0 (LiCl)	28.5±0.8 (0.998)	35.0±2.6 (0.987)	25.3±0.5 (0.999)
	1.5 (LiCl)	27.3±0.8 (0.998)	34.8±1.9 (0.993)	30.5±0.9 (0.998)
	1.0 ($LiClO_4$)	29.7±0.5 (0.999)	26.4±1.9 (0.987)	30.3±2.7 (0.981)
	1.5 ($LiClO_4$)	29.6±0.8 (0.998)	32.3±2.6 (0.985)	33.1±1.4 (0.996)
[OMIM]Br (50% w/w)	Aqueous Salt(mol kg^{-1}) (50% w/w)			
	H_2O	19.4±2.1 (0.969)	29.8±3.9 (0.960)	17.5±0.9 (0.992)
	1.0 (LiCl)	23.0±1.6 (0.987)	32.1±2.8 (0.981)	20.7±0.5 (0.999)
	1.5 (LiCl)	25.5±0.9 (0.997)	29.5±3.3 (0.970)	18.8±2.3 (0.962)
	1.0 ($LiClO_4$)	20.4±2.3 (0.965)	30.7±0.9 (0.998)	18.1±1.7 (0.978)
	1.5 ($LiClO_4$)	21.5±1.6 (0.986)	29.5±1.1 (0.996)	19.4±1.0 (0.993)
[OMIM]Br (80% w/w)	Aqueous Salt(mol kg^{-1}) (20% w/w)			
	H_2O	38.2±1.2 (0.998)	32.7±0.7 (0.999)	24.9±0.8 (0.997)
	1.0 (LiCl)	40.5±0.8 (0.999)	35.5±0.6 (0.999)	29.3±1.3 (0.995)
	1.5 (LiCl)	37.0±1.0 (0.998)	36.3±0.6 (0.999)	29.0±0.2 (0.999)
	1.0 ($LiClO_4$)	37.9±1.0 (0.998)	33.3±1.3 (0.996)	30.7±1.8 (0.991)
	1.5 ($LiClO_4$)	35.1±1.6 (0.995)	33.2±1.2 (0.997)	23.0±0.8 (0.997)

The addition of Li^+ salts bears negligible effect on both the activation energy of viscous and diffusive flow and is within the error limits. However, a significant change in the activation energy of viscous and diffusive flow has been observed with the change in the composition of ILs. The E_η values increase about 1.5 order of magnitude with the increase in the composition of [BMIM]Br from 50 to 80 wt% in its aqueous solutions. On the other hand, there is a two fold increase in the E_η values are observed with the increase in the composition of [OMIM]Br from 50 to 80 wt% in its aqueous solutions. The

magnitude of activation energy of viscous flow, E_η for [BMIM]Br is nearly similar to that of [OMIM]Br in its 50 wt% composition. However, in the 80 wt% composition of IL, the magnitude of E_η value for [OMIM]Br is nearly 1.3 order of magnitude higher as compared to that of the [BMIM]Br.

The activation energy of diffusive flow for ILs, $E_{D,[IL]+}$ are higher as compared to that of the $E_{D,H2O}$. This signifies that the $[IL]^+$ requires more energy to flow from one position to other as compared to that of the water molecules. The magnitude of both the $E_{D,[IL]+}$ and $E_{D,H2O}$ are increase with the increase in the composition of ILs. However, at a fixed composition of IL, there is an insignificant change in the magnitude of activation energy for diffusive flow of water molecules, $E_{D,H2O}$ are observed. This indicates that increase in the alkyl group substitution in ILs does not alter the activation energy of diffusive flow of water molecules. On the other hand, there is a significant increase in the activation energy of diffusive flow of ILs (50 wt%) is observed with the increase in the alkyl chain length of ILs. However, a mild enhancement in the $E_{D,[IL]+}$ is observed with the increase in the composition of ILs to 80 wt% possibly due to the increased aggregation at higher composition.

We have also made an attempt to calculate and understand the activation energy of rotational motion of $[IL]^+$ ($E_{\tau 2,[IL]+}$) and water molecules ($E_{\tau 2,H2O}$); and activation energy of translational motion of $[IL]^+$ ($E_{\tau t,[IL]+}$) and water molecules ($E_{\tau t,H2O}$) in the aqueous Li^+ salt solutions of ILs by applying the Arrhenius equation as:

$$\tau_{2,[IL]+} = \tau_{2,0,[IL]+}\, exp^{-E_{\tau 2,[IL]+}/RT} \quad (11)$$

$$\tau_{t,[IL]+} = \tau_{t,0,[IL]+}\, exp^{-E_{\tau t,[IL]+}/RT} \quad (12)$$

$$\tau_{2,H2O} = \tau_{2,0,H2O}\, exp^{-E_{\tau 2,H2O}/RT} \quad (13)$$

$$\tau_{t,H2O} = \tau_{t,0,H2O}\, exp^{-E_{\tau t,H2O}/RT} \quad (14)$$

where $\tau_{2,[IL]+}$, $\tau_{2,H2O}$, $\tau_{t,[IL]+}$ and $\tau_{t,H2O}$ are the rotational correlation time of $[IL]^+$, rotational correlation time of water molecules, translational correlation time of $[IL]^+$ and translational correlation time of water molecules; and $E_{\tau 2,[IL]+}$, $E_{\tau 2,H2O}$, $E_{\tau t,[IL]+}$ and $E_{\tau t,H2O}$

are their activation energy, respectively. $\tau_{2,0,[IL]+}$, $\tau_{2,0,H2O}$, $\tau_{t,0,[IL]+}$ and $\tau_{t,0,H2O}$ are their preexponential factors. The calculated values of $E_{\tau 2,[IL]+}$, $E_{\tau 2,H2O}$, $E_{\tau t,[IL]+}$ and $E_{\tau t,H2O}$ are represented in the Table 5.

Table 5. Temperature Dependent (300-315 K) Activation Energy of Translational ($E_{\tau t,[IL]+}$ and $E_{\tau t,H2O}$) and Rotational Motion ($E_{\tau 2,[IL]+}$ and $E_{\tau 2,H2O}$) of $[IL]^+$ and Water Molecules in the Aqueous Li^+ Salt Solutions of ILs. (The Correlation Coefficient, r^2 Values are given in the Parenthesis.)

IL	System	$E_{\tau t,[IL]+}$ /kJ mol^{-1} (r^2)	$E_{\tau t,H2O}$ /kJ mol^{-1} (r^2)	$E_{\tau 2,[IL]+}$/kJ mol^{-1} (r^2)	$E_{\tau 2,H2O}$/ kJ mol^{-1} (r^2)
[BMIM]Br (50% w/w)	Aqueous Salt(mol kg^{-1}) (50% w/w)				
	H_2O	22.1±2.9 (0.954)	17.2±2.4 (0.949)	22.6±1.1 (0.993)	22.1±0.8 (0.998)
	1.0 (LiCl)	23.9±1.1 (0.994)	21.1±0.4 (0.999)	23.8±1.0 (0.995)	23.6±1.2 (0.993)
	1.5 (LiCl)	24.9±1.7 (0.988)	22.7±1.7 (0.986)	22.3±0.5 (0.999)	22.6±0.2 (0.999)
	1.0 ($LiClO_4$)	26.6±3.4 (0.958)	20.9±0.2 (0.999)	22.3±1.1 (0.993)	22.0±0.9 (0.996)
	1.5 ($LiClO_4$)	23.7±2.1 (0.980)	19.4±1.0 (0.992)	22.9±0.9 (0.996)	22.9±0.8 (0.997)
[BMIM]Br (80% w/w)	Aqueous Salt(mol kg^{-1}) (20% w/w)				
	H_2O	30.0±0.7 (0.998)	24.8±0.5 (0.999)	30.7±0.9 (0.998)	30.9±0.8 (0.998)

	1.0 (LiCl)	33.0±1.9 (0.992)	25.8±0.5 (0.999)	31.3±0.8 (0.998)	31.0±0.8 (0.998)
	1.5 (LiCl)	33.3±1.5 (0.995)	30.0±0.7 (0.999)	29.9±0.8 (0.998)	29.9±0.7 (0.999)
	1.0 ($LiClO_4$)	27.4±1.5 (0.992)	22.1±6.7 (0.783)	32.2±0.5 (0.999)	32.2±0.4 (0.999)
	1.5 ($LiClO_4$)	33.7±1.9 (0.992)	32.1±1.1 (0.997)	32.1±0.9 (0.998)	32.1±0.8 (0.999)
[OMIM]Br (50% w/w)	Aqueous Salt(mol kg^{-1}) (50% w/w)				
	H_2O	30.8±3.2 (0.974)	18.0±0.9 (0.993)	22.1±2.1 (0.975)	22.1±2.2 (0.975)
	1.0 (LiCl)	29.5±2.8 (0.977)	20.9±0.5 (0.999)	25.6±1.6 (0.990)	25.4±1.6 (0.990)
	1.5 (LiCl)	32.3±2.9 (0.980)	19.7±2.2 (0.968)	28.1±0.9 (0.997)	28.1±0.9 (0.997)
	1.0 ($LiClO_4$)	30.8±0.9 (0.998)	19.0±1.4 (0.986)	23.0±2.4 (0.972)	23.0±2.2 (0.976)
	1.5 ($LiClO_4$)	28.7±0.9 (0.997)	20.0±1.1 (0.992)	24.1±1.5 (0.989)	24.2±1.5 (0.990)
[OMIM]Br (80% w/w)	Aqueous Salt(mol kg^{-1}) (20% w/w)				
	H_2O	33.4±0.6 (0.999)	25.1±0.7 (0.999)	40.8±1.2 (0.998)	40.8±1.2 (0.998)
	1.0 (LiCl)	36.1±0.6 (0.999)	28.6±1.0 (0.997)	43.1±0.8 (0.999)	43.1±0.8 (0.999)

1.5 (LiCl)	36.4±0.5	28.9±0.2	39.6±1.0	39.8±3.1
	(0.999)	(0.999)	(0.998)	(0.986)
1.0 ($LiClO_4$)	34.1±1.0	29.2±1.6	40.5±1.0	40.4±1.0
	(0.998)	(0.993)	(0.999)	(0.999)
1.5 ($LiClO_4$)	34.1±0.9	23.3±0.8	37.7±1.6	37.7±1.6
	(0.998)	(0.997)	(0.996)	(0.996)

An insignificant change in the activation energy of translational and rotational motions is observed with the increase in the composition of Li^+ salts. However, there is a considerable increase in the activation energy of both the translational and rotational motions are observed with the increase in the composition of ILs. This is due to the increase in the viscosity of the medium. The activation energy of translational motion of $[OMIM]^+$ is more in each compositions of Li^+ salts as compared to that of the water molecules. However, there is an insignificant change in the rotational activation energy is observed for the above mentioned molecules. The compositions of [OMIM]Br shows interesting behavior on the activation energy of translational and rotational motions. The activation energy of translational motion of $[OMIM]^+$ is more as compared to that of its rotational activation energy in its 50 wt% mixtures; and the reverse order is observed in higher 80 wt% of [OMIM]Br. On the other hand, in each compositions of [OMIM]Br, the translational activation energy of water molecules are lower as compared to that of the rotational activation energy. However, the magnitude of enhancement in the rotational activation energy of water molecules is more as compared to the translational activation energy in the 80 wt% composition of [OMIM]Br as compared to the lower 50 wt% composition. The higher rotational activation energy of $[OMIM]^+$ as compared to the translational activation energy in its 80 wt% composition of [OMIM]Br is possibly due to the stronger π-π interactions between the imidazolium ring of $[OMIM]^+$ which makes the rotation of the cation difficult.

4.3.1.6. Average Flip Distance

The average flip distance of ^{1}H NMR active nuclei is the translational distance travelled by the nuclei during its one flip and is obtained from the equation 15 as

$$< R >= \sqrt{6D\,\tau_2} \qquad (15)$$

where, D and τ_2 are the self-diffusion coefficient and the rotational correlation time of the molecules, respectively.[50] Figure 12a and b represents the average flip distance of $[BMIM]^+$ and $[OMIM]^+$ in their aqueous Li^+ salt solutions, respectively. Increase in the temperature of the medium increase the translational distance travelled by the $[IL]^+$. It is due to the fact that, the local environment of the $[IL]^+$ is more free with the rise in the temperature resulting in the increased $[IL]^+$ jump distance. The reported van der Waals radius from the MM2 and *ab initio* molecular orbital calculations for $[BMIM]^+$ and $[OMIM]^+$ are 0.330 and 0.373 nm, respectively.[53-55] It means the average translational distance travelled by each of the ILs cation is greater than their van der Waals radii indicates that the translational and rotational motion of $[IL]^+$ are not coupled with each other in the studied temperature range.

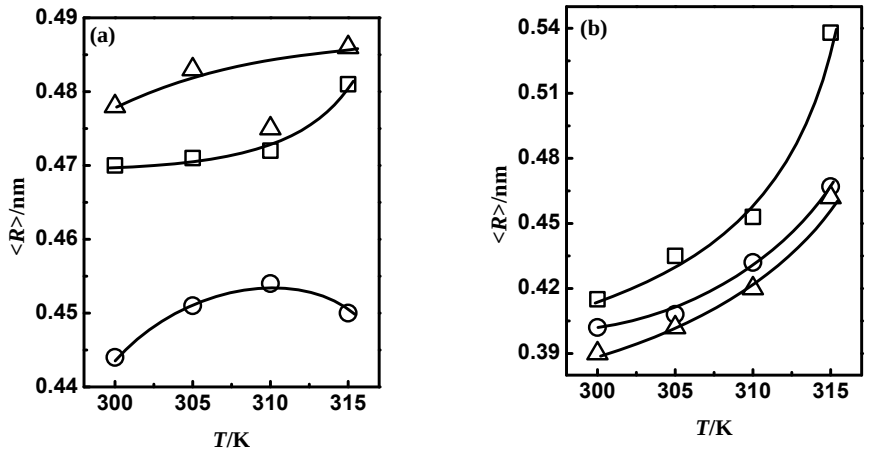

Figure 12. The variation of average flip distance, <*R*> of $[IL]^+$ with the increase in the temperature for [BMIM]Br (a) and [OMIM]Br (b) in its aqueous solutions (□), 0.5 mol kg^{-1} of aqueous LiCl (○) and 0.5 mol kg^{-1} of aqueous $LiClO_4$ (△). The compositions of ILs in each case are fixed as 40% (w/w).

4.3.2. CONCLUSIONS

1) The 3-D nanostructural organization of [OMIM]Br is weakens by the $LiClO_4$ in its aqueous mixtures of [OMIM]Br.

2) The diffusional motion of water molecules are faster as compared to the $[IL]^+$ and the relative diffusional motion ($D_{H2O}/D_{[IL]+}$) decreases with the increase in both the temperature and composition of Li^+ salts.

3) The Li^+ salts decreases the dynamics of $[BMIM]^+$ more as compared to that of the water molecules in the aqueous Li^+ salt solutions of [BMIM]Br.

4) On the other hand, the Li^+ salts decreases the dynamical behavior of $[OMIM]^+$ in its aqueous Li^+ salt solutions of [OMIM]Br as compared to the pure system (without Li^+ salts). However, the dynamics of $[OMIM]^+$ is faster in $LiClO_4$ mixtures as compared to the LiCl. Contrary to this, the water molecule shows opposite behavior.

5) The diffusional motion of the $–C_8H_{17}$ side chain of [OMIM]Br increases in the order of $D_f < D_g < D_h$ in the aqueous Li^+ salt solutions of [OMIM]Br and the trend is not altered with the rise in the temperature of the medium.

6) The acidic nature of C2 proton of imidazolium ring increases by LiCl whereas $LiClO_4$ decrease it in its aqueous Li^+ salt solutions of ILs as compared to the pure system (without any Li^+ salts).

7) An increase in the temperature of the medium increases the bond length of both the C2 proton and terminal alkyl group protons (h) of ILs suggesting the increased acidic nature of protons.

8) Increase in the compositions of ILs increase the acidic nature of the C2 proton whereas it decreases the acidic nature of terminal alkyl group protons (h) of ILs.

9) The rotational motion of $[IL]^+$ is faster as compared to the translational motion and increase in the compositions of ILs increase their correlation time values suggesting the slower in their translational and rotational motion.

10) The addition of Li^+ salts has insignificant effect in both the translational and rotational motion of $[BMIM]^+$; however, $LiClO_4$ increase both the motion of $[OMIM]^+$ more as compared to the LiCl.

11) The deviation in the magnitude of translational motion of water molecules is insignificant with the change in both the ILs and compositions of Li^+ salts. However, rotational motion of water molecules shows substantial change with the change in both the ILs and Li^+ salts.

12) Increase in the compositions of ILs increase both the activation energy of viscous, E_η and diffusive flow ($E_{D,[IL]+}$ and $E_{D,H2O}$).

13) The activation energy of translational motion of $[OMIM]^+$ is more as compared to the rotational activation energy in its 50 wt% composition and the trend is being reversed with the increase in the compositions to 80 wt% possibly due to the stronger π-π interactions between the imidazolium ring. On the other hand, the rotational activation energy of water molecules is more as compared to the translational activation energy in both the compositions of [OMIM]Br.

14) The average flip distance travelled by each of the ILs is greater than their van der Waals radii suggesting that the $\tau_{t[IL]+}$ and $\tau_{2[IL]+}$ are not coupled with each other.

4.4. On the Validity of Stokes-Einstein Equation in the Aqueous Li^+ Mixtures of ILs

4.4.1. RESULTS AND DISCUSSION

4.4.1.1 Stokes-Einstein Relationship

The relationship between the self-diffusion of a 'stokes' (hydrodynamic) particle with the bulk viscosity of the medium can be explained by the help of Stokes-Einstein equation 16 as

$$D = \frac{1}{ca}\frac{kT}{\pi\eta} \qquad (16)$$

and is generally valid for classical hydrodynamic systems.[56] In the Stokes-Einstein equation D, η, a, k and T are the self-diffusion coefficient, bulk viscosity, van der Waals radii of diffusing particle, Boltzmann constant and absolute temperature of the medium, respectively. c, the coupling factor is theoretically ranges between 4 and 6 for slip and stick boundary conditions, respectively.[57,58]

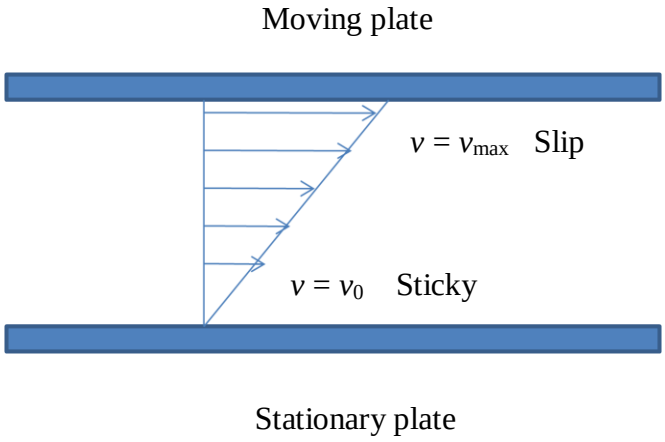

Figure 13. Schematic representation of a fluid showing the 'slip' and 'sticky' boundary condition.

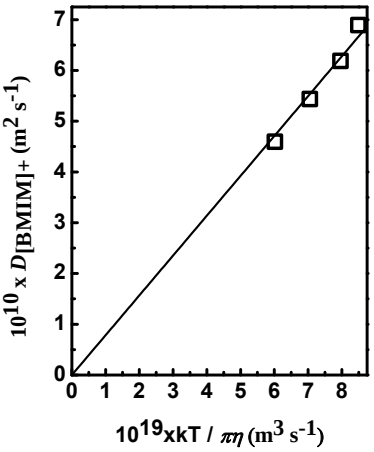

Figure 14. Stokes-Einstein (SE) plot for the $D_{[BMIM]+}$ in the aqueous solutions of [BMIM]Br (40 wt%). The line is of the linear fit with the correlation coefficient (r^2) value of 0.999.

The physical meaning of the boundary condition can be well understood from the Figure 13. Consider the flow of a fluid which is placed in between the two plates as represented in the Figure 13. The bottom plate is the stationary plate and the fluid attached to it has the zero velocity (v_0) and is considered as 'sticky' in nature. On the other hand, the top plate is moving and the fluid attached to it has the maximum velocity (v_{max}) and is considered to be 'slipy' in nature. The boundary condition of a diffusing particle can be obtained by the plot of the D with the $kT/\pi\eta$ by fixing the intercept value to zero. The slope represents the $1/ca$ from which the value of c can be calculated. In the Figure 14, a sample Stokes-Einstein (SE) plot is represented for the $D_{[BMIM]+}$ in its 40 wt% aqueous solutions of [BMIM]Br. The SE coupling factor (c) for the $[IL]^+$ and water molecules are given in the Table 6 and 7, respectively. The values of c for the $[IL]^+$ are in the range of 3.8-4.4 and are closer to the 'slip' boundary conditions. On the other hand, the c values for the water molecules are in between the range of 0.4-1.7 and are deviating from the Stokes-Einstein boundary conditions. It means the classical hydrodynamic conditions are strictly invalid when the diffusing particle is the water molecules in the aqueous Li^+ salt solutions of ILs. It was reported that the value of SE coupling factor, c is 6 for the ideal hydrodynamic systems and is nearly 4 for ionic liquids.[59] The value of c closer to 4 for the $[IL]^+$ in the aqueous Li^+ salt solutions of ILs is in accordance with the reported literature values.[59]

Table 6. The SE Coefficient Values for the $[IL]^+$ in the Aqueous Li^+ Salt Solutions of ILs.

IL	System	m (1/ca)/m^{-1}	ca/nm	c ($[IL]^+$)
[BMIM]Br	Aqueous salt (mol kg^{-1}),			
(40 wt%)	60 wt%			
	H_2O	7.85×10^8	1.27	3.86
	0.5 mol kg^{-1} LiCl	7.07×10^8	1.41	4.28
	0.5 mol kg^{-1} $LiClO_4$	8.04×10^8	1.24	3.77
[OMIM]Br	Aqueous salt (mol kg^{-1}),			
(50 wt%)	50 wt%			

	H_2O	6.68×10^8	1.50	4.01
	0.5 mol kg^{-1} LiCl	6.28×10^8	1.59	4.27
	0.5 mol kg^{-1} $LiClO_4$	6.10×10^8	1.64	4.39

Table 7. The SE Coefficient Values for the H_2O Molecules in the Aqueous Li^+ Salt Solutions of ILs.

IL	System	m (1/ca)/m^{-1}	ca/nm	c (H_2O)
[BMIM]Br	Aqueous salt (mol kg^{-1}),			
(40 wt%)	60 wt%			
	H_2O	2.40×10^9	0.42	1.48
	0.5 mol kg^{-1} LiCl	2.07×10^9	0.48	1.71
	0.5 mol kg^{-1} $LiClO_4$	2.50×10^9	0.41	1.45
[OMIM]Br	Aqueous salt (mol kg^{-1}),			
(50 wt%)	50 wt%			
	H_2O	1.03×10^{10}	0.10	0.35
	0.5 mol kg^{-1} LiCl	1.01×10^{10}	0.10	0.35
	0.5 mol kg^{-1} $LiClO_4$	8.98×10^9	0.11	0.39

4.4.1.2 Frictional Coefficient (*f*) and Microviscosity

According to Stokes the value of frictional coefficient, $f = 6\pi\eta a$ for a particle of spherical nature of radius a moving with a uniform velocity in a continuous fluid of viscosity, η.[56] The principle of classical hydrodynamics states that, the movement of a spherical particle is obstructed by a force due to the pressure built in front of it (= $4\pi\eta a$) and a frictional force parallel to its surface (= $2\pi\eta a$). Therefore, the cost of energy required for the flow of a particle inside a fluid is equal to the frictional coefficient, *f*. Therefore, for a 'perfectly sticking' condition both the forces add up to give the value of $f = 6\pi\eta a$. On the other hand, for the 'perfectly sliding' condition no frictional forces are

acting parallel to the flow of the particle and in that condition the frictional coefficient is reduced to $f = 4\pi\eta a$. Similarly, the $[IL]^+$ and water molecules also have to overcome certain amount of frictional force (f) in order to flow inside its fluid mixtures. Thus, by applying this concept, we have calculated the values of frictional coefficient, f for the $[OMIM]^+$ inside the aqueous Li^+ salt solutions of [OMIM]Br and the values are given in the Table 8. The dimension of the frictional coefficient, f is similar to that of the dimension of force per unit displacement of the particle. It means the frictional coefficient of the particles is a measure of the frictional force experienced by the particle inside its fluid mixtures per unit displacement. As microviscosity of a particle or molecule is the frictional force experienced by it per its unit motion. Therefore, this frictional coefficient factor, f can be used as an alternative qualitative measurement for the microviscosity experienced by the diffusing particle inside the fluid mixtures. It is illustrated in the Table 8 that the increase in the temperature of the medium decreases the frictional coefficient, f experienced by the $[OMIM]^+$. It means the microviscosity experienced by the $[OMIM]^+$ decreases with the increase in the temperature of the medium.

Table 8. The Frictional Coefficients (f) Experienced by the $[OMIM]^+$ Inside its Aqueous Solutions.

System	T/K	η/mPa.s	f ($c\pi\eta a$) / kg.s^{-1}
[OMIM]Br 50 % (w/w) in H_2O	300	11.10	5.22×10^{-11}
	305	9.33	4.38×10^{-11}
	310	8.48	3.98×10^{-11}
	315	7.68	3.61×10^{-11}

4.4.1.3 Hole Formation

The diffusional motion of charged species inside the solutions can also be explained by the help of Hole theory. It was Furth[60] who first introduced the Hole theory in order to

explain the liquid state of a material and later on developed by Bockris et al. for the use of molten salts.[61] The Hole formation theory can also be successfully applied to Deep Eutectic Solvents (DES) in which the diffusional motion of different species present in it can be correlated with the availability of appropriate dimension of hole to accommodate the diffusing particles.[62] Many reports are also available in the literature in order to explain the diffusional motion of ionic liquids through the help of Hole formation theory.[56,62,63] Recently, Abbott and co-workers proposed a hole-hopping mechanism in order to explain the diffusional motion of ILs.[63-65] They have explained that there is a successive destruction and creation of holes are taking place inside the IL fluids due to its random fluctuations and the diffusional motion of IL molecules takes place through a series of 'jumps' between these 'holes'. To the best of our knowledge there has not been a single report is available in the literature to describe the Hole formation in the aqueous salt solutions of ILs.

Table 9. The Calculated Size of Hole of $[IL]^+$ in the Aqueous Li^+ Salt Solutions of ILs.

System	T/K	$D_{[IL]^+}\times10^{10}$/m^2 s^{-1}	η/mPa.s	ξ/pm
50%[BMIM]Br (w/w) (in H_2O)	300	3.535	2.97	209
	305	4.271	2.57	203
	310	4.934	2.26	203
	315	5.273	2.05	213
50%[OMIM]Br (w/w) (in H_2O)	300	0.727	11.10	271
	305	0.861	9.33	277
	310	1.134	8.48	235
	315	1.267	7.68	236

Here, we have applied this Hole formation theory in order to explain the diffusional motion of ILs in its aqueous Li^+ salt solutions of ILs. According to the hole formation theory, the correlation length, ξ, is a measure of the size of the hole into which the diffusing particle can jump. This correlation length of the diffusing particle is physically

related to the hydrodynamic radii and can be obtained from the Stokes-Einstein equation 17 as

$$\xi = \frac{k_B T}{6\pi\eta D} \qquad (17)$$

where, the symbols have their usual meaning.[56] The calculated values of the hole-radii for the $[IL]^+$ in its aqueous Li^+ salt solutions of ILs are shown in the Table 9. The hole-radii for the $[OMIM]^+$ is greater than that of $[BMIM]^+$ and also is smaller than their van der Waals radii of 330 and 373 pm for $[BMIM]^+$ and $[OMIM]^+$, respectively.[53,54] The temperature dependent deviation in the values of the hole-radii for $[IL]^+$ is may be due to the inaccuracy in their estimation. Therefore, more accurate estimation of the hole-radii is necessary to test and understand the applicability of hole formation theory in the diffusion-based studies of aqueous salt solutions of ILs.

4.4.2. CONCLUSIONS

In short, we conclude:

1) The frictional coefficient, f of a diffusing particle can qualitatively gives the information regarding the microviscosity experienced by the diffusing particles in the aqueous Li^+ salt solutions of ILs,

2) The classical Stokes-Einstein equation is not valid for the diffusional motion of water molecules, and

3) The calculated size of the hole for $[BMIM]^+$ is less as compared to that of the $[OMIM]^+$ and are less than their van der Waals radii.

4.6. REFERENCES

(1) Wang, Y.; Voth, G. A. *J. Am. Chem. Soc.* **2005**, *127*, 12192-12193.

(2) Wang, Y.; Voth, G. A. *J. Phys. Chem. B* **2006**, *110*, 18601-18608.

(3) J.N.A.C. Lopes, A. A. H. P. *J. Phys. Chem. B* **2006**, *110*, 3330-3335.

(4) Raabe, G.; Kohler, J. *J. Chem. Phys.* **2008**, *128*, 154509.

(5) Xiao, D.; Rajian, J. R.; Cady, A.; Li, S.; Bartsch, R. A.; Quitevis, E. L. *J. Phys. Chem. B* **2007**, *111*, 4669-4677.

(6) Tran, C. D.; De Paoli Lacerda, S. H.; Oliveira, D. *Appl. Spectrosc.* **2003**, *57*, 152-157.

(7) Jiang, W.; Wang, Y.; Voth, G. A. *J. Phys. Chem. B* **2007**, *111*, 4812-4818.

(8) Niu, J.; Qiu, H.; Li, J.; Liu, X.; Jiang, S. *Chromatographia* **2009**, *69*, 1093-1096.

(9) Qiu, H.; Zhang, Q.; Chen, L.; Liu, X.; Jiang, S. *J. Sep. Sci.* **2008**, *31*, 2791-2796.

(10) Bowers, J.; Butts, C. P.; Martin, P. J.; Vergara-Gutierrez, M. C.; Heenan, R. K. *Langmuir* **2004**, *20*, 2191-2198.

(11) Zhang, H.; Li, K.; Liang, H.; Wang, J. *Colloids and Surf. A: Physicochemical and Engineering Aspects* **2008**, *329*, 75-81.

(12) Dong, B.; Zhao, X.; Zheng, L.; Zhang, J.; Li, N.; Inoue, T. *Colloids and Surf. A: Physicochemical and Engineering Aspects* **2008**, *317*, 666-672.

(13) Luczak, J.; Hupka, J.; Thoming, J.; Jungnickel, C. *Colloids and Surf. A: Physicochemical and Engineering Aspects* **2008**, *329*, 125-133.

(14) Fazio, B.; Triolo, A.; Di Marco, G. *J. Raman Spectrosc.* **2008**, *39*, 233-237.

(15) Sun, B.; Jin, Q.; Tan, L.; Wu, P.; Yan, F. *J. Phys. Chem. B* **2008**, *112*, 14251-14259.

(16) Bhargava, B. L.; Klein, M. L. *J. Phys. Chem. B* **2009**, *113*, 9499-9505.

(17) Bowers, J.; Vergara-Gutierrez, M. C.; Webster, J. R. P. *Langmuir* **2004**, *20*, 309-312.

(18) Baldelli, S. *J. Phys. Chem. B* **2003**, *107*, 6148-6152.

(19) Lynden-Bell, R. M. *Mol. Phys.* **2003**, *101*, 2625-2633.

(20) Lynden-Bell, R. M.; Del Popolo, M. *Phys. Chem. Chem. Phys.* **2006**, *8*, 949-954.

(21) Lynden-Bell, R. M.; Kohanoff, J.; Del Popolo, M. G. *Faraday Discuss.* **2005**, *129*, 57-67.

(22) Yan, T.; Li, S.; Jiang, W.; Gao, X.; Xiang, B.; Voth, G. A. *J. Phys. Chem. B* **2006**, *110*, 1800-1806.

(23) Kazarian, S. G.; Briscoe, B. J.; Welton, T. *Chem. Commun.* **2000**, 2047-2048.

(24) Sudhir, N. V. K. *Chem. Commun.* **2001**, 413-414.

(25) Cammarata, L.; Kazarian, S. G.; Salter, P. A.; Welton, T. *Phys. Chem. Chem. Phys.* **2001**, *3*, 5192-5200.

(26) Hofmeister, F. *Archiv. Exp. Pathol. Pharmakl.* **1888**, *24*, 247-260.

(27) Zhang, Y.; Furyk, S.; Bergbreiter, D. E.; Cremer, P. S. *J. Am. Chem. Soc.* **2005**, *127*, 14505-14510.

(28) Breslow, R.; Rizzo, C. J. *J. Am. Chem. Soc.* **1991**, *113*, 4340-4341.

(29) Lo Nostro, P.; Ninham, B. W. *Chem. Rev.* **2012**, *112*, 2286-2322.

(30) Collins, K. D. *Methods* **2004**, *34*, 300-311.

(31) Freire, M. G.; Neves, C. M. S. S.; Silva, A. M. S.; Santos, L. s. M.; Marrucho, I. M.; Rebelo, L. P. N.; Shah, J. K.; Maginn, E. J.; Coutinho, J. A. P. *J. Phys. Chem. B* **2010**, *114*, 2004-2014.

(32) Bonhote, P.; Dias, A.-P.; Papageorgiou, N.; Kalyanasundaram, K.; Gratzel, M. *Inorg. Chem.* **1996**, *35*, 1168-1178.

(33) Suarez, P. A. Z.; Einloft, S.; Dullius, J. E. L.; De Souza, R. F.; Dupont, J. *J. Chim. Phys.* **1998**, *95*, 1626-1639.

(34) Huddleston, J. G.; Visser, A. E.; Reichert, W. M.; Willauer, H. D.; Broker, G. A.; Rogers, R. D. *Green Chem.* **2001**, *3*, 156-164.

(35) Noda, A.; Hayamizu, K.; Watanabe, M. *J. Phys. Chem. B* **2001**, *105*, 4603-4610.

(36) Nanda, R.; Kumar, A. *Ind. J. Chem.* **2013**, *52*, 1377-1382.

(37) Nanda, R.; Kumar, A. *J. Phys. Chem. B* **2015,** *119*, 1641-1653.

(38) Gibbs, S. J.; Johnson Jr, C. S. *J. Magn. Reson.* **1991**, *93*, 395-402.

(39) Stejskal, E. O.; Tanner, J. E. *J. Chem. Phys.* **1965**, *42*, 288-292.

(40) Zhang, Q.-G.; Xue, F.; Tong, J.; Guan, W.; Wang, B. *J. Solution Chem.* **2006**, *35*, 297-309.

(41) Isono, T. *J. Chem. Eng. Data* **1984**, *29*, 45-52.

(42) Lopez□Leon, T.; Ortega□Vinuesa, J. L.; Bastos□Gonzalez, D. *ChemPhysChem* **2012**, *13*, 2382-2391.

(43) Franks, F. *Water, a Comprehensive Treatise: Recent advances*; Plenum Press, 1972.

(44) Tokuda, H.; Tsuzuki, S.; Susan, M. A. B. H.; Hayamizu, K.; Watanabe, M. *J. Phys. Chem. B* **2006**, *110*, 19593-19600.

(45) Zhao, Y.; Gao, S.; Wang, J.; Tang, J. *J. Phys. Chem. B* **2008**, *112*, 2031-2039.

(46) Miran, M. S.; Kinoshita, H.; Yasuda, T.; Susan, M. A. B. H.; Watanabe, M. *Chem. Commun.* **2011**, *47*, 12676-12678.

(47) Singh, T.; Kumar, A. *J. Chem. Thermodyn.* **2011**, *43*, 958-965.

(48) Breslow, R.; Guo, T. *Proc. Natl. Acad. Sci.* **1990**, *87*, 167-169.

(49) Golubev, N. S.; Denisov, G. S.; Smirnov, S. N.; Shchepkin, D. N.; Limbach, H.-H. *Zeitschrift Phys. Chemie* **1996**, *196*, 73-84.

(50) Hayamizu, K.; Tsuzuki, S.; Seki, S.; Umebayashi, Y. *J. Chem. Phys.* **2011**, *135*, 084505.

(51) Hayamizu, K.; Tsuzuki, S.; Seki, S.; Fujii, K.; Suenaga, M.; Umebayashi, Y. *J. Chem. Phys.* **2010**, *133*, 194505.

(52) Kumar, A. *Chem. Rev.* **2001**, *101*, 1-20.

(53) Ue, M. *J. Electrochem. Soc.* **1994**, *141*, 3336-3342.

(54) Ue, M.; Murakami, A.; Nakamura, S. *J. Electrochem. Soc.* **2002**, *149*, A1385-A1388.

(55) Tokuda, H.; Hayamizu, K.; Ishii, K.; Susan, M. A. B. H.; Watanabe, M. *J. Phys. Chem. B* **2005**, *109*, 6103-6110.

(56) Lovelock, K. R. J.; Ejigu, A.; Loh, S. F.; Men, S.; Licence, P.; Walsh, D. A. *Phys. Chem. Chem. Phys.* **2011**, *13*, 10155-10164.

(57) Price, W. S. *NMR Studies of Translational Motion: Principles and Applications*; Cambridge University Press, 2009.

(58) Tyrrell, H. J. V.; Harris, K. R. *London, England* **1984**.

(59) Martinelli, A.; Marechal, M.; Ostlund, A.; Cambedouzou, J. *Phys. Chem. Chem. Phys.* **2013**, *15*, 5510-5517.

(60) Furth, R. In *Mathematical Proceedings of the Cambridge Philosophical Society*; Cambridge Univ Press: 1941; Vol. 37, p 252-275.

(61) Bockris, J. M.; Hooper, G. W. *Discuss. Faraday Soc.* **1961**, *32*, 218-236.

(62) Abbott, A. P.; Boothby, D.; Capper, G.; Davies, D. L.; Rasheed, R. K. *J. Am. Chem. Soc.* **2004**, *126*, 9142-9147.

(63) Abbott, A. P.; Harris, R. C.; Ryder, K. S. *J. Phys. Chem. B* **2007**, *111*, 4910-4913.

(64) Taylor, A. W.; Licence, P.; Abbott, A. P. *Phys. Chem. Chem. Phys.* **2011**, *13*, 10147-10154.

(65) Abbott, A. P. *ChemPhysChem* **2005**, *6*, 2502-2505.

CHAPTER 5

An Insight into the Microviscosity and Microporsity in the Ionic Liquid-based Microemulsion

The physical properties like microviscosity, micropolarity, diffusion coefficients and pH of the aqueous ionic liquid (IL) confined media has been discussed in this chapter. NMR relaxation technique has been used to estimate the microviscosity and pH of the aqueous IL confined media. A comparative discussion between the bulk viscosity, η_{bulk} and microviscosity, η_{micro} has been presented. A model is proposed to estimate the mole fraction of bound and free water molecules present inside the miceller core. The rate of proton transfer phenomenon has been discussed by the approach of NMR spin-spin relaxation time, T_2 and correlated with the pH of the aqueous IL confined media.

5.1. INTRODUCTION

This chapter is devoted to the measurement and understanding of transport properties of aqueous ionic liquid confined media. The confined water is ubiquitous in nature like in cellular organelle of biological species,[1] water inside the reverse micelles,[2-7] and microemulsions.[8-14] Reverse micelles or microemulsions are thermodynamically stable, an isotropic mixture of oil and water with a surfactant or a mixture of surfactants and frequently in combination with a cosurfactant.[15] Structurally, there are three different kinds of microemulsions are present; water in oil (W/O) where water is the dispersed phase and oil is the dispersion medium, oil in water (O/W) where oil is the dispersed phase and water is the dispersion medium, and the bicontinuous structure where both the oil and water is present as the continuous phase.[15-17] Many reports are available in the literature regarding the study of aqueous[8-14] and non-aqueous[18] microemulsions with oil as a dispersion medium. However, the use of volatile organic solvents for the preparation of microemulsions or reverse micelles is not an environmental benign process. These hazardous volatile organic solvents are therefore replaced by ionic liquids (ILs). There are reports are available in the literature for the preparation and characterization of IL-based microemulsions by using a variety of techniques.[13,16,17] ILs are either used as hydrophobic solvents by the replacement of oil phase[13,16,17] or used as the hydrophilic phase[19-24] by replacing the aqueous phase in IL-based microemulsions. The most studied hydrophobic IL in the case of aqueous hydrophobic IL-based microemulsions is [BMIM][PF_6].[13,16,17] However, the hydrolysis of [PF_6]$^-$ of ILs yields HF molecules and makes the system acidic.[25,26] This is a severe limitation of using [PF_6]$^-$ as anion in ILs for the preparation of microemulsions. For that reason incorrect information about the physicochemical properties of aqueous confined media may be obtained. Therefore we have replaced the use of [PF_6]$^-$ by a [NTf_2]$^-$ based IL and the cation of the IL is dibutylimidazolium ([BBIM]$^+$) which are stable towards the hydrolysis. There are reports in the literature regarding the determination of physicochemical properties of water in IL microemulsions by taking hydrophobic IL as the dispersion medium.[16,27] However to the best of our knowledge there has not been a single report is available in the literature regarding the determination of physicochemical properties of aqueous microemulsions containing hydrophobic [NTf_2]$^-$ based ionic liquids. In this report for the first time we

have studied the physicochemical properties of [BBIM][NTf_2]/H_2O/TX-100 microemulsions and are discussed below.

5.2. EXPERIMENTAL SECTION

5.2.1. Materials.

Materials required for the synthesis of ionic liquid like 1-butyl imidazole (99.9% purity), butyl bromide (99.9% purity) and $LiNTf_2$ (99.98% purity) were purchased from Sigma Aldrich. Non-ionic surfactant, Triton X-100 (98.5% purity) was purchased from Fluka Analyticals. $K_4Fe(CN)_6$ (99.95% purity), used as an electrochemically active probe for the cyclic voltammetric study was purchased from Sigma Aldrich. Methyl orange (MO) (99% purity) used for the UV-vis spectrophotometric study was purchased from Sigma Aldrich. Distilled deionized water having electrical resistivity of 18.2 MΩ cm was obtained from a Millipore MilliQ unit for the preparation of microemulsions.

5.2.2. Synthesis of Ionic Liquid.

The hydrophobic dibutylimidazolium bis(trifluoromethanesulfonyl)imide ([BBIM][NTf_2]) ionic liquid was synthesized according to the reported procedure.[28] First the quaternization reaction between the butylimidazole and butyl bromide yields the dibutylimidazolium bromide [BBIM]Br. In the next step the exchange of anion between the Br^- of [BBIM]Br and NTf_2^- of $LiNTf_2$ (metathesis reaction) takes place in water as the solvent medium. Then the prepared IL was separated through a separating funnel with dichloromethane (DCM). High vacuum was used to remove the excess amount of solvent (both the water and DCM) from the IL. It was ensured that the water content in each IL sample was less than 50 ppm. ^1H NMR spectra was taken for the synthesized ionic liquid which did not show any trace amount of impurity in the sample. The IL was also checked for any halide impurities which was less than 50 ppm.[29]

5.2.3. Preparation of Microemulsions.

[BBIM][NTf_2]/H_2O/TX-100 microemulsions were prepared by fixing I = 0.05 and 0.1 with the varying wt% of water. Then the solutions were stirred in a vortex mixer up to the formation of clear, homogeneous and optically transparent solutions. Those solutions were kept over months and no phase separation was observed which indicates the stability of the prepared microemulsions.

5.3. APPARATUS AND PROCEDURE

5.3.1. Phase Equilibria.

Solubility measurements were performed to construct the ternary phase diagram for [BBIM][NTf_2]/H_2O/TX-100. The samples were placed in a glass jacket with an inlet-outlet water circulating system connected externally to a Julabo thermostat to regulate the temperature of the system. All the measurements were performed at a temperature of 298.15±0.01 K. The ternary phase diagram for the [BBIM][NTf_2]/H_2O/TX-100 system was constructed through the visual detection of solution with a transition from a clear to a turbid solution.

5.3.2. Cyclic Voltammetry.

Electrochemical properties were investigated by cyclic voltammetric (CV) technique[17] using a BioLogic Science Instrument in a conventional three-electrode cell, where Pt foil was used as the counter electrode, Ag/AgCl as the reference electrode and glassy carbon as the working electrode (WE). Before its use (WE) in the electrochemical study it was polished with a 0.3μm aluminum oxide slurries and was sonicated several times alternately with deionized water and ethanol and dried under lamp. The area of the WE was determined using cyclic voltammetric experiment by taking a reversible system of 4 mM $K_3Fe(CN)_6$ in 1 M KCl solution with the diffusion coefficient D = 6.36 X 10^{-10} m^2 s^{-1}.[17] The calculated surface area of the working electrode was found to be 1.53 X 10^{-2} m^2. The potential was scanned between +0.5 to -0.5 V and the sweep rate were changed from 25-100 mV s^{-1}. Potassium ferrocyanide $K_4Fe(CN)_6$ was used as the electrochemically active probe in all the microemulsion systems and the temperature used throughout the study was kept constant as 298.15±0.1 K.

5.3.3. Dynamic Light Scattering.

The hydrodynamic diameters of aqueous ionic liquid microemulsions were determined by dynamic light scattering technique (BIC 90 Plus Particle Size Analyser, Brookhaven Instruments Corporation, USA). All the microemulsion samples were filtered through the 0.22μm PTFE membrane filters procured from RanDisc. The samples were prepared under the condition of inert atmosphere and were taken in a cuvette. Precautions were made to avoid any kind of bubbles formed inside the microemulsion samples. All the

measurements were made with a scattering angle of 90^0 at a temperature of 298.15±0.1 K.

5.3.4. UV-vis Spectroscopy.

The stock solutions of the methyl orange (UV-vis spectroscopic probe) were prepared in the methanol prior to their use. The stock solution was added dropwise into the microemulsion samples and the methanol (solvent) was evaporated under vacuum. The sample containing the probe was transferred to a quartz cuvette under a nitrogen atmosphere and sealed with a septum. The λ_{max} values were measured at 298.15 K by using a UV-visible spectrophotometer and the temperature of the cell was monitored using a single cell accessory with an accuracy of ±0.01 K.

5.3.5. pH Measurements.

Different pH solutions were prepared by titrating 0.1 M NaOH (98.5% purity, Fluka) with 0.5 M H_2SO_4 (98.5% purity, Fluka). A digital pH meter was used (Global Digital pH Meter, Model No-504) to measure the pH of the aqueous core (pH of the aqueous solutions were measured externally prior to the formation of microemulsions) in the range of 2.0-9.5.

5.3.6. Viscosity Measurement.

The viscosity of aqueous ionic liquid microemulsion systems were measured using Brookfield-ultra rheometer with cone plate arrangement. Temperature of the samples was monitored by a Julabo constant temperature thermostat bath with an accuracy of ±0.01 K. The viscosity (η) values of the solutions were obtained through the equation as:

$$\eta = (100/RPM)\ (TK)\ (Torque)\ (SMC) \qquad (1)$$

Where RPM, TK (0.09373) and SMC (0.327) are the speed, viscometer torque constant and spindle multiplier constant respectively. The calibration of the instrument was performed by taking the reported viscosity data of aqueous solutions of $CaCl_2$, $MgCl_2$ and [BMIM][BF_4] with different concentration.[30,31] The accuracy of the instrument was obtained as ±1%.

5.3.7. NMR Study.

All NMR experiments were performed on a Bruker-400 NMR spectrometer operating at a ^{1}H resonance frequency of 400MHz, at 298.15±0.1 K. Analysis of neat samples was performed in a 5 mm (outside diameter) NMR tube using D_2O in a capillary tube as external lock. All the spectra were collected by using a one pulse sequence, [30^0-flip angle] with 32k complex data points. A spectral width of 20 ppm and a repetition time of 2s were used with the averaging of eight signals. Heteronuclear single quantum coherence (HSQC) experiment was performed to differentiate the water signal from other signals present in the microemulsion system. Spin-lattice relaxation times (T_1) were measured by inversion recovery method, [180^0_x-τ-90^0_x-acq], performing 34 experiments with delay time (τ) ranging from 2 ms to 5 s. Spin-spin relaxation times (T_2) were measured by using CPMG method, [90^0_x-(τ-180^0_y-τ)$_m$-acq], performing 34 experiments with varying the numbers of echoes.

5.4. RESULTS AND DISCUSSION

5.4.1. The Ternary Phase Diagram.

In the following we describe the results of our investigation. The construction of phase diagram is essential for the study of microemulsions because the hydrophilic part of the non-ionic TX-100 surfactant molecule is greater than that of the hydrophobic part and for that reason the phase behavior might be very sensitive to the nature of solvent used.[32]

Herein, we have taken a hydrophobic IL i.e. [BBIM][NTf_2], which acts as the oil phase and one of the most common non-ionic surfactant, TX-100 for constructing the ternary phase diagram with water. The phase diagram of the ternary system containing H_2O, [BBIM][NTf_2] and TX-100 was constructed through the solubility measurements and is depicted in Figure 1. The ternary phase diagram constitutes of one multiphase zone and one single phase zone. Our study was mainly focused on the single phase zone. The single phase-zone constitutes of three microheterogeneous regions.[16] The W/IL system, in which water is the dispersed phase and IL as the dispersion medium, IL/W where IL is the dispersed phase and water is the dispersion medium, and the bicontinuous zone[33], where both water and IL are present as the continuous phase. These microheterogeneous

regions have been detected through the measurement of bulk viscosity[34] and the measurements of diffusion coefficients of an electrochemically active probe with the help of cyclic voltammetric technique.[35]

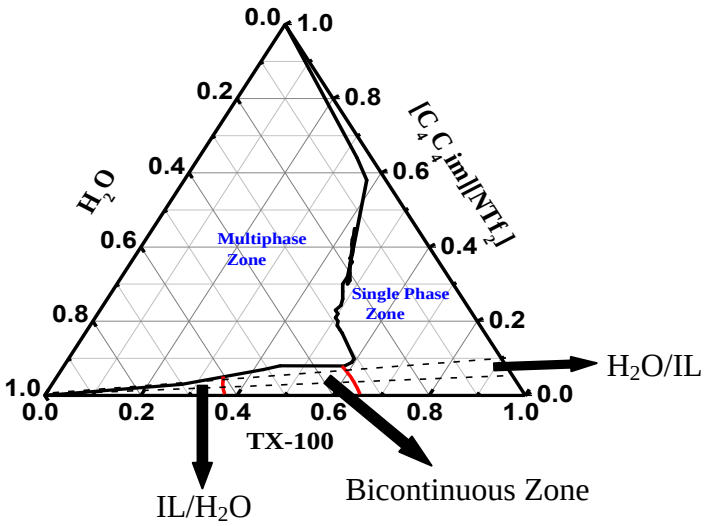

Figure 1. The ternary phase diagram of the [BBIM][NTf_2]/H_2O/TX-100 system showing change in the microheterogeneous regions from H_2O/IL to bicontinuous to IL/H_2O at 298.15 K. The dashed lines are chosen for studying the apparent diffusion coefficient with initial [IL]/[TX-100] weight fractions are 0.05 and 0.1.

5.4.2. Viscosity.

To detect the microheterogeneous regions we measured the viscosity by taking I = 0.05 (I = [BBIM][NTf_2]-to-TX-100 weight ratio). The plot of viscosity of the mixtures with the increase in wt% of water is shown in Figure 2. The plot shows an initial shoot in the viscosity at about 40 wt% reaching to a maximum value at about 45 wt% before falling further in higher wt% of water. There is a change in the shape of the plot at about 65-70 wt%. The initial increase in the viscosity with the addition of water suggests the formation of microstructure inside the single phase zone of the ternary phase diagram.[34] If there are no microheterogeneous regions inside the single phase zone, the initial addition of water should lower the viscosity of the ternary mixture. The zone up to about 40 wt% of water indicates the structural transition from W/IL microemulsions to bicontinuous structural zone supported by the reports about the structural transition from

droplet W/O to bicontinuous microemulsions.[36] The deviation from the linearity observed at around 70 wt% of water indicates the structural transition from bicontinuous to IL/W microemulsion zone.[34] Inside the bicontinuous microemulsions regions, the change in the viscosity behavior is may be due to the possibility of formation of some kind of structural changes at around 45 wt% of water.[36] The continuous decrease in viscosity observed in the case of bicontinuous microemulsions zones may be due to the dynamic nature of the region.

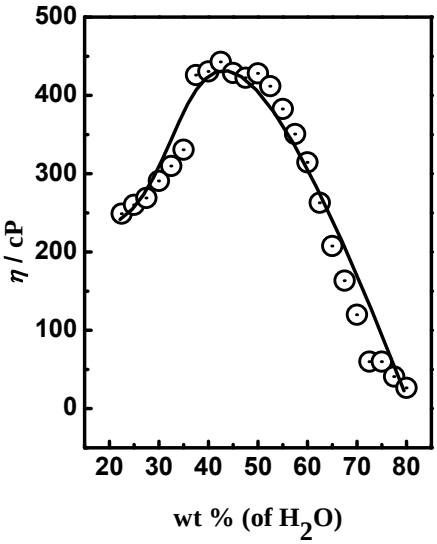

Figure 2. Dynamic viscosity, η of the [BBIM][NTf_2]/H_2O/TX-100 microemulsions with increasing wt % of water (I = 0.05).

In this region, the discrete particle nature of W/IL microemulsion droplets vanishes and both the water and ionic liquid phases are in a state of continuous dynamics with each other. Therefore the viscosity of the bicontinuous microstructure decreases continuously with the increase in the wt% of water. Again, as viscosity is a bulk property, therefore it does not give us the correct information regarding the determination of structural transition points inside the single phase zone of microemulsions. For this reason, we carried out the diffusion coefficients measurements of an electrochemically active probe inside the microemulsion system with the help of cyclic voltammetric technique. This is discussed below:

5.4.3. Diffusion Behavior of Electrochemically Active $K_4Fe(CN)_6$ Probe Inside the Microemulsion.

Several techniques like pulsed-gradient spin echo NMR,[37-39] dynamic light scattering[40,41] and cyclic voltammetry[42,43] are used for the study of microstructural transition of the miceller systems. In this investigation, we used the cyclic voltammetric technique for the detection of microheterogeneous regions inside the ternary phase diagram. The apparent diffusion coefficient measurements were performed through the cyclic voltammetric technique by taking the potassium ferrocyanide [$K_4Fe(CN)_6$] as the electrochemically active probe[17] inside the [BBIM][NTf_2]/H_2O/TX-100 ternary system and is represented in Table 1. The peak currents of the redox reversible systems (Fe^{+2}/Fe^{+3}) are measured with different scan rate and the apparent diffusion coefficients are calculated by applying the Randles-Sevick equation given by:

$$i_P = \frac{0.447F^{3/2}An^{3/2}D^{1/2}Cv^{1/2}}{R^{1/2}T^{1/2}} \qquad (2)$$

where *n* is the number of electrons involved in the redox reaction, *A* is the working area of the electrode, *D* is the diffusion coefficient of the electrochemically active probe in the solution, *C* is the concentration of the electroactive probe in the solution, ν is the sweep rate or scan rate used, *F* is the Faraday constant, *R* is the universal gas constant, and *T* is the absolute temperature. For the study of microstructural transition, it is essential that the electrochemical charge transfer must be diffusion controlled in nature.[41] The plots of peak current i_p versus $v^{1/2}$ shown in Figure 3 are straight line passing through the origin indicating that the electron transport reaction for the redox system inside the microemulsions are diffusion controlled in nature.[42,43] The change in the apparent diffusion coefficient values with an increase in the wt% of water gives us the indication about the microstructural transition points inside the single phase zone of the ternary phase diagram. For the detection of microheterogeneous regions the two *I* values (*I* = [BBIM][NTf_2]-to-TX-100 weight ratio) are chosen as 0.05 and 0.10, as shown in Figure 1. Figure 4(a) and (b) represents the plot of the apparent diffusion coefficients, D_{app} of the electrochemically active probe, $K_4Fe(CN)_6$ with the increasing wt% of water at *I* = 0.05 and 0.1, respectively. It has been clearly shown in the above drawings that with the increase in the weight percentage of water the diffusion coefficients of the

electrochemically active probe goes on increases. The probe being ionic in nature is only soluble in the water phase.

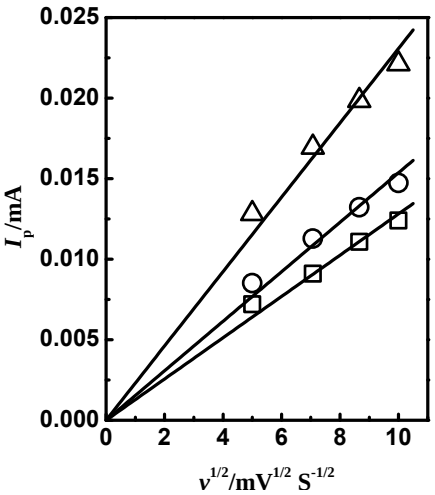

Figure 3. The plot of the peak current (i_p) versus square root of scan rate ($v^{1/2}$) for 25 wt% H_2O (□), 30 wt% H_2O (O) and 40 wt% H_2O with IL-to-TX-100 weight fraction as 0.1. The lines are obtained by the linear fit.

Initially, a mild increment in the diffusion coefficients values are observed in low wt% of water that is below 34% for I = 0.05 and below 31% for I = 0.1. This is due to the reason that the ionic electrochemically active probe remains inside the water pool possessing high viscosity. With the increase in the wt% of water the microviscosity of the confined water droplets decreases.[44] The D_{app} values of the probe inside the pool increases with an increase in the fluidity of droplets. A mild enhancement in the D_{app} values of the probe is due to an increase in the content of water and not due to any change in the microstructure of the microemulsions. The microemulsions formed in these regions are of the kind of W/IL type.[16]

Table 1. The Values of the Apparent Diffusion Coefficients (D_{app}) with the Increasing Wt% of H_2O for I = 0.05 and 0.1, Respectively.

I = 0.05		I = 0.1	
Wt% (H_2O)	D_{app} x 10^{10} / m^2S^{-1}	Wt% (H_2O)	D_{app} x 10^{10} / m^2S^{-1}
22.5	7.1	20.0	6.6
25.0	9.8	22.5	8.0

27.5	14.8	25.0	11.9
30.0	18.6	27.5	15.6
32.5	21.0	30.0	17.2
35.0	29.2	32.5	26.9
37.5	35.3	35.0	32.1
40.0	42.1	37.5	42.1
42.5	55.4	40.0	64.0
45.0	76.6	42.5	60.2
47.5	82.9	45.0	68.0
50.0	102.1	47.5	91.7
52.5	108.5	50.0	102.1
55.0	116.4	52.5	104.5
57.5	140.4	55.0	122.0
60.0	148.7	57.5	146.4
62.5	155.2	60.0	150.5
65.0	167.7	62.5	157.6
67.5	177.2	65.0	161.2
70.0	179.5	67.5	166.7
72.5	182.0	70.0	171.6
75.0	186.7	72.5	173.8
77.5	183.0	75.0	172.3
80.0	184.3	77.5	175.2
		80.0	177.8

Standard uncertainties in the measurements, u (D_{app}) = ± 2.0%

The increase in the D_{app} values of the probe are again slow down in the water-rich phase zone and a mild enhancement in the D_{app} values are observed with the higher wt% of water i.e. above 60% for I = 0.05 and 57.5% for I = 0.10, respectively. In these regions the microemulsions are of the kind of IL/W type.[16] In this region the IL molecules are trapped by the hydrophobic core of the surfactant molecules and remain as in the pool form and forms the IL/W microemulsion.[16] The IL molecules act as the dispersed phase

with water as the dispersion medium. The electrochemically active $K_4Fe(CN)_6$ probe molecules are now in the dispersion water medium, present in the bulk quantity and the D_{app} values of probe molecules are higher and resembles to that of diffusion in the neat water.[16]

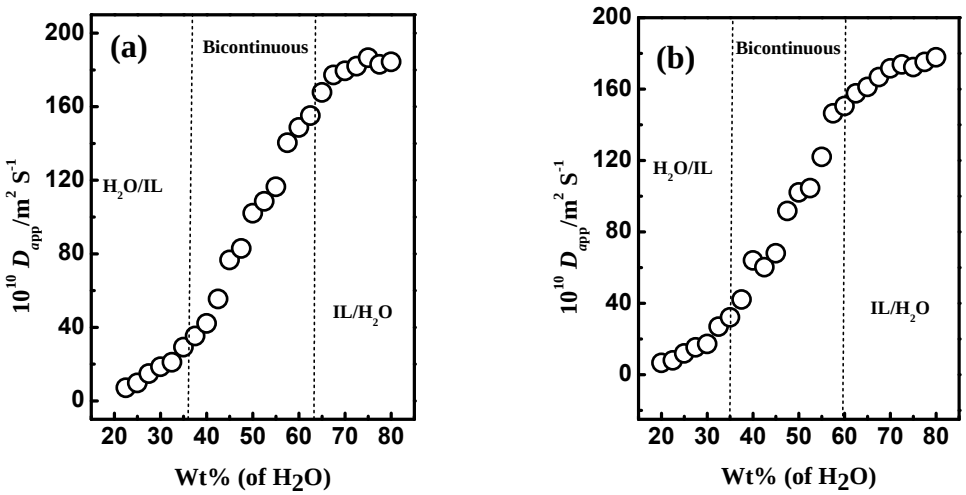

Figure 4. Apparent diffusion coefficient, D_{app} of $K_4Fe(CN)_6$ in [BBIM][NTf_2]/H_2O/TX-100 microemulsion system showing the structural transition from W/IL to bicontinuous to IL/W as a function of water content at a temperature of 298.15 K. ([BBIM][NTf_2]/TX-100 weight ratio = 0.05 (a) and 0.1 (b)).

Thus, an increase in the amount of water has a very minimal effect on the diffusion coefficient of $K_4Fe(CN)_6$ and the structure of the microemulsions is insensitive to the compositions of water in this region. However, a dramatic change in the D_{app} values is observed in the intermediate water compositions. This indicates that the environment of the microemulsions is different from that of the droplet structure.[45] Our results infer that when the water compositions are between 34-60% (I = 0.05) and 31-57.5% (I = 0.1), a bicontinuous microstructure is formed, in which both the water and hydrophobic [BBIM][NTf_2] are present as the continuous phase.[45] The diffusion of molecules in the continuous medium is faster as compared to the molecules confined in the closed domains[45] and thus the probe inside the bicontinuous structure has higher diffusion coefficient value as compared to that of W/IL droplet microemulsion. The increment in the diffusion coefficient values with an increase in wt% of water follows the sigmoidal

trend and the three different kinds of microheterogeneous regions can be detected by the transition points obtained from the Figure 4 are given in the Table 2.

Table 2. Microstructural transition points for [BBIM][NTf_2]/H_2O/TX-100 microemulsions system at different *I* values. The values are given in wt% of water. (*I* = [BBIM][NTf_2]-to-TX-100 weight ratio)

I	W/IL-to-Bicontinuous transition point	Bicontinuous-to-IL/W transition point
0.05	36	63.5
0.1	35	60.0

Thus from all of the above investigations, we can deduce that three different microheterogeneous regions are present inside the single phase zone and those are W/IL, bicontinuous and IL/W microemulsions and are represented in the Figure 1.

The interfacial reactions occurring on the electrode surface of both the W/IL and IL/W microemulsions are different from that of the pure water system. It has been reported that the organic species like TX-100 and [BMIM][PF_6] are active towards the surface of the electrode.[46] Being organic in nature both [BBIM][NTf_2] and TX-100 are active towards the surface and adsorb on the electrode surface. In the case of W/IL microemulsions, the $K_4Fe(CN)_6$ molecules remain inside the water pool. Due to thermal motion, there is an exchange of masses between the nano-droplets of W/IL microemulsions containing $K_4Fe(CN)_6$. Because of this thermal motion the electrochemically active probe molecules passes through the organic surfactant layer and come in contact with the electrode surface leading to the electrochemical reaction occurs.[46] On the other hand the electrochemical reaction for IL/W microemulsions is very similar to that of the pure water as the probe molecules reside in the water bulk phase.

5.4.4. Dynamic Light Scattering (DLS) Measurements.

With the phase diagram and cyclic voltammetric studies yielding information on the presence of three different regions of microemulsions, we now move to investigate the

systems by using DLS studies to know whether the water molecules are entrapped by the surfactant molecules to form W/IL microemulsions or the IL molecules confined inside the surfactant layer to form the IL/W microemulsions. The hydrodynamic radii (D_h) of IL/W microemulsions because of their low viscosity values are given in Table 3. The D_h of different IL/W microemulsions are measured by varying *I* values. With the increase in the *I* values, the D_h values of the microemulsion increase for a fixed wt % of water (Figure 5). The drawing represents the change in the D_h values of the IL/W microemulsion droplets with the increase in the *I* values for two different fixed compositions of water (67.5% and 72% of water). This is due to the reason that with the increase in *I* values, the content of IL in the system increases causing the swelling of the microemulsions and thereby increasing the sizes of microemulsion droplets.

Table 3. Measured hydrodynamic radii (D_h) of microemulsions obtained through the dynamic light scattering measurements. (*I* and *R* represents the [BBIM][NTf_2]-to-TX-100 weight and molar ratio, respectively)

H_2O/Wt%	IL/Wt%	TX-100/Wt%	*I*	*R*	D_h/nm
67.5	1.55	30.96	0.05	0.07	4.6
72.5	1.31	26.20	0.05	0.07	5.0
77.5	1.07	21.42	0.05	0.07	5.5
67.5	2.41	30.08	0.08	0.11	5.2
72.5	2.04	25.46	0.08	0.11	5.4
77.5	1.67	20.83	0.08	0.11	5.7
67.5	2.95	29.54	0.1	0.14	5.6
72.5	2.50	25.00	0.1	0.14	5.6
77.5	2.04	20.45	0.1	0.14	5.7

Our findings are supported by the work of Falcone *et al.*[47] who observed that with the increase in the IL content, an increase in the droplet size of the non-aqueous microemulsions was observed. This swelling behavior of confined media is reported for aqueous microemulsion systems.[48] This suggests that the IL molecules are entrapped by

the surfactant molecules in order to form IL/W microemulsions. The increase in the droplet size of the microemulsions can also be explained with the help of packing parameter (*P*) and can be represented as $P = v/al$, where *v*, *a* and *l* signify the volume of the hydrocarbon chain, effective head group area of the surfactant and the length of the hydrocarbon chain, respectively.[47]

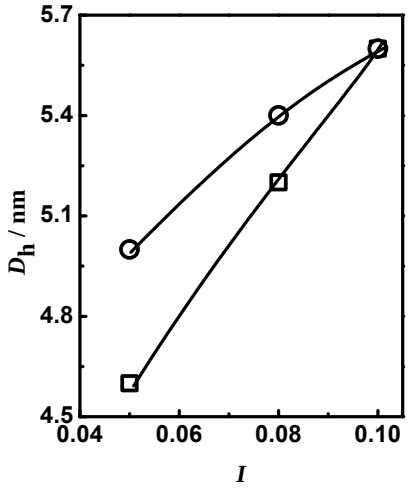

Figure 5. Hydrodynamic radii (D_h) of the IL/W microemulsion droplets with *I* values for [BBIM][NTf_2]/H_2O/TX-100 system with a fixed wt% of water (67.5%, □ and 72.5% O) showing the swelling of the microemulsion droplets.

It has been reported that the size of the confined media depends upon the effective packing parameter of the surfactants used.[47] Decreasing the packing parameter of surfactant molecules increases the size of confined media and vice versa.[49] With the increase in the content of IL into the system by increasing the *I* values, the IL molecules penetrate into the surfactant layer and interact with the headgroup of the TX-100 surfactant molecules. This interaction results into an increase in the effective headgroup area, *a* of the surfactant molecules. The interactions between the cationic part of [BMIM][PF_6] with the polar headgroup of non-ionic TX-100 surfactant in the case of [BMIM][PF_6]/H_2O/TX-100 microemulsion system also supports the above statement.[14] Thus, the value of *a* increases which in turn decreases the packing parameter, *P* of the surfactant molecules. Consequently, the droplet size of the IL/W microemulsions increases. It is suggested in the literature that a linear dependence of the D_h values on *I*

points to spherical droplets of microemulsions.[50] However, a slightly non-linear dependence in our case seems to be with the increase in the wt % of water to 72.5%. However we currently are not aware of any reasons behind it.

5.4.5. ^{1}H NMR and NMR Relaxation Study.

Many workers have studied the properties of this water present inside the reverse micelles through the help of different experimental techniques like DLS,[40,41] IR spectroscopy,[6] UV-vis spectroscopy,[51,52] fluorescence spectroscopy[32,44] and NMR spectroscopy.[3,4] In most of these reports different spectroscopic probe molecules are used

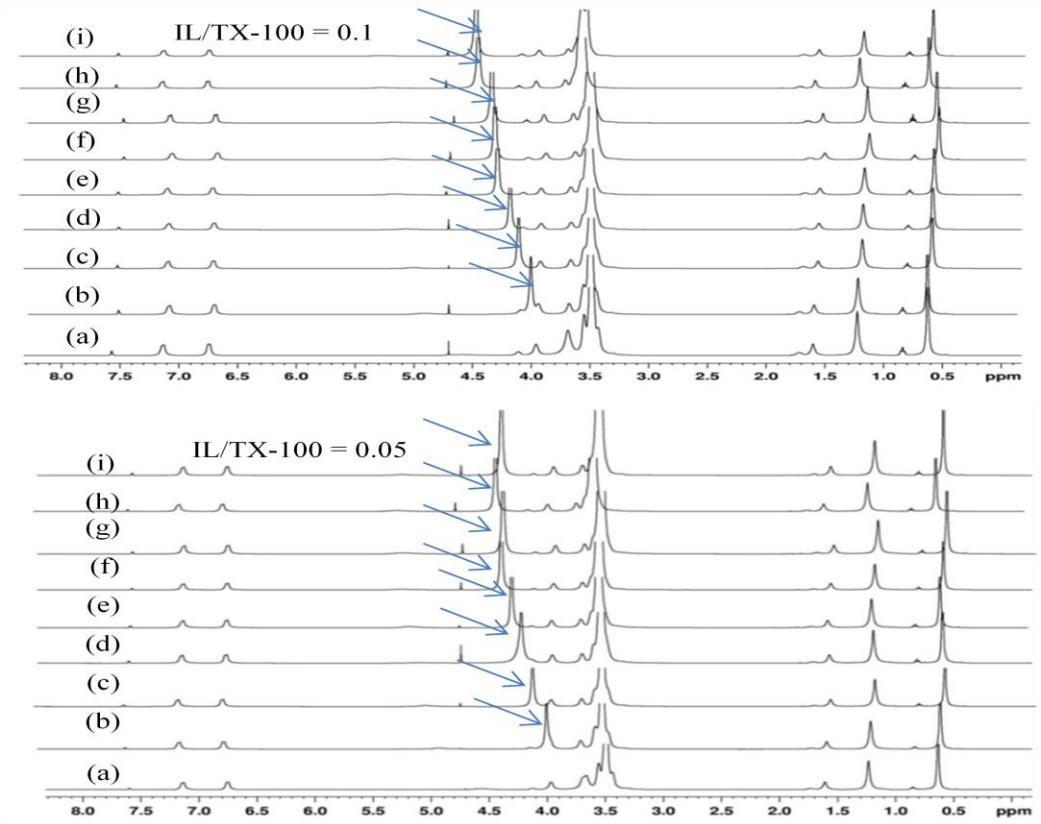

Figure 6. Stacking of ‘H NMR spectra showing the types of H_2O molecules present inside the W/IL microemulsions with different wt% of water: 5.0 wt% (a), 7.5 wt% (b), 10.0 wt% (c), 15.0 wt% (d), 17.5 wt% (e), 20.0 wt% (f), 22.5 wt% (g), 25.0 wt% (h), 27.5 wt% (i). (Top: weight ratio of IL/TX-100 = 0.1, bottom: IL/TX-100 = 0.05)

for the determination of physicochemical properties of different confined media. The location of probe molecules inside the reverse micelles however creates problems in

finding the true physical properties of these confined media. In our work, we have carried out the NMR spectroscopic measurements of water inside the W/IL confined media, which gives the information related to the physical properties of these confined media without the help of any spectroscopic probe.[53,54] Figure 6 represents the stacking of ^{1}H NMR spectra of different W/IL microemulsions with an increase in the wt% of water. The upper and lower parts of the figure illustrate about the IL-to-TX-100 weight ratio (*I*) as 0.1 and 0.05, respectively.

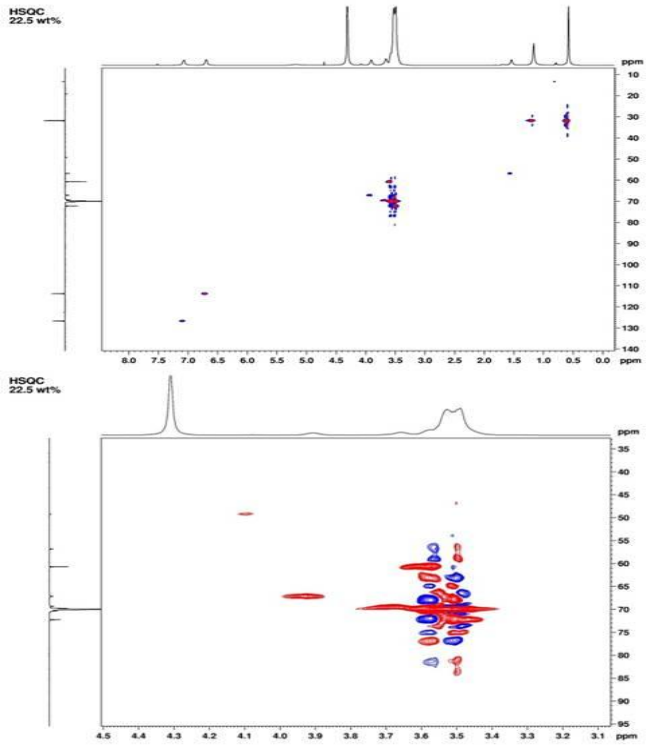

Figure 7. NMR ^{1}H-^{13}C heteronuclear single quantum coherence (HSQC) spectra of W/IL microemulsion containing 22.5 wt% of water showing the confirmation of H_2O signal at 4.27 ppm. (*I* = 0.05)

It has been shown in Figure 6 that with the increase in the water content from 5.0 wt% to 27.5 wt%, the peak at around 4.0 ppm (5.0 wt% of water) is nearly shifted to 0.4 ppm towards the deshielded region leaving rest of the peaks unchanged. It signifies that the peak is the indication of the proton of water molecules present inside the reverse micelles. To confirm the water signal emerging out from the microemulsion samples, we

also carried out the two-dimensional ^{1}H-^{13}C heteronuclear single quantum coherence spectroscopy (HSQC) and the results are shown in Figure 7. The drawing represents the HSQC spectra for 22.5 wt% of water with IL-to-TX-100 wt. ratio, I = 0.05. As we have recorded the ^{1}H-^{13}C HSQC spectra the water signal must not have the contour plot due to the absence of carbon atom in the molecule. The enlarged bottom view of the graph shows the absence of such contour plot at 4.27 ppm on the ^{1}H-NMR spectra axis, which confirms the signal emerging from the water molecule. With the lower wt% of water, the peak coming out from the water molecules are mixed up with the proton of the TX-100 molecules.[55] H-bonding interaction between the –OH group of TX-100 molecules with the water molecules inside the [BMIM][PF_6]/H_2O/TX-100 microemulsions supports the above statement.[14] This suggests that the interfacial water present around the surface of headgroups of TX-100 molecules experiencing a different interacting environment as compared to that of the core water molecules.

It was reported that there are three types of miceller water are present namely trapped water, bound water and free water.[56] The dissolved water molecules present in the non-polar solvents are known as trapped water molecules. The water molecules, which are H-bonded with the head group of surfactant molecules, are called as the bound water molecules and the core water molecules of the reverse micelles are termed as the free water molecules. The initial addition of water to the [BBIM][NTf_2]/H_2O/TX-100 microemulsions system binds with the head group of surfactant molecules through the help of hydrogen bonding interaction between the H-atom of water with the oxygen atom of oxyethylene unit of TX-100 and experience a shielding effect.[57] With the increase in the wt% of water, the water molecules form a pool inside the surfactant layer and behave like that of the bulk water molecules. These water molecules are not interacted with the head group of surfactant molecules and are termed as free water molecules with a slightly deshielding effect as compared to that of the bound water molecules. It means protons of bound water molecules are experiencing a higher electron density as compared to that of the protons of free water molecules. The lower IR stretching frequency of –OH bond of free water molecules (3220 ± 20 cm^{-1}) as compared to that of bound water molecules (3400 ± 20 cm^{-1}) also supports the above statement.[57] ^{1}H-NMR spin-lattice relaxation time (T_1) study of water molecules was carried out to understand the dynamics of the

water molecules present inside the [BBIM][NTf_2]/H_2O/TX-100 microemulsions. By applying the Bloembergen, Purcell, and Pound (BPP) theory[58] the reorientational correlation time (τ_c) of water molecules can be calculated from the measured T_1 relaxation time of water molecules and are illustrated in the Figure 8. According to BPP theory both the spin-lattice relaxation time T_1 and reorientational correlation time τ_c are inversely related to each other as represented in the following equation 2,

$$\frac{1}{T_1} = \frac{3}{10}\frac{\gamma^4\hbar^2}{b^6}\left[\frac{\tau_c}{1+\omega^2\tau_c^2} + \frac{4\tau_c}{1+4\omega^2\tau_c^2}\right] \qquad (3)$$

where T_1 is the NMR spin-lattice relaxation time, γ the gyromagnetic ratio of the proton, $\hbar$ the Planck's constant, b the intra-proton distance of water molecule, τ_c the reorientational correlation time and ω the resonance frequency.

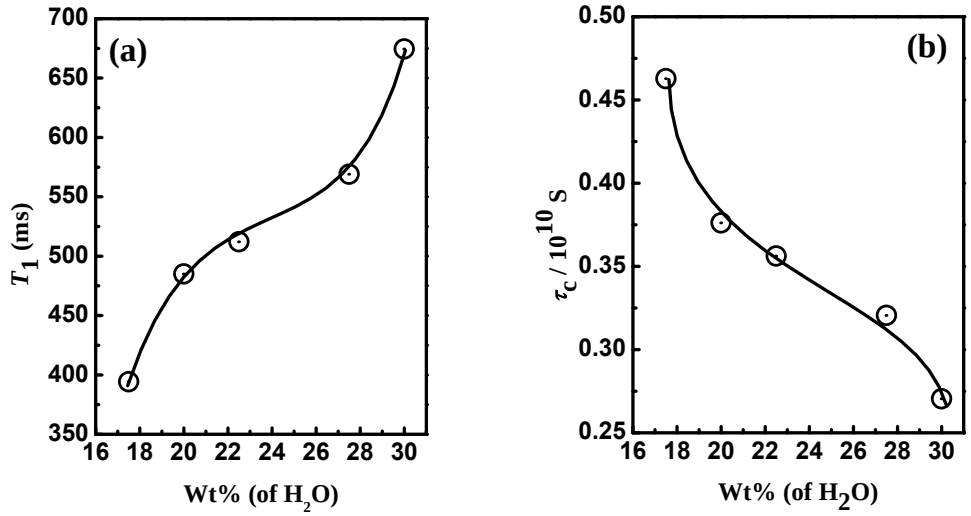

Figure 8. Variation of NMR spin lattice relaxation time T_1, (a) and their calculated reorientational correlation time τ_c, (b) with the increase in the wt% of water.

Figure 8(a) and (b) represent the variation of T_1 and τ_c values, respectively with the increase in the wt% of water. It is seen from the plots given in Figure 8 that with the increase in the wt% of water the T_1 values increase where as the τ_c values decrease.

It is reported that the relaxation time observed in the case of H_2O/hexanol/TX-100/cyclohexane was the weighted average of the signals coming out from the protons of

the H_2O molecules, -OH group of hexanol and the -OH group of the TX-100 molecules.[53] As in the case of [BBIM][NTf_2]/H_2O/TX-100 microemulsions system, the TX-100 molecule contain a hydroxyl proton, therefore there is the possibility of fast exchange of proton takes place between this proton with the proton of water molecules which must be faster than our observed relaxation time. Therefore the observed T_1 values are the weighted average of these two signals. The increase in the T_1 values with the increase in the wt% of water indicates that the mobility of proton inside the miceller core increases as confirmed by the decreased reorientational correlation time, τ_c shown in Figure 8(b). The τ_c values of water molecules present inside the miceller core of the [BBIM][NTf_2]/H_2O/TX-100 microemulsions are in the range of 0.25×10^{-10} to 0.46×10^{-10} s. It is reported that the overall tumbling motion of W/O microemulsions are of the order of 10^{-9} s.[59] If we consider the tumbling motion of these W/IL microemulsions in the range to that of the W/O microemulsions, we can then signify that the motion of water molecules is not coupled with the overall tumbling motion of these W/IL microemulsions and is different from them.

Therefore, the bulk transport property like viscosity of these W/IL microemulsions is different from that of the microscopic transport properties like microviscosity of the confined water. Reports are available in the literature regarding the determination of microviscosity of the reverse micelles or microemulsions by the use different spectroscopic probe molecules.[2,44] The location of probe molecules inside the miceller core is however questioned by many workers leading to a problem in the determination of exact microviscosity of miceller core.[3,4] In our study, we attempted to estimate the η_{micro} of the miceller core of the [BBIM][NTf_2]/H_2O/TX-100 microemulsions system with the help of NMR spin-lattice relaxation (T_1) measurements.[54] Assuming the Debye-Stokes equation to be valid in these microemulsion systems the microviscosity of the miceller core is estimated from the reorientational correlation time as:

$$\tau_c = \frac{4\pi\eta a^3}{3kT} \qquad (4)$$

where a is the radius of the molecule, k is the Boltzmann constant, T is the absolute temperature and η is the microviscosity experienced by the molecule inside the miceller system.

From the Figure 9 it is seen that the η_{micro} experienced by the water molecules inside the water pool of W/IL microemulsion decreases with increasing wt% of water. The physicochemical properties of aqueous confined media of small reverse micelles are significantly different from that of the bulk water,[7,44] whereas with the increase in the size of the aqueous miceller phase, its properties approach to that of bulk liquid water.[53,54]

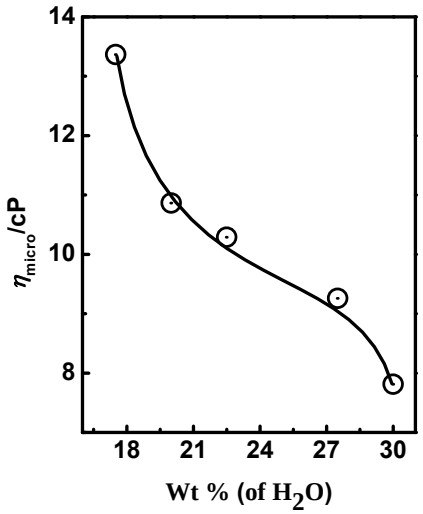

Figure 9. Variation of the microviscosity of the water present inside the miceller core of the [BBIM][NTf_2]/H_2O/TX-100 system with the increase in the wt% of water for IL-to-TX-100 weight fraction, I as 0.05.

With the lower content of water, it interacts with the non-ionic headgroups of TX-100 molecules.[14] Due to this the water molecules present near to the surfactant head groups experienced higher viscosity and these water molecules are termed as the bound water molecules.[56] The higher correlation time value for the lower wt% of water also supports the above statement. With the higher water content the water molecules lose their connectivity with the headgroups of surfactant molecules and form pool of water molecules inside the miceller core.[53,54] Therefore, these water molecules experience a higher fluidity and in turn a decrease in their microviscosity values.[53,54] These water

molecules are termed as free water molecules and their NMR rotational correlation time remains invariant with the addition of water.[59] We have however observed a continuous decrease in the correlation time of the water molecules and their microviscosity values with the increase in the wt% of water. This contradictory observation may be due to the reason that the so called free water molecules present inside the miceller core of the microemulsions are not actually free from the interacting influence of the headgroups of TX-100 surfactant molecules. Another interesting observation in the case of these W/IL microemulsions is there that exist an inverse relationship between the microviscosity and the bulk viscosity as illustrated in the Table 4.

Table 4. A comparison between the microviscosity (η_{micro}) with the bulk viscosity (η_{bulk}) and the spin-lattice relaxation time (T_1) with the relaxation rates (R) of the microemulsions samples with the increase in the wt% of water (I = 0.05)

Sl. No.	Wt.% of H_2O	η_{micro}/cP	η_{bulk}/cP	T_1/ms	$R=(1/T_1)/s^{-1}$
1	17.5	13.36		394.20	2.54
2	20.0	10.86		484.99	2.06
3	22.5	10.29	248.90	512.06	1.95
4	27.5	9.26	269.10	569.08	1.76
5	30.0	7.81	290.80	674.50	1.48

It means within the studied W/IL microemulsion zones the increase in the amount of water decreases the micorviscosity of the water nano-droplets on the other hand it increases the bulk viscosity of the microemulsion mixtures. The decrease water-surfactant interaction is the primary cause for the decreased η_{micro}, however the increasing droplet-droplet interactions with the increase in the wt% of water are responsible for the enhancement in the η_{bulk} of the W/IL microemulsion system. Also the relaxation rate of the water molecules in the W/IL microemulsion zones decreases with the increasing composition of water. It means that the rate of relaxation of water molecules is directly related to the microviscosity of the nano-droplets. Higher is the

microviscosity of the medium, higher is the time required for the protons of water molecule to be relaxed.

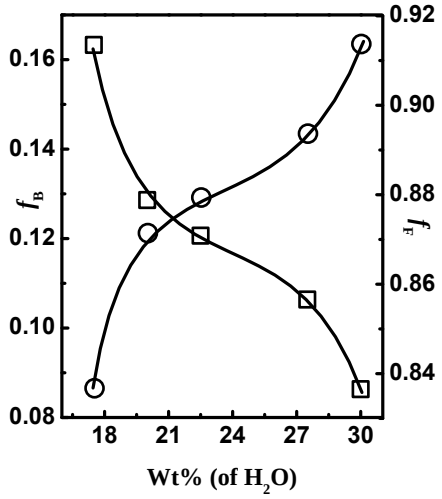

Figure 10. Variation of mole fraction of bound water molecules f_B, (○) and free water molecules f_F, (□) which are present inside the aqueous nano-droplets of [BBIM][NTf_2]/H_2O/TX-100 microemulsion systems with the wt% of water.

As both the free and bound water molecules are present inside the W/IL microemulsion systems therefore it is of interest to know the fraction of each water molecules. For this purpose, we used the model of Hansen[54] for W/O microemulsions system. According to him

$$T_1^{-1} = f_B\, T_{1B}^{-1} + f_F\, T_{1F}^{-1} \qquad (5)$$

where T_1, T_{1B} and T_{1F} are the experimentally observed relaxation time, relaxation time of bound water molecules and relaxation time of free water molecules present inside the miceller core, respectively. f_B and f_F are the mole fraction of bound and free water molecules, respectively and $f_B + f_F = 1$.

By replacing the relaxation rate, R in place of relaxation time, T_1, equation 4 can be rewritten as:

$$R = f_B\, R_B + f_F\, R_F \qquad (6)$$

where R, R_B and R_F are the observed relaxation rate, relaxation rate of bound water molecules and relaxation rate of free water molecules, respectively. Rearranging equation 5, the fraction of bound water molecules can be calculated by applying the following equation 6.

$$R = f_B R_B + (1\text{-}f_B) R_F$$

$$f_B = (R - R_F) / (R_B - R_F) \quad (7)$$

Assuming the relaxation rate of free water molecules is similar to that of the bulk water molecules as 0.278 s^{-160} and that of bound water molecules as 14.08 s^{-1} which is obtained from the intercept of the linear fitting of relaxation time with the wt% of water. Figure 10 represents the calculated mole fraction of bound and free water molecules with the increasing composition of water. The mole fraction of bound water molecules decreases where as the mole fraction of free water molecules are increases with the increase in the composition of water. This suggests that the probability of interactions between the water molecules with the surfactant molecules are increases with the decreasing composition of water where as increasing water content strengthen the water-water interactions.

Table 5. The Mole Fraction of Bound Water Molecules (f_B) with the Increase in the Wt% of Water.

Wt% (H_2O)	f_B
17.5	0.16
20.0	0.13
22.5	0.12
27.5	0.11
30.0	0.09

It also infers that the reverse micelles contain more amounts of free water molecules as compared to that of the bound water molecules within the studied W/IL microemulsions zone. Reports are available in the literature that the mole fraction of

bound water gets saturated beyond a particular composition of water.[54] However in the case of W/IL microemulsions zone of [BBIM][NTf_2]/H_2O/TX-100 microemulsions we have observed a continuous decrease in the value of mole fraction of bound water molecules as illustrated in the Table 5 and is confirms from the observed spin-lattice relaxation time T_1. Reports are available in the literature regarding the determination of pH of the aqueous miceller media by the use of different spectroscopic molecular probe.[3,61]

Table 6. Influence of pH on the spin-spin relaxation time, T_2 of water molecules present inside the miceller core of [BBIM][NTf_2]/H_2O/TX-100 microemulsions with IL-to-TX-100 weight fraction as 0.1. The line widths of the spectra are calculated from the measured T_2 values.

pH	T_2/ms	$\Delta\nu_{1/2}$ $(1/\pi T_2)$/ ms^{-1}
2.00	21.336	0.015
3.00	1.060	0.300
4.00	4.950	0.064
5.10	6.302	0.051
6.14	6.408	0.050
7.03	6.403	0.050
9.08	6.474	0.049
9.50	6.546	0.049

However as stated above, the use of probe molecules creates problem in finding out the exact physical properties of different miceller media because of its difficulty in find out the exact location of it inside the reverse miceller media.[3,4] To avoid this problem we have used the NMR spin-spin relaxation time, T_2 of water molecules as a probe to

measure the pH of the aqueous reverse miceller core of the [BBIM][NTf_2]/H_2O/TX-100 microemulsion systems, as T_2 relaxation time is sensitive to the pH of the aqueous miceller medium.[55] Figure 11 represents the variation of NMR spin-spin relaxation time, T_2 of water molecules present inside the reverse miceller core of the [BBIM][NTf_2]/H_2O/TX-100 microemulsion systems with the pH of the medium.

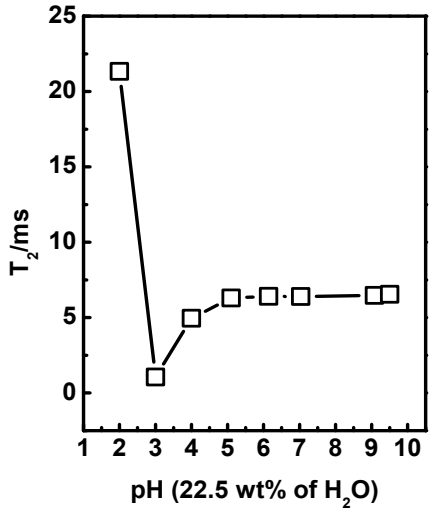

Figure 11. Variation of NMR spin-spin relaxation time, T_2 of water molecules (signal at 4.27 ppm) with the pH of the miceller core for the [BBIM][NTf_2]/H_2O/TX-100 microemulsion system with a fixed wt% of water as 22.5 wt%. The pH of the aqueous miceller systems are externally measured before the use of it for the experimental purposes. (I = 0.1)

At higher proton concentrations, the NMR spin-spin relaxation time, T_2 of water molecules shows its maximum value as 21.336 ms. However with the increase in the pH of the aqueous miceller medium this value sharply drops to a minimum at 1.06 ms as represented in Table 6. Afterwards a continuous increase in the T_2 relaxation time values was observed with the increase in the pH of the aqueous reverse micelles. The reason for this variation in T_2 relaxation time values are due to the possibility of variation in the rate of proton exchange between the water molecules and the hydroxyl proton of TX-100 molecules.[55] At the high proton concentration, the rate of proton exchange between the water and TX-100 molecules are faster. Here the magnetically excited protons switch their precessional frequency faster causing slower dephasing of their transverse

magnetization vector and consequently, we obtain a higher value of T_2 relaxation time.[62] The calculated line width from the measured T_2 relaxation time given in Table 6 also supports the above statement. At the higher proton concentration and with the maximum value of T_2 relaxation time the calculated line width of the signal is minimum as 0.015 ms^{-1} which indicates the sharpening of the signal that emerges out from the protons of both the water and TX-100 (alcoholic proton) molecules due to the faster rate of exchange between them.[63] At the minimum value of T_2 relaxation time (1.06 ms at pH = 3) the rate of proton exchange is in between the fast and slow intermediate regimes.[62] Here the calculated line width of the signal is highest as 0.3 ms^{-1} which indicates the broadening of the peak due to the fusion of the two peaks coming out from the water and TX-100 molecules. The peak coalesces also occurs at the minimum value of T_2 relaxation time between the protons of water and –OH group of hexanol molecules inside the CTAB microemulsioins.[55] However with the increasing the pH of the aqueous reverse miceller media of [BBIM][NTf_2]/H_2O/TX-100 microemulsion systems from 3.0 to onwards the concentration of proton inside the aqueous confined nano-droplets are decreases and consequently the rate of proton exchange decreases.

Table 7. Micropolarity of aqueous confined media of [BBIM][NTf_2]/H_2O/TX-100 microemulsions with the increasing wt% of water (IL-to-TX-100 weight ratios as 0.05 and 0.1, respectively)

IL/TX-100 = 0.05 Wt% H_2O	λ_{max}	IL/TX-100 = 0.1 Wt% H_2O	λ_{max}
10.0	426.0	7.5	427.9
15.0	428.0	12.5	429.0
22.5	429.0	20.0	429.9
27.5	430.1	25.0	431.0

The decrease in the proton concentration creates a heterogeneous environment in the local magnetic field inside the aqueous IL microemulsion systems causing the faster dephasing of the transverse magnetization vector.[62] This results in the decrease in the

values of the T_2 relaxation time with the increase in the pH of the aqueous IL miceller core. The calculated line width of the water signal is around 0.05 ms^{-1} and remains invariant with the further increase in the pH of the aqueous IL microemulsions. This may be due to the splitting of the two proton signal coming out both from the water and TX-100 molecule (alcoholic proton).

We also investigates the micropolarity of the aqueous nano-droplets of [BBIM][NTf_2]/H_2O/TX-100 microemulsions by the use of methyl orange (MO) as the UV-vis spectroscopic molecular probe. Due to the hydrophilic nature of MO, it is soluble in the aqueous miceller core and insoluble in the hydrophobic ionic liquid phase. Therefore MO is considered to be a very good polarity probe for the determination of micropolarity of the microheterogeneous medium. The electronic transition energy coming out from the measured λ_{max} values of MO is sensitive to the polarity of the microenvironment.

The measured λ_{max} values of aqueous confined media of [BBIM][NTf_2] H_2O/TX-100 microemulsions are given in Table 7 for the IL-to-TX-100 wt. ratio *I*, as 0.05 and 0.1, respectively.

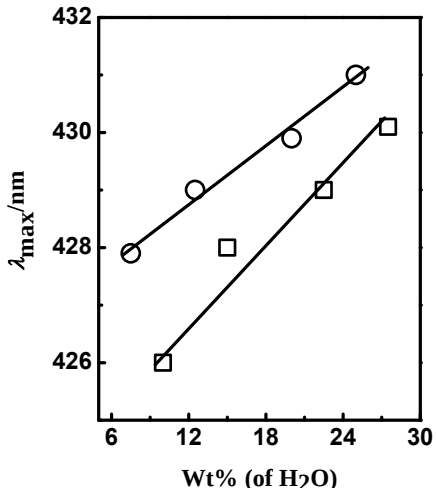

Figure 12. Variation of λ_{max} values of MO as the UV-vis spectroscopic absorption probe as a function of wt% of water for *I* = 0.05 (□) and 0.1 (O), respectively.

From the above Table 7 it is very clear that the λ_{max} values of MO increase with an increase in the wt% of water. This indicates that the micropolarity of the aqueous confined media increases with an increase in the λ_{max} values of MO.[32] The variation of λ_{max} values of MO with the wt% of water is illustrated in Figure 12. We have observed nearly a linear dependence of λ_{max} values with the change in the composition of water agreeing with the published reports.[63] This may be due the possibility of the change in the state of water present inside the miceller core. Thus the linear dependency of λ_{max} values of MO in case of [BBIM][NTf_2]/H_2O/TX-100 microemulsion systems indicates that the water molecules present inside the miceller core are not completely free from the interacting influence of the polar hydrophilic part of the non-ionic TX-100 surfactant molecules as discussed above from the NMR relaxation studies.

5.5. CONCLUSIONS

In conclusion, we show that the NMR T_1 relaxation time of water molecules can be used as an alternative parameter to indicate the microviscosity of the aqueous IL confined media. Both the microviscosity and the bulk viscosity values of aqueous IL microemulsions are inversely related to each other. The NMR T_2 relaxation time of water molecules varies with pH of the aqueous IL confined media and gives an indication of the pH of the aqueous miceller core. Two kinds of water molecules (the bound water and free water molecules) are present inside the aqueous IL confined media. The fraction of bound water molecules decreases whereas the fraction of free water molecules increases with an increase in the composition of water. However, at each composition of water the fraction of free water molecules are higher than as compared to that of fraction of bound water molecules. High proton concentration inside the aqueous IL confined media leads to faster exchange of protons and a decrease in the proton concentration lowers the rate of proton exchange.

5.6. REFERENCES

(1) Chance, B. *Proc. Natl. Acad. Sci. U.S.A.* **1970**, *67*, 560-571.

(2) Correa, N. M.; Silber, J. J.; Riter, R. E.; Levinger, N. E. *Chem. Rev.* **2012**, *112*, 4569-4602.

(3) Crans, D. C.; Rithner, C. D.; Baruah, B.; Gourley, B. L.; Levinger, N. E. *J. Am. Chem. Soc.* **2006**, *128*, 4437-4445.

(4) Baruah, B.; Roden, J. M.; Sedgwick, M.; Correa, N. M.; Crans, D. C.; Levinger, N. E. *J. Am. Chem. Soc.* **2006**, *128*, 12758-12765.

(5) Moilanen, D. E.; Levinger, N. E.; Spry, D. B.; Fayer, M. D. *J. Am. Chem. Soc.* **2007**, *129*, 14311-14318.

(6) Piletic, I. R.; Moilanen, D. E.; Levinger, N. E.; Fayer, M. D. *J. Am. Chem. Soc.* **2006**, *128*, 10366-10367.

(7) Riter, R. E.; Willard, D. M.; Levinger, N. E. *J. Phys. Chem. B* **1998**, *102*, 2705-2714.

(8) Moniruzzaman, M.; Kamiya, N.; Goto, M. *Langmuir* **2008**, *25*, 977-982.

(9) Murgia, S.; Palazzo, G.; Mamusa, M.; Lampis, S.; Monduzzi, M. *J. Phys. Chem. B* **2009**, *113*, 9216-9225.

(10) Shipovskov, S.; Oliveira, C. L. P.; Hoffmann, S. V.; Schauser, L.; Sutherland, D. S.; Besenbacher, F.; Pedersen, J. S. *ChemPhysChem* **2012**, *13*, 3179-3184.

(11) Fathi, H.; Kelly, J. P.; Vasquez, V. R.; Graeve, O. A. *Langmuir* **2012**, *28*, 9267-9274.

(12) Ventura, S. P. M.; Santos, L. D. F.; Saraiva, J. A.; Coutinho, J. A. P. *Green Chem.* **2012**, *14*, 1620-1625.

(13) Anjum, N.; Guedeau-Boudeville, M.-A.; Stubenrauch, C.; Mourchid, A. *J. Phys. Chem. B* **2008**, *113*, 239-244.

(14) Lian, Y.; Zhao, K. *Soft Matter* **2011**, *7*, 8828-8837.

(15) Langevin, D. *Acc. Chem. Res.* **1988**, *21*, 255-260.

(16) Gao, Y.; Han, S.; Han, B.; Li, G.; Shen, D.; Li, Z.; Du, J.; Hou, W.; Zhang, G. *Langmuir* **2005**, *21*, 5681-5684.

(17) Gao, Y. a.; Li, N.; Zheng, L.; Zhao, X.; Zhang, S.; Han, B.; Hou, W.; Li, G. *Green Chem.* **2006**, *8*, 43-49.

(18) Zech, O.; Kunz, W. *Soft Matter* **2011**, *7*, 5507-5513.

(19) Liu, J.; Cheng, S.; Zhang, J.; Feng, X.; Fu, X.; Han, B. *Angew. Chem., Int. Ed.* **2007**, *46*, 3313-3315.

(20) Gao, Y.; Li, N.; Zheng, L.; Zhao, X.; Zhang, J.; Cao, Q.; Zhao, M.; Li, Z.; Zhang, G. *Chem. – Eur. J.* **2007**, *13*, 2661-2670.

(21) Gao, Y.; Li, N.; Zheng, L.; Bai, X.; Yu, L.; Zhao, X.; Zhang, J.; Zhao, M.; Li, Z. *J. Phys. Chem. B* **2007**, *111*, 2506-2513.

(22) Eastoe, J.; Gold, S.; Rogers, S. E.; Paul, A.; Welton, T.; Heenan, R. K.; Grillo, I. *J. Am. Chem. Soc.* **2005**, *127*, 7302-7303.

(23) Gao, Y.; Voigt, A.; Hilfert, L.; Sundmacher, K. *ChemPhysChem* **2008**, *9*, 1603-1609.

(24) Atkin, R.; Warr, G. G. *J. Phys. Chem. B* **2007**, *111*, 9309-9316.

(25) Freire, M. G.; Neves, C. M. S. S.; Marrucho, I. M.; Coutinho, J. A. P.; Fernandes, A. M. *J. Phys. Chem. A* **2009**, *114*, 3744-3749.

(26) Porada, J. H.; Mansueto, M.; Laschat, S.; Stubenrauch, C. *Soft Matter* **2011**, *7*, 6805-6810.

(27) Harada, M.; Yamada, M.; Kimura, Y.; Saijo, K. *J. Colloid Interface Sci.* **2013**, *406*, 94-104.

(28) Huddleston, J. G.; Visser, A. E.; Reichert, W. M.; Willauer, H. D.; Broker, G. A.; Rogers, R. D. *Green Chem.* **2001**, *3*, 156-164.

(29) Seddon K. R.; Stark, A.; Torres, M-J. *Pure Appl. Chem.* **2000**, *72*, 2275-2278.

(30) Isono, T. *J. Chem. Eng. Data* **1984**, *29*, 45-52.

(31) Zhang, Q.-G.; Xue, F.; Tong, J.; Guan, W.; Wang, B. *J. Solution Chem.* **2006**, *35*, 297-309.

(32) Andrade, S. M.; Costa, S. M. B.; Pansu, R. *J. Colloid Interface Sci.* **2000**, *226*, 260-268.

(33) Clausse, M.; Peyrelasse, J.; Heil, J.; Boned, C.; Lagourette, B. *Nature* **1981**, *293*, 636-638.

(34) Kaur, G.; Chiappisi, L.; Prevost, S.; Schweins, R.; Gradzielski, M.; Mehta, S. K. *Langmuir* **2012**, *28*, 10640-10652.

(35) Mo, C.; Zhong, M.; Zhong, Q. *J. Electroanal. Chem.* **2000**, *493*, 100-107.

(36) Garti, N.; Yaghmur, A.; Leser, M. E.; Clement, V.; Watzke, H. J. *J. Agric. Food Chem.* **2001**, *49*, 2552-2562.

(37) Chew, C. H.; Gan, L. M.; Ong, L. H.; Zhang, K.; Li, T. D.; Loh, T. P.; MacDonald, P. M. *Langmuir* **1997**, *13*, 2917-2921.

(38) Kataoka, H.; Eguchi, T.; Masui, H.; Miyakubo, K.; Nakayama, H.; Nakamura, N. *J. Phys. Chem. B* **2003**, *107*, 12542-12548.

(39) Johannessen, E.; Walderhaug, H.; Balinov, B. *Langmuir* **2003**, *20*, 336-341.

(40) Laia, C. s. A. T.; Brown, W.; Almgren, M.; Costa, S. l. M. B. *Langmuir* **1999**, *16*, 465-470.

(41) Velazquez, M. M.; Valero, M.; Ortega, F. *J. Phys. Chem. B* **2001**, *105*, 10163-10168.

(42) Mo, C. *Langmuir* **2002**, *18*, 4047-4053.

(43) Mandal, A. B.; Nair, B. U. *J. Phys. Chem.* **1991**, *95*, 9008-9013.

(44) Hirose, Y.; Yui, H.; Sawada, T. *J. Phys. Chem. B* **2004**, *108*, 9070-9076.

(45) Guering, P.; Lindman, B. *Langmuir* **1985**, *1*, 464-468.

(46) Ying, X.; Zhou, H.; Hu, J.; Xu, Y.; Zeng, J.; Chen, J.; Kuang, Y. *J. Appl. Electrochem.* **2009**, *39*, 1273-1278.

(47) Falcone, R. D.; Correa, N. M.; Silber, J. J. *Langmuir* **2009**, *25*, 10426-10429.

(48) Riter, R. E.; Undiks, E. P.; Kimmel, J. R.; Levinger, N. E. *J. Phys. Chem. B* **1998**, *102*, 7931-7938.

(49) Evans, D. F.; Ninham, B. W. *J. Phys. Chem.* **1986**, *90*, 226-234.

(50) Gao, H.; Li, J.; Han, B.; Chen, W.; Zhang, J.; Zhang, R.; Yan, D. *Phys. Chem. Chem. Phys.* **2004**, *6*, 2914-2916.

(51) Belletete, M.; Lachapelle, M.; Durocher, G. *J. Phys. Chem.* **1990**, *94*, 7642-7648.

(52) Tamura, K.; Schelly, Z. A. *J. Am. Chem. Soc.* **1981**, *103*, 1013-1018.

(53) Kumar, C.; Balasubramanian, D. *J. Phys. Chem.* **1980**, *84*, 1895-1899.

(54) Hansen, J. R. *J. Phys. Chem.* **1974**, *78*, 256-261.

(55) Halliday, N. A.; Peet, A. C.; Britton, M. M. *J. Phys. Chem. B* **2010**, *114*, 13745-13751.

(56) Li, Q.; Weng, S.; Wu, J.; Zhou, N. *J. Phys. Chem. B* **1998**, *102*, 3168-3174.

(57) Li, N.; Zhang, S.; Ma, H.; Zheng, L. *Langmuir* **2010**, *26*, 9315-9320.

(58) Bloembergen, N.; Purcell, E. M.; Pound, R. V. *Phys. Rev.* **1948**, *73*, 679-712.

(59) Wong, M.; Thomas, J. K.; Nowak, T. *J. Am. Chem. Soc.***1977**, *99*, 4730-4736.

(60) Krynicki, K. *Physica* **1966**, *32*, 167-178.

(61) Menger, F. M.; Saito, G. *J. Am. Chem. Soc.* **1978**, *100*, 4376-4379.

(62) Levitt, M. H. *Spin Dynamics: Basics of Nuclear Magnetic Resonance*; Wiley, 2001.

(63) Qi, L.; Ma, J. *J. Colloid Interface Sci.* **1998**, *197*, 36-42.

CHAPTER 6

An Insight into the Kosmotropic/Chaotropic Behavior of Solutes in the Ionic Liquid Mixtures

The present chapter deals with the understanding of the behavior of added chaotropic/kosmotropic solute in the ionic liquid mixtures. This chapter is divided into two sections. In the first section 6.1, the unusual behavior of urea in its aqueous solutions of ionic liquids has been discussed. In the consequent section 6.2, the behavior of different kosmotropic and chaotropic solutes in the ionic liquid systems are presented. The magnitude of kosmotropic/chaotropic behavior of salts is altering with the variation in the hydrophobic alkyl group substitution in ionic liquid cations. A plausible explanation for the behavior of each of the kosmotropic/chaotropic solutes in the ionic liquid mixtures has been presented in this section of the chapter.

6.1. INTRODUCTION

On the basis of effect of salt on the structure of water, the salts can be classified into two categories; water structure-breaker/salting-in (S-I) salts and water structure-maker/salting-out (S-O) salts.[1,2] It was Hofmeister who proposed a series for anions and cations of salt on their ability to precipitate proteins and macromolecules in their aqueous salt solutions.[3-6]

$$CO_3^{2-} > SO_4^{2-} > S_2O_3^{2-} > H_2PO_4^{-} > F^{-} > Cl^{-} > Br^{-} \approx NO_3^{-} > I^{-} > ClO_4^{-} > SCN^{-}$$

$$Zn^{+2} > Mg^{+2} > Ca^{+2} > Li^{+} > Na^{+} > K^{+} > NH_4^{+} > Rb^{+} > Cs^{+}$$

The ions on the left hand side of the series are called as S-O or kosmotropes or water structure-maker while on the right hand side of the series are known as S-I or chaotropes or water structure-breaker.[7] There is an increasing interest in this subject to understand the molecular mechanism by which ions operate in its aqueous solutions containing hydrophobes and macromolecules.[8] Zhang *et al.* proposed a model to describe the S-I/S-O phenomenon by measuring the low critical solution temperature of [poly(N-isopropylacrylamide)] in aqueous solutions of different electrolytes.[8] The model is based on the three different types of interactions to explain the S-I/S-O effects: (i) the destabilization of the hydrated polar groups of the solute by the polarization effect of ions; (ii) increased surface tension of solvent by salts; (iii) direct binding of ions to the polar groups of solute molecules. The interactions denoted as (i) and (ii) lead to the S-O phenomenon, whereas the interaction denoted by (iii) is responsible for the S-I phenomena. The MD simulation study shows that the strength of hydrophobic interactions is induced by high charge density ions by making hydration complexes with water away from the hydrophobic surfaces.[9] This effect is purely entropic in origin, similar to the S-O phenomenon. On the other hand, the reduction of hydrophobic interaction, similar to the S-I phenomenon are induced by the binding of low charge density ions to the hydrophobic surface and the effect being either entropic or enthalpic in origin.[9] Research on ionic liquids has received considerable attention because of its special physicochemical properties like very low vapor pressure, high thermal stability, recyclability, wide liquidus range and wide electrochemical window.[10,11] ILs have been

used in a variety of application purposes such as in electrochemistry, biological and chemical processes, energy and food processing.[12-15] In the literature exists a few reports describing the effect of salt on the properties of ILs.[16-18] For example, the mechanism of S-I/S-O phenomenon of salts in their aqueous solutions containing ILs is not fully explored. Freire et al.[19] proposed a mechanism of S-I/S-O phenomenon in the aqueous salt solutions of ionic liquids and found out the direct interactions of polarizable S-I ions with the hydrophobic alkyl group of ionic liquids.

All the ionic liquids used in this chapter of the thesis are of alkyl imidazolium cation based with a variation in their alkyl group substitution. These are 1-octyl-3-methylimidazolium bromide ([OMIM]Br), 1-octyl-3-methylimidazolium tetrafluoroborate ([OMIM][BF_4]), 1-hexyl-3-methylimidazolium bromide ([HMIM]Br), 1-hexyl-3-methylimidazolium tetrafluoroborate ([HMIM][BF_4]), 1-butyl-3-methylimidazolium bromide ([BMIM]Br) and 1-butyl-3-methylimidazolium tetrafluoroborate ([BMIM][BF_4]) and their structures are given in Figure 1.

This chapter is divided into two sections. The first section of the chapter 6, deals with all the six selected ILs presented above and describes about the interesting chaotropic or S-I behavior of urea on the viscosity of the IL mixtures. It has been reported that, non-electrolyte like urea, which does not alter the arrangement of water molecules to an appreciable extent has attracted several investigations to ascertain the nature of urea in several systems.[20,21] Urea decreases the hydrophobic bonding between hydrophobic particles and increases the solubility of hydrocarbons and organic compounds[22-26] and hence considered as the "water structure-breaker". Considering the importance of urea and ionic liquids in biological-related problems, it is essential to understand how the solution viscosity is altered in such systems and has been discussed in this section of the chapter 6.

In the second section of the chapter 6, we have focused our research about the S-I/S-O behavior of salts in its aqueous solution containing ILs through the viscosity measurements. Here all the selected ILs is of the alkyl group substituted imidazolium bromide based with the variation in their hydrophobic alkyl group substitution. The selected salts are LiCl, $LiClO_4$, $NaClO_4$, GnCl and Gn_2SO_4 with their wide nature of

effects on the structure of water. The concepts of hard and soft nature of ions, Hofmeister effects and the concept of surface viscosity are used to explain the results.

6.2. EXPERIMENTAL SECTION

6.2.1. Materials

1-Methylimidazole (Sigma Aldrich with 99.5% *w/w* purity), 1-Bromobutane (Sigma Aldrich with 99.5% *w/w* purity), 1-Bromohexane (Sigma Aldrich with 99.8% *w/w* purity) and 1-Bromoocatne (Sigma Aldrich with 99.9% *w/w* purity) were procured and used after distillation. $NaBF_4$ (Fluka, purity > 98%), LiCl (Fluka with 99.8% *w/w* purity), $LiClO_4$ (Fluka with 99.5% *w/w* purity), $NaClO_4$ (Fluka with 99.5% *w/w* purity), guanidinium chloride (GnCl) (Sigma Aldrich with 99.9% *w/w* purity), Gn_2SO_4 (Sigma Aldrich with 99.9% *w/w* purity) and urea (Sigma Aldrich with 99.8% *w/w* purity) were purchased and heated in an oven at 120 °C for 5 h before their use.

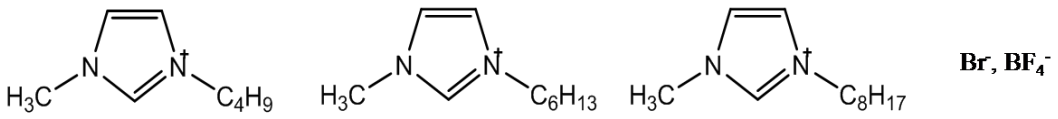

[BMIM] [HMIM] [OMIM]

Figure 1. Cationic and anionic structure of imidazolium based ILs employed in the study.

The aqueous salt solutions were prepared in deionized water (specific conductance of < 0.055×10^{-6} S cm^{-1}) on the basis of molality with an accuracy of ± 0.0002 mol kg^{-1}. All the alkylimidazolium bromide based ILs employed in the present study were synthesized according to the reported procedure.[27-30] The freshly synthesized ILs were dried and purified under high vacuum with a constant heating at 323.15 K for 12 h. The water content was measured using a Karl-Fischer titrator and was observed to be < 100 ppm. The imidazolium tetrafluoroborate-based ILs was also checked for any halide impurities by Vollahard's titration and was obtained to be > 50 ppm. Note that the standard Volhard titration has been validated using a chloride-selective electrode.[31,32] The ^{1}H NMR spectra

of the synthesized ILs did not show any traces of impurities and are in good agreement with the reported values.[27-30]

6.2.2. Experimental procedure

Brookfield-ultra rheometer with a cone plate arrangement was used for the measurement of viscosity of IL solutions and the sample required for each measurement was 0.5 ml. The viscosity (η) values of the solutions were obtained through the equation as:

$$\eta = (100/RPM)\ (TK)\ (\text{Torque})\ (SMC) \qquad (1)$$

where *RPM*, *TK* (0.09373) and *SMC* (0.327) are the speed, viscometer torque constant and spindle multiplier constant, respectively. The calibration of the instrument was performed by taking the reported viscosity data of aqueous solutions of $CaCl_2$, $MgCl_2$ and [BMIM][BF_4] in different concentration. The accuracy of the instrument was obtained as ±1%.[33,34] The reported experimental viscosity data are the average of triplicate measurement with a precision of 0.25%. All the experiments were carried out at 298.15±0.01 K and the temperature of the experimental set up was monitored by using a julabo temperature thermostat bath.

Now the results and discussion of each section of the chapter 6 are discussed as below.

6.3. UNUSUAL BEHAVIOR OF UREA IN THE AQUEOUS UREA-IONIC LIQUID SYSTEM

6.3.1. RESULTS AND DISCUSSION

In this study we have reported the effect of urea on the aqueous solutions of ionic liquids using the viscometric technique. Figure 2 shows the concentration dependence of the viscosity, η data for aqueous urea in ionic liquid mixtures. From the drawing, it is seen that urea does not exhibit any pronounced effect on the η in the presence of [BMIM]Br and [HMIM]Br when compared against the η values of aqueous urea alone. The interactions between the water and urea molecules in turn reduce the strength of hydrophobic bonding prevailing between the ionic liquid cations. It may be noted that the nonpolar solutes like hydrocarbons and hydrocarbon moieties, dissolve interstitially in water and in aqueous urea solutions. Urea actively participates in the formation of

clusters. The increased cluster formation is directly related to the weakening of hydrophobic bonding upon addition of urea as evidenced by many solution properties.[35] Weakening of the hydrophobic bonding results into loosening of the ionic liquid structure and hence the viscosity is reduced. Also, the presence of urea in water increases the relative permittivity of water,[36-39] which helps in further weakening of the coulomb interactions prevailing between $[OMIM]^+$ and Br^-.

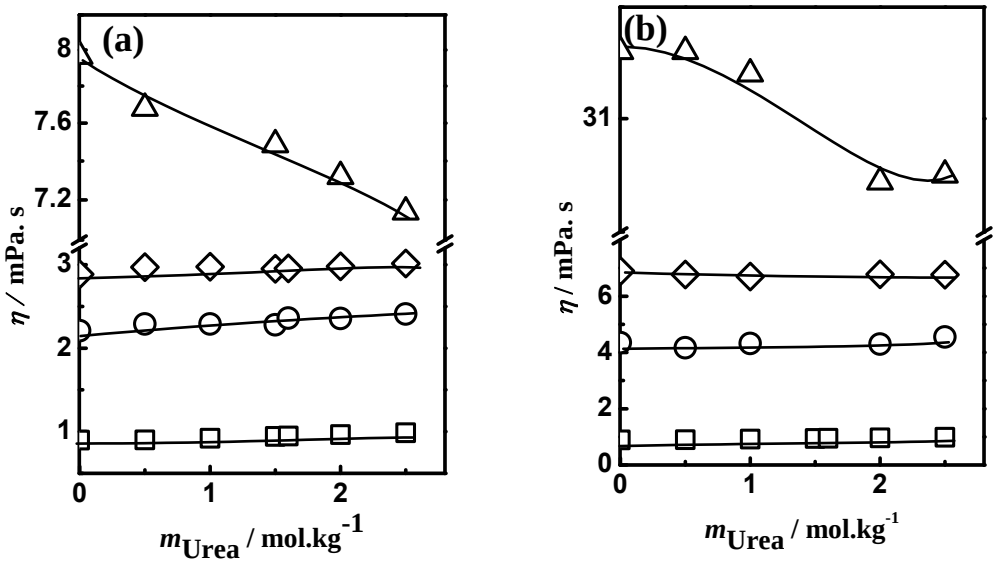

Figure 2. The comparative plots of η vs. concentration of aqueous urea solution for urea+water mixture (□), [BMIM]Br (O), [HMIM]Br (◇), [OMIM]Br (Δ) at $x_{[BMIM]Br/[HMIM]Br/[OMIM]Br}$= (a) 0.05 and (b) 0.1.

Hence, the favourable interactions between the urea molecules and the "iceberg" region of the cation lead to the weakening of the ionic liquid structure and the mixture containing [OMIM]Br ionic liquid shows the lowering of the viscosity as shown in Figure 2. Alternatively, the micelle formation in $[OMIM]^+$ type of ionic liquids and its impact on the viscosity cannot be discounted.[35] This behaviour is seen both at x_{IL} = 0.05 and 0.1. The magnitude of the viscosity of the mixture however increases due to increase in the concentration of the ionic liquid in the mixture. The observed enhancement is not abnormal for the lower alkylated ionic liquids possessing $-C_4H_9$ and $-C_6H_{13}$ groups. Conversely, in the case of $-C_8H_{17}$ containing imidazolium based ionic liquid, the enhancement in the viscosity is nearly 4 times (at x_{IL} = 0.1) as compared to the viscosities noted in the lower composition range of ionic liquid at x_{IL} = 0.05.

In Figure 3, we show the effect of change in the counter anion of the ionic liquids. It is noted that for the ionic liquids containing -C_4H_9 and -C_6H_{13} groups, the magnitude of the viscosity is the nearly same for both the tetrafluoroborate-based and for bromide based aqueous ionic liquids with urea mixtures. With the alkyl substitution of -C_8H_{17}, the magnitude of the viscosity for the mixture containing tetrafluoroborate based ionic liquid is lower as compared to the mixture containing bromide based ionic liquid (see Figures. 2(a) and 3).

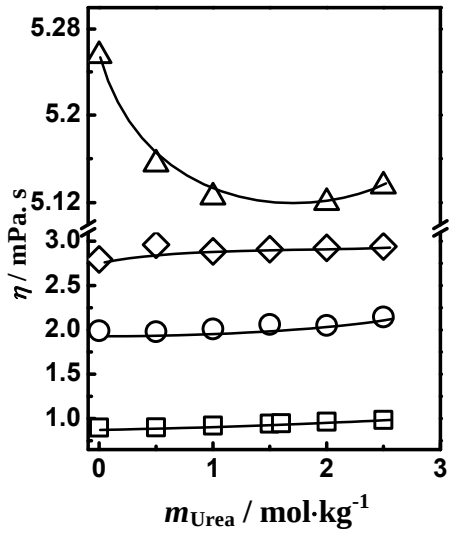

Figure 3. A comparative plot of η vs. molality of aqueous solutions of urea for $x_{[BMIM][BF4]}$ (O), $x_{[HMIM][BF4]}$ (◇), $x_{[OMIM][BF4]}$ (Δ) all at 0.05; and aqueous solution of urea (□).

Upon increasing the concentration of urea the viscosity of the mixture containing tetrafluoroborate based ionic liquid is further reduced, a trend also followed by the bromide based ionic liquid. This suggests that the anion replacement in the mixture does not have any effect for the smaller alkyl group substituted ionic liquids however, for –C_8H_{17} based ionic liquid and the substitution aids to the further suppression of the viscosity. The reason for this effect can be correlated to the increased relative permittivity, ε of aqueous urea mixture as compared to that of pure water.[35,37-40] The increased ε value of aqueous urea mixture is expected to reduce the coulombic interaction between the -C_8H_{17}-based imidazolium cation and tetrafluoroborate anion. The

coulombic interactions are weaker in the tetrafluoroborate ionic liquid as compared to the bromide based ionic liquid because of the low charge density of the tetrafluoroborate anion. Hence, it would be easier for the urea + water mixture to dissociate the tetrafluoroborate based ionic liquid into its counter -C_8H_{17} substituted imidazolium cation and tetrafluoroborate anion. The dissociated cation and anion are then solvated by the water molecules. The dissolved -C_8H_{17} substituted imidazolium cation would form -C_8H_{17} imidazolium-water-urea complexes, whereas the anion would also be hydrated in the aqueous solution. In order to discern the effect of the salting agents, in Figure 4 is shown a comparison of the structure-breaking behaviour of urea and the structure-making behaviour of LiCl in aqueous ionic liquid solutions.

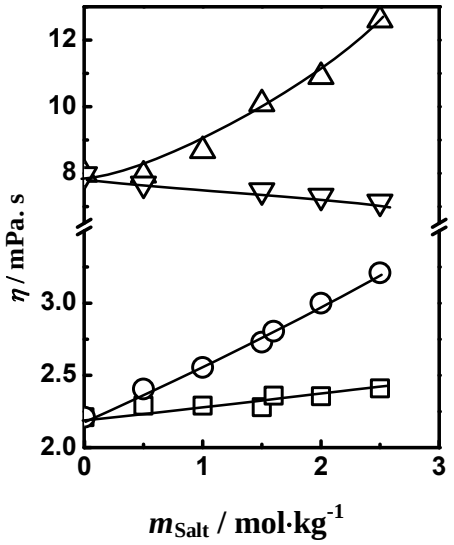

Figure 4. The η values as a function of salt concentration for [OMIM]Br in aqueous solutions of urea (▽) and LiCl (△), and [BMIM]Br in aqueous solutions of urea (□) and LiCl (O), at $x_{[OMIM][Br]/[BMIM][Br]} = 0.05$

LiCl shows an expected structure-making behaviour in aqueous solution of both -C_4H_9 and -C_8H_{17} substituted ionic liquids. Li^+ cation owing to its small size and strong electric field reorient the water molecules very strongly around itself and form rigid hydration shells. This results into the availability of less water molecules for the ionic liquid constituents resulting into the ions to come at closer proximity with each other thus they

form larger aggregates with very small amount of the water molecules. The presence of these aggregates leads to the enhancement in the viscosity of the system. However, in the case of urea, for lower alkylated ionic liquids there is a mild increment observed in the viscosity of the mixture upon changing the concentration of urea. The reason for this mild increment may be due to the fact that the coulombic interactions between the cations substituted with lower alkyl chains and the anions are reasonably strong. These interactions are not affected due to the presence of urea. Therefore, this mild enhancement in the viscosity of such systems is directly a function of concentration alone i.e. the increase in the number of particles.

For higher alkylated ionic liquids, the behaviour of urea in the mixture reverses ensuring a considerable decrease in the viscosity. It is known that in the presence of water, ionic liquids dissociate into its counter cations and anions. The water molecules are enforced to reorient around the long hydrophobic tails of the cations due to hydrophobic hydration phenomenon.[2] As discussed earlier, urea molecules form stable complexes with these water patches around the non polar part of the ionic liquids cations.[35] This results into the decrease in the hydrophobic interaction between the alkyl tails and also suppresses the coulombic interaction between the ionic liquid cations and anions. This leads to a reduction in the viscosity of the mixture containing the higher alkyl group substituted ionic liquid. Hence in the presence of higher alkyl group substituted ionic liquids, urea behaves as a structure-breaker in its aqueous solution.

In Figure 5, we show 1) the effect of increase in the carbon content in the ionic liquid cations on altering the viscosity of the mixture and 2) the effect of increasing concentration of urea on the mixture viscosity. An increase in the carbon content in the alkyl tails substituted on ionic liquid cations gradually increases the viscosity of the mixture. As a general trend the viscosities of pure ionic liquids increases with increasing the cationic size, particularly with increase in the alkyl chain length. The mixture of aqueous ionic liquid mixtures with urea follows the same trend of increasing viscosities as observed for the pure ionic liquids. Interestingly, the increasing concentration of urea has a nullifying effect on the mixture viscosity. As seen from Figure 5, for the lower alkylated ionic liquids the increasing concentration of urea in the mixture does not produce any noteworthy effect on the mixture viscosity. However, as the number of

carbon atoms in the alkyl chain increases to -C_8, a distinct increase in the mixture viscosity on all the concentrations of urea is observed. The aqueous solution of -C_8H_{17} substituted ionic liquids exhibits the maximum viscosity suggesting the maximum structuredness of ionic liquid in its binary mixtures. In the ternary mixtures of aqueous ionic liquid with urea, where urea concentration is 0.05 mol·kg^{-1}, the mixture viscosity reduces as compared to the viscosity of ionic liquid in its aqueous solution. Upon increasing the concentration of urea from 0.05 to 2.5 mol·kg^{-1}, the viscosity of the ternary mixture is further decreased.

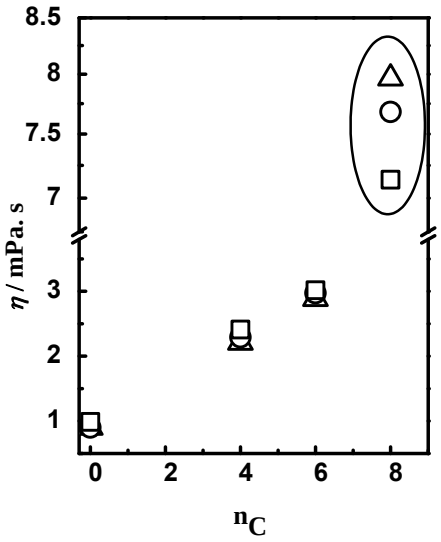

Figure 5. The η values as a function of number of carbon atom of [$C_n$mim]Br based ionic liquids (where, n_C = 4, 6, 8 and "0" stands for the absence of ionic liquid); aqueous solutions of ionic liquid (∆), 0.5 urea (O) and 2.5 mol·kg^{-1} m urea (□).

This observation suggests that urea shows the chaotropic behaviour in a mixture of higher alkylated ionic liquid and water, resulting into a decrease in the viscosity of mixtures.

6.3.2. CONCLUSIONS

In summary, we conclude that urea exhibits mild kosmotropic behaviour in aqueous mixtures of ionic liquid, in which the ionic liquid component is substituted with lower alkyl group. However, this behaviour of urea is reversed into the chaotropic, when the ionic liquid is substituted with -C_8H_{17} group on the imidazolium ring. In addition to this increase in the urea concentration, the chaotropic behaviour becomes more pronounced.

Therefore, this aqueous mixture of the ionic liquid with urea in higher composition of urea is far less viscous as compared to the aqueous solution of ionic liquid. These observations can prove to be very important in the industrial applications as urea can prove to be a potential viscosity reducer for ionic liquids.

6.4. DO SALTING EFFECT IS A FUNCTION OF HYDROPHOBIC ALKYL GROUP SUBSTITUTION IN IONIC LIQUID CATION?

6.4.1. RESULTS AND DISCUSSION

6.4.1.1. Effect of S-I and S-O Salts on the Alkyl Chain of ILs

In this section we discuss about the effect of S-I/S-O salts in their aqueous solutions containing ILs. All the ILs is of the alkyl group substituted imidazolium bromide based and their structures are given in Figure 1.

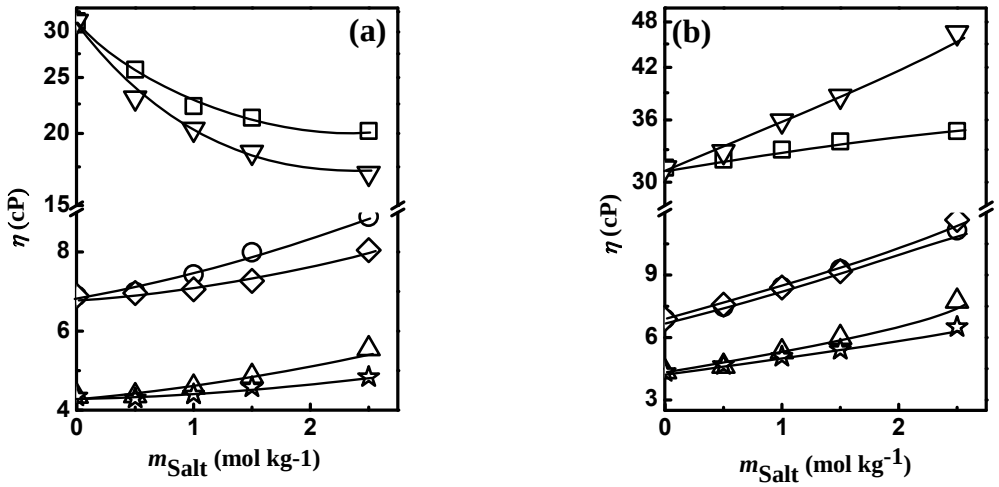

Figure 6. The η versus m_{Salt} plots for (a) [OMIM]Br in aqueous solutions of $LiClO_4$ (□), $NaClO_4$ (▽), [HMIM]Br in $LiClO_4$ (○), $NaClO_4$ (◇), [BMIM]Br in $LiClO_4$ (Δ), $NaClO_4$ (☆), (b) [OMIM]Br in Gn_2SO_4 (□), LiCl (▽), [HMIM]Br in Gn_2SO_4 (O), LiCl (◇), [BMIM]Br in Gn_2SO_4 (△), LiCl (☆).The composition of ILs in all the systems are fixed as x_{IL} = 0.1.

Figure 6. (a) represent the variation in viscosity (η) with the increase composition of S-I salts viz. $LiClO_4$ and $NaClO_4$ for [$C_n$mim]Br (n = 4, 6, 8). The composition of ILs for the

experiment was taken as x_{IL} = 0.1. The addition of $LiClO_4$ and $NaClO_4$ salt increase the magnitude of η of the mixtures containing the lower alkyl chain length substituted ILs viz. [BMIM]Br and [HMIM]Br. From the Figure 6 (a) it has been observed that the magnitude of enhancement in the η is higher for $LiClO_4$ as compared to that of $NaClO_4$. This effect can be described on the basis of the high charge density of Li^+ ion as compared to that of Na^+ ion; as the contribution towards the η from the ClO_4^- ion is common in both the electrolytes. The kosmotropicity of Li^+ ion is higher as compared to that of Na^+ ion and for that reason the high charge density kosmotropic Li^+ ion orients the water molecules around them more strongly as compared to that of Na^+ ion.[7] Therefore, the local ordering of water molecules around the Li^+ ion is stronger as compared to that of the Na^+ ion. Consequently, the local viscosity (or microviscosity, η_{micro}) experienced by the water molecules surrounding the high charge density Li^+ ion is more as compared to that of the Na^+ ion. Therefore, the enhancement in the bulk viscosity, η_{bulk} for $LiClO_4$ is higher as compared to that of the $NaClO_4$ in [BMIM]Br and [HMIM]Br mixtures. The enhancement in viscosity by the ClO_4^- salts are also in accordance with the Hofmeister series.[8] Li^+ comes before the Na^+ ion in the Hofmeister series[8] and are more S-O in nature as compared to Na^+ ion. Therefore the effect of Li^+ salt on the viscosity is more as compared to the Na^+ salt as represented in the Figure 6 (a). Interestingly, with the increase in the alkyl chain length of IL to $-C_8H_{17}$ as in the case of [OMIM]Br, these S-I salts ($LiClO_4$ and $NaClO_4$) shows an anomalous decrease in their bulk viscosity, η_{bulk} and has been discussed later on in a separate section of the manuscript.

We have also studied the effects of S-O salts like LiCl and Gn_2SO_4[22,41] on the viscosity of IL mixtures. Figure 6 (b) illustrates the effect of these S-O salts on the viscosity of the IL mixtures by keeping the composition of IL fixed as x_{IL} = 0.1. Both the S-O salts increase the viscosity of the ternary mixture of imidazolium-based ILs. The S-O nature of LiCl is due to the strong dominating kosmotropic effect of the Li^+ ion[41] over the mild chaotropic Cl^- ion.[41] On the other hand, in case of Gn_2SO_4 the strong S-O nature of SO_4^{2-} anion dominates over the S-I nature of Gn^+ ion and the salt is overall behaves as a S-O salt.[22] As the SO_4^{2-} ion is placed much above to that of Li^+ ion in the Hofmeister series therefore, the overall S-O effect of Gn_2SO_4 is higher than that of LiCl. Also, as the

Gn_2SO_4 is a combination of S-I Gn^+ cation and S-O SO_4^{2-} anion therefore, its effect on the viscosity is different than that of other S-O LiCl salt.

Interestingly, we have observed a change in the S-O nature of these salts with the increase in the alkyl chain length of ILs as shown in Figure 7. The enhancement in viscosity by Gn_2SO_4 is more as compared to that of LiCl for lower alkyl group substituted ILs viz. [BMIM]Br and [HMIM]Br. However with the increase in the alkyl chain length to $–C_8H_{17}$ as in the case of [OMIM]Br the trend in viscosity is being reversed and LiCl shows more enhancement in viscosity as compared to Gn_2SO_4 as represented in Figure 7(a) and (b) for x_{IL} = 0.05 and 0.1, respectively. This suggests that the S-O behavior of Gn_2SO_4 is higher as compared to that of LiCl in case of lower alkyl chain length [BMIM]Br and [OMIM]Br mixtures. On the other hand, in case of higher alkyl chain length [OMIM]Br mixtures, the S-O behavior of LiCl is more as compared to that of Gn_2SO_4. By taking the two extreme parts of alkyl chain length of ILs viz. $-C_4H_9$ and $-C_8H_{17}$, the order of S-O behavior of LiCl and Gn_2SO_4 are represented as in the Chart 1.

It was reported that Gn^+ of Gn_2SO_4 decreases the S-O effect of SO_4^{2-} in the system as the former is a S-I cation.[22] If the S-O effect of salts is only due to the ion-water interactions between the salt and water, then we should observed the same trend of S-O behavior for both the salts in all the imidazolium bromide-based ILs. However, as we observe a change in the S-O behavior of these salts with the change in the hydrophobic alkyl chain length of ILs; therefore, it indicates that the hydrophobic alkyl groups attached to the imidazolium ring of IL plays a significant role in the salting phenomenon. And, besides salt ion-water interactions other interactions are also plays important role in the S-O phenomenon for Gn_2SO_4 which become prominent with the increase in the alkyl chain length of ILs. It was reported that the hydration number of higher alkyl chain length substituted ILs are higher as compared to that of its lower alkyl chain length counterpart.[42] Thus, more numbers of hydrophobic hydrated water molecules (icebergs) are present around the $–C_8H_{17}$ chain as compared to that of $–C_4H_9$ chain.[42] The high negative surface charge density SO_4^{2-} ion strongly attracts the dipole of water molecules towards itself by the addition of S-O Gn_2SO_4 into the IL system. As a result of which less

number of water molecules are available for the hydration of ILs. To gain the cost of their hydration energy, the van der Waals interactions between the alkyl chain length of IL increase[43,44] resulting into the formation of aggregated species inside the mixtures. Strong and definite aggregates are formed in case of [OMIM]Br and weaker aggregates are formed for [HMIM]Br and [BMIM]Br.[43]

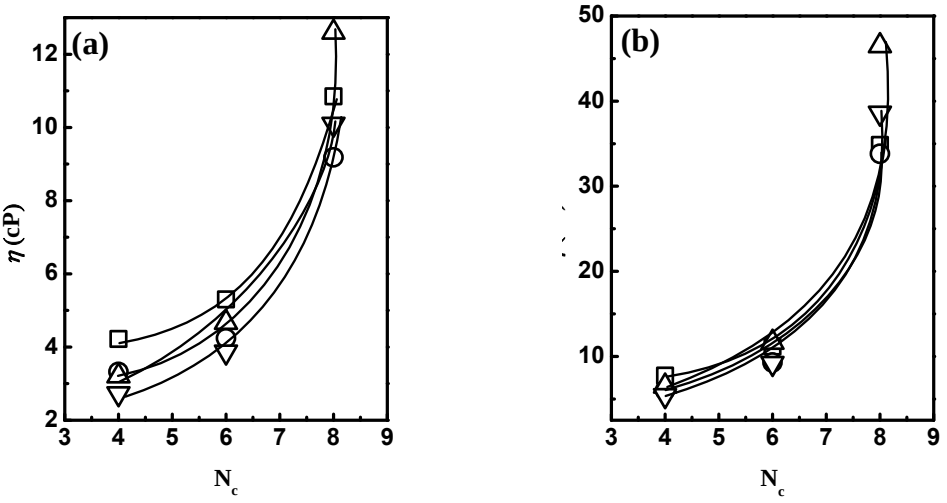

Figure 7. The plots of η versus the number of carbon atom (N_c) of alkyl chain length of [$C_n$mim]Br-based ILs for 2.5 mol kg^{-1} Gn_2SO_4 (□), 1.5 mol kg^{-1} Gn_2SO_4 (○), 2.5 mol kg^{-1} LiCl (△) and 1.5 mol kg^{-1} LiCl (▽) with x_{IL} = 0.05 (a) and 0.1(b), respectively.

However, the chaotropic effect of Gn^+ ion of Gn_2SO_4 becomes prominent with the increase in the alkyl chain length of IL from $–C_4H_9$ to $–C_8H_{17}$ as more numbers of iceberg structures[42] with stronger and definite aggregates[43] are broken in the case of higher alkyl chain length [OMIM]Br due to their higher hydrophobic surface area as compared to the lower alkyl chain length substituted [BMIM]Br with lower hydrophobic surface area. The direct interactions between the polarizable S-I ions with the hydrophobic alkyl group of ILs is also in support of the above statement.[19] The overall S-O effect of Gn_2SO_4 therefore decreases with the increase in the alkyl chain length of ILs from $–C_4H_9$ to $–C_8H_{17}$. For that reason, the enhancement in the bulk viscosity, η_{bulk} by Gn_2SO_4 is less as compared to that of LiCl for higher hydrophobic $–C_8H_{17}$ group substituted [OMIM]Br. On the other hand, the enhancement in viscosity by Gn_2SO_4 is more than that of LiCl for

[HMIM]Br and [BMIM]Br and that can be understood by higher value of ΔS_{hyd} for SO_4^{2-} (-199 $JK^{-1}mol^{-1}$) as compared to that of Li^+ (-148 $JK^{-1}mol^{-1}$).[41]

Chart 1. Representation of the order of S-O nature of salts with the increase in the alkyl chain length of ILs.

Surface viscosity may also be considered as a factor to understand the experimental observation. It is reported that S-I salts decrease the surface viscosity of the aqueous solutions of surfactant, whereas the S-O salts increase the surface viscosity.[45] Therefore, both LiCl and Gn_2SO_4 being S/O in nature, increase the surface viscosity of the IL mixtures which are reflected in the enhancement in the bulk dynamic viscosity.

In the above section we have presented a comparative explanation for the S-O and S-I salts. Now in the following sections we are going to discuss about the effect of individual salts on the viscosity of its aqueous solutions containing ILs.

6.4.1.2. Effects of LiCl

Figure 8(a) and (b) represent the 3D plot for η with the increase in the compositions of LiCl in [BMIM]Br and [OMIM]Br, respectively and also with the increase in the x_{IL}. The addition of LiCl increases the viscosity of the ternary mixtures for a fixed composition of IL. The trend in viscosity remains same in all the studied compositions of IL. In the case of aqueous solutions of LiCl containing ILs, the enhancement in viscosity is mainly due to the high charge density of Li^+ cation, which orients the dipole of water molecules strongly around itself resulting in the enhancement in the microviscosity, η_{micro} around the Li^+ and is reflected in the bulk viscosity, η_{bulk} of the mixtures. More number of water molecules is involved in the hydration of kosmotropic Li^+ ions by the increase in the compositions of LiCl. As a result of which the number of water molecules available for

the hydrophobic hydration ('iceberg') of alkyl chain length of IL becomes less and this effect increases with the increase in the alkyl chain length of ILs; as more number of water molecules are required for the hydration of $[OMIM]^+$ as compared to that of $[BMIM]^+$.In addition to that, the hydration number of $-C_4H_9$ substituted IL is more as compared to that of $-C_8H_{17}$ substituted IL [27, 31] and the demand of the hydration energy of the IL is increase with the increase composition of LiCl.[44]

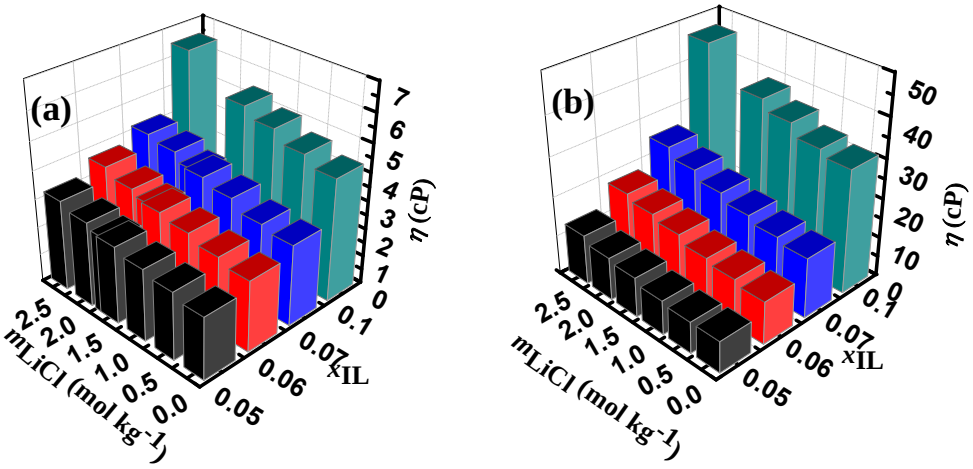

Figure 8. The η versus m_{LiCl} plots for aqueous solutions of LiCl with x_{IL} = 0.05 (black), 0.06 (red), 0.07 (blue) and 0.1(dark cyan) for [BMIM]Br (a) and [OMIM]Br (b), respectively.

For that reason the IL molecules minimize their water accessible surface area in order to reduce their hydration energy[43,44] and form aggregates by the increased van der Waals interactions between the hydrophobic alkyl chain length of IL molecules.[43] In addition to that the addition of LiCl increases the surface viscosity of the IL mixtures as IL molecules with hydrophobic alkyl chain length behaves as surfactant in its aqueous solutions.[45,46] Thus four factors contribute to the enhancement in the viscosity in aqueous solutions of LiCl containing ILs. (I) The contribution from the increased microviscosity around the high charge density Li^+ cations; (II) the contribution from the increased aggregates of IL; (III) the contribution from the increased surface viscosity of the fluids; and (IV) the contribution from the increased number of particles with the increase in the compositions of LiCl. In addition to this, the model proposed by Zhang *et al.*[8] can also be

applied to explain the S-O behavior of LiCl in its aqueous solutions containing ILs. Firstly, because of higher affinity of Li^+ ions towards water molecules, it disturbs the hydrated water molecules surrounding the IL cations. Secondly, increase in the composition of LiCl increases the surface tension of the mixtures. As a result of which the formation of cavity[47] becomes difficult to incorporate the IL molecules. Therefore, the interactions between the IL molecules increase leading to the formation of aggregated particles inside the solutions; resulting into the enhancement in the bulk viscosity, η_{bulk} of the mixtures. Similarly, the enhancement in the viscosity for Gn_2SO_4 in their aqueous solutions containing IL behaves in a similar way to that of LiCl.

6.4.1.3. The Effect of Perchlorate Salts

The perchlorate ion is known to be a well known water structure-breaker or S-I (chaotropic) in nature.[47-49] In the current investigation, we have taken two perchlorate salts ($LiClO_4$ and $NaClO_4$) with the variation in their cationic counterpart and studied its effect on the viscosity of its aqueous solutions containing different hydrophobic alkyl group substituted imidazolium based ILs which are depicted in Figure 9. Figure 9(a) and (b) represents the effects of $LiClO_4$ and Figure 9(c) and (d) illustrate the effects of $NaClO_4$ on the viscosity of its aqueous solutions containing [BMIM]Br (Figure 9a and c) and [OMIM]Br (Figure 9b and d), respectively. In the case of [BMIM]Br, both the ClO_4^- salts increase the viscosity of the mixtures with the increase in their composition and the same trend is observed in all the studied compositions of ILs. The magnitude of viscosity is higher for $LiClO_4$ as compared to that of $NaClO_4$. This is due to the more kosmotropic nature of Li^+ cation as compared to that of Na^+ ion.[49] Also the value of change in the structural entropy (ΔS_{str}) provides the information of local ordering of water molecules around the ions.[41] The ΔS_{str} value for Li^+ is six times higher as compared to that of Na^+ (-96 J. K^{-1}. mol^{-1} for Li^+ and -16 J. K^{-1}. mol^{-1} for Na^+).[41] It means the water molecules are more structured around the Li^+ ion as compared to that of Na^+. This result in the more enhancements in the local viscosity or microviscosity, η_{micro} around the former ion as compared to the later one and therefore, the η_{bulk} for $LiClO_4$ mixture is more as compared to that of $NaClO_4$ mixture. However, for [OMIM]Br mixtures an unusual behavior in viscosity is observed with the increase in the compositions of ClO_4^-. It has been observed

that an initial decrease in the viscosity with the increase in the compositions of ClO_4^- followed by an enhancement at lower compositions of [OMIM]Br. It suggests viscosity versus composition of ClO_4^- passes through a minima and is vanished at higher compositions of [OMIM]Br. The minima observed for ClO_4^- containing salts are shown in one of our previous report.[50]

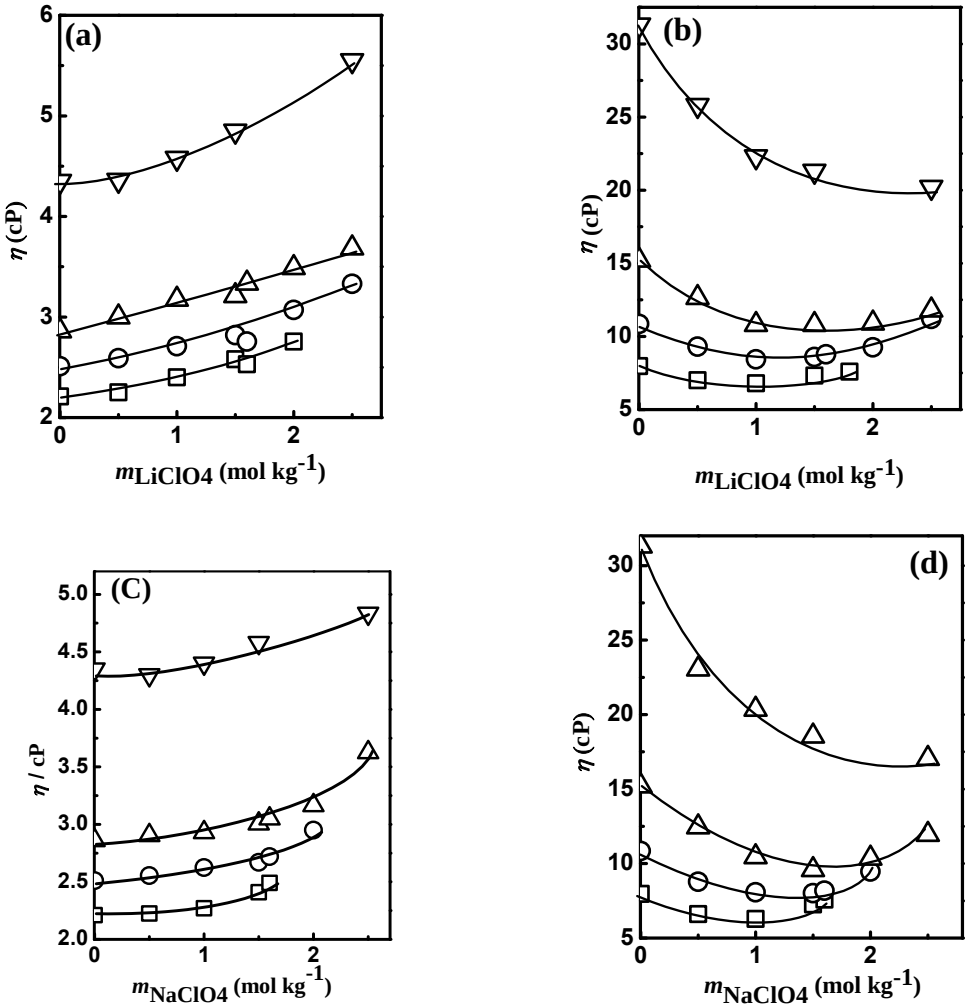

Figure 9. The η versus m_{salt} plots for x_{IL} = 0.05 (□), 0.06 (○), 0.07 (△), and 0.1 (▽) for $LiClO_4$ in [BMIM]Br (a) and [OMIM]Br (b); and $NaClO_4$ in [BMIM]Br (c) and [OMIM]Br (d), respectively.

In the case of aqueous perchlorate solutions of [OMIM]Br, there is the possibility of hydrogen bonding interactions between the C2-H atom of imidazolium ring with the oxygen atom of ClO_4^- ion.[8,51] Also the density of water molecules is more around a

hydrophobic surface as compared to that of the bulk.[52] These water molecules are more compressible[52] and forms 'iceberg' around the hydrophobic surface.[42] Thus, beside the interactions of the polarizable ClO_4^- anions with the C2-H atom of imidazolium ring of ILs, it also interacts with the hydrophobic hydrated water molecules present around the hydrophobic alkyl chain length of ILs.[19] It was also reported that the polarizable, low charge density halide ions like I^- (chaotrope) shows more surface preference as compared to that of the bulk and the cost of cavitational energy required to form a cavity around a water-hydrophobic interface is nearly half of that in the bulk.[52] It means chaotropic ions prefer to stay around the hydrophobic surface and are thermodynamically more stable as compared to that in the bulk. Lopez-Leon *et al.* reported that the rigid chaotropic ion-water complex create difficulty in the approaching of the two hydrophobic surfaces to come closer to each other.[53] Thus, from all of the above reports we can infer that with the increase in the compositions of ClO_4^- ions it interacts with the hydrophobic hydrated water molecules present around the hydrophobic alkyl chain length of ILs and thereby breaks the iceberg networks[42,43] and forms semi-hydrated species[53] around the hydrophobic alkyl chain length of ILs and get satisfied its rest of the hydration energy through the dispersion interactions with the hydrophobic alkyl chain length of ILs. This increased dispersion interactions between the semi-hydrated ClO_4^- anion[53] with the hydrophobic alkyl chain length of ILs increases the repulsion between the alkyl chain lengths of ILs and therefore, the attractive component of the van der Waals interactions between the alkyl chain length of ILs[43] is being reduced resulting in the breakdown of the aggregated species inside their aqueous solutions containing S-I salts and are schematically shown in the Figure 10. However, ClO_4^- salts increase the viscosity of [BMIM]Br mixtures whereas it decreases the viscosity of [OMIM]Br mixtures. Weak attractive van der Waals interactions are broken in case of [BMIM]Br mixtures as this IL forms weaker aggregates in their aqueous solutions.[43] However, strong and definite aggregates[43] are broken in the case of higher $-C_8H_{17}$ chain length substituted [OMIM]Br. In addition to that more number of icebergs are broken in case of [OMIM]Br as compared to that of the [BMIM]Br due to the higher hydrophobic surface area with higher hydration number in case of former IL as compared to the later one.[42] However, as the contribution towards the viscosity of the mixtures from the increases in the number of

particles due to increased compositions of salt dominates over the contribution coming out from the sum of the decreased van der Waals interactions between the $–C_4H_9$ group of IL and less number of breaking of iceberg; results in the enhancement in the viscosity of the [BMIM]Br mixtures with the increase in the compositions of ClO_4^- ions. On the other hand, in the case of [OMIM]Br mixtures the sum of the contribution from the decreased van der Waals interactions between the hydrophobic $–C_8H_{17}$ chain length of [OMIM]Br[43] and breakdown of icebergs[42] dominates over the increased number of particles with the increase in the compositions of ClO_4^- salt resulting in the decrease in the viscosity of the [OMIM]Br mixtures.

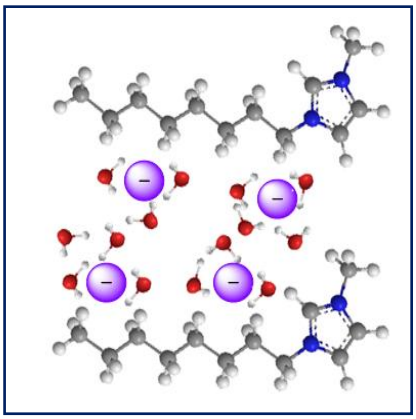

Figure 10. Proposed schematic representation of the interactions of polarizable ClO_4^- anions (light violet circle) with its rigid hydration shell (red circle represents the oxygen atom of water molecule) with the aggregates of [OMIM]Br IL (bromide anions and cationic part of salts are not shown for better representation) representing the increase repulsion between the hydrophobic $–C_8H_{17}$ chain length of IL.

However, this decrease in the viscosity values is limited up to a particular composition and yielding a minimum in the viscosity. The viscosity of the mixtures is again increase beyond that minimum. This behavior is only specific for lower compositions of ILs that is up to x_{IL} = 0.07 and is being disappear with the increase in the x_{IL} to 0.1. This study clearly demonstrates that with the increase in the compositions of higher alkyl chain length [OMIM]Br in the mixture, more number of aggregated species are formed[42] in its aqueous salt solutions and for that reason it requires higher composition of ClO_4^- salts to

break all the formed aggregates. The change in the structural entropy, ΔS_{stru} for ClO_4^- ion (+38 J K^{-1} mol^{-1}) in its aqueous solution is also in support of the above discussions.[41] This positive change in the value of ΔS_{stru} for perchlorate ion in its aqueous solution indicates that the local ordering of water molecules around the ClO_4^- ion get reduced as compared to the system without it. Therefore, the local viscosity or microviscosity, η_{micro} around the ions is being reduced. Consequently, the bulk viscosity, η_{bulk} is being reduced for the mixtures containing perchlorate ions.

It was reported that the surface viscosity of diethanolamine derivatives of n-alkylsuccinic anhydride (alkyl = dodecyl, tetradecyl, and octadecyl) in aqueous S-O, NaCl salt is more as compared to that of S-I, NH_4NO_3 salt.[45] The imidazolium-based ILs behaves as surfactant in their aqueous solutions and critical aggregation concentration (cac) of the $[OMIM]^+$ based ILs are smaller as compared to that of $[BMIM]^+$ based ILs.[46] It means [OMIM]Br has more surface preference as compared to that of [BMIM]Br. Therefore, the S-I salts like $LiClO_4$ and $NaClO_4$ reduce the surface viscosity whereas in case of S-O LiCl and Gn_2SO_4, the value of surface viscosity is increases for its aqueous solutions of IL mixtures. This effect is more pronounced in case of [OMIM]Br compare to that of [BMIM]Br because of the higher surface preference for the former IL as compare to that of the later one. The aggregated [OMIM]Br present on the surface of the ternary mixtures are being disturbed by the S-I salts[45] resulting in the decrease in their surface viscosity values and is reflected in the bulk viscosity, η_{bulk} observed in case of aqueous S-I salts of [OMIM]Br. However, in case of lower hydrophobic [BMIM]Br and [HMIM]Br the value of surface viscosity is insignificant because of its negligible surface preference.

Though both the GnCl and ClO_4^- salts are S-I in nature; the purpose of discussing the effect of GnCl on the viscosity of IL mixtures in a separate section is because of its different molecular mechanism as compared to that of the ClO_4^- salts.

6.4.1.4. Effect of GnCl

Guanidinium chloride (GnCl) is widely used over a three quarter of a century as a protein denaturant,[54] decreases the hydrophobic interactions between hydrophobic particles[55] and increases the solubility of hydrophobic and organic compounds in their aqueous

solutions.[48] It has negative value of enthalpy of hydration, ΔH_{hyd} (-602 kJ mol^{-1}) and entropy of hydration, ΔS_{hyd} (-63.7 J K^{-1} mol^{-1}),[56] positive value of viscosity B_η coefficient (0.058 dm^3 mol^{-1})[56] and increases the surface tension of water.[56] These properties support the kosmotropic or structures-making (S-O) behavior of GnCl.

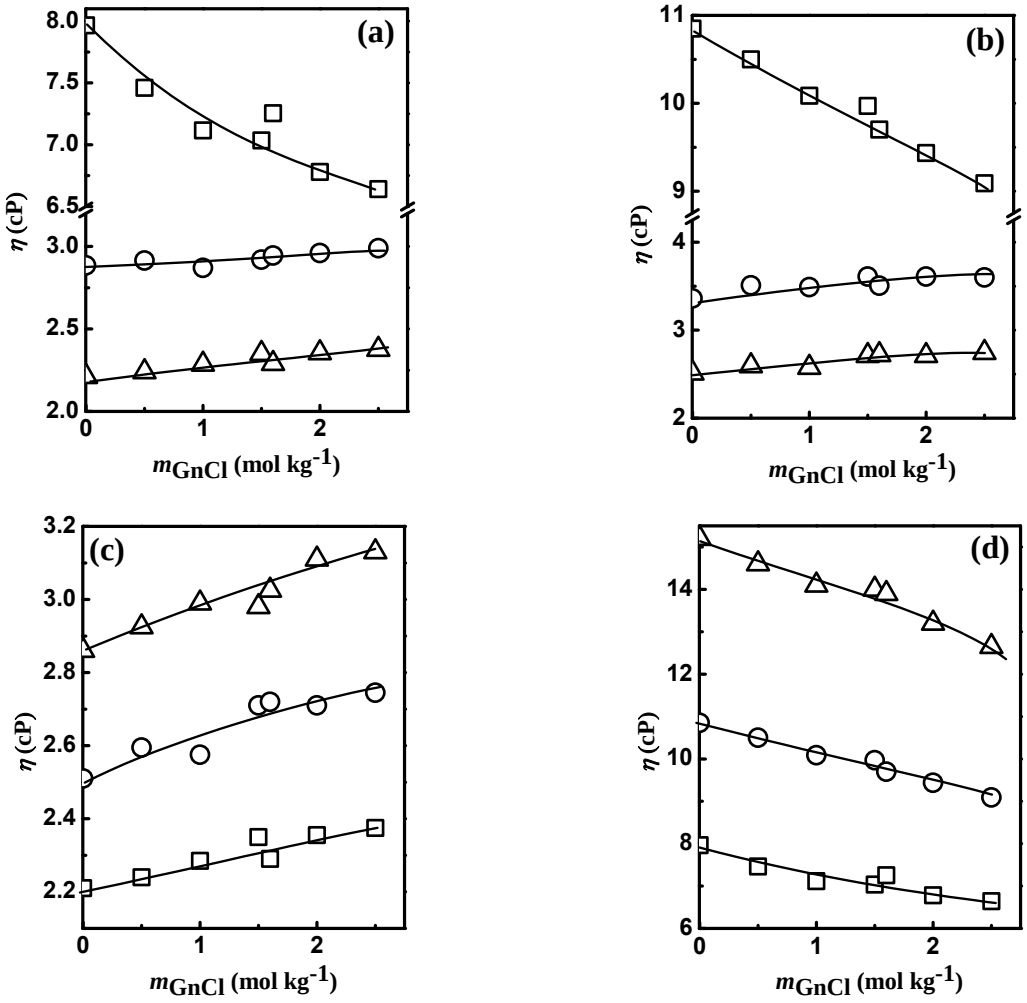

Figure 11. The η versus m_{GnCl} plots for [OMIM]Br (□), [HMIM]Br (○), [BMIM]Br (△) for 0.05x_{IL} (a) and 0.06x_{IL} (b). Also plots for [BMIM]Br (c) and [OMIM]Br (d) with 0.05x_{IL} (□), 0.06x_{IL} (○),0.07x_{IL} (△) are shown for better comparison purposes.

However, the positive value of structural entropy of hydration, ΔS_{stru} (83 J K^{-1} mol^{-1})[56] is in support of the chaotropic or structure-breaking (S-I) behavior of GnCl in its aqueous solutions. Others reports also suggest the chaotropic nature of GnCl.[55,57,58] It was reported

that the viscosity of the salt solutions of surfactants gives an indirect information about the hydrophobic interactions between hydrophobic particles,[59] means a decrease in hydrophobic interactions decreases the viscosity of solutions and vice versa. The work of these authors leads to the motivation of choosing GnCl in our current investigation to understand its effects on the viscosity of its aqueous solutions containing hydrophobic alkyl group substituted imidazolium bromide-based ILs which is depicted in Figure 11. Increase in the composition of GnCl increase the viscosity of mixtures containing lower hydrophobic alkyl group substituted ILs viz. [BMIM]Br and [HMIM]Br. However, increase in the hydrophobic alkyl group of IL to $-C_8H_{17}$ as in [OMIM]Br, a decrease in the viscosity of mixtures are observed and the results are shown in the Figure 11 (a) and (b) for the x_{IL} = 0.05 and 0.06, respectively. The trend in the viscosity is same with the varying in the compositions of ILs as are shown in the Figure 11(c) and (d) for [BMIM]Br and [OMIM]Br, respectively.

It has been reported that the number of Gn^+ ions near a hydrophobic polymer are more as compared to that of the bulk.[55] Also the dehydrated guanidinium ions[60] bind and stay parallel to the flat hydrophobic plates and place it in between the two non polar surfaces.[58] Being hydrophobic in nature, Gn^+ ions are expelled from the bulk water and displace the hydrophobic hydrated water molecules (icebergs) present around the hydrophobic polymer and thereby enhancing its density around it.[55] As we have taken different hydrophobic alkyl group substituted ILs; therefore the mechanism of interactions of GnCl with the hydrophobic alkyl chain length of ILs are similar to that of its interactions with the hydrophobic polymer.

First it will create a cavity[47] for itself in its aqueous solutions containing ILs. In the next step the Gn^+ cation starts interacting with the hydrophobic hydrated water molecules[60] as the possibility of axial interactions are blocked due to the steric hindrance and consequently break the icebergs of water molecules present around the hydrophobic alkyl group of ILs.[42] Then accumulation of Gn^+ ions takes place[55] with their cationic plane facing parallel towards the hydrophobic alkyl chain length.[60] Increasing the composition of GnCl increase the stacking of Gn^+ ions around the hydrophobic alkyl chain length[55,60] and exert a repulsive interaction between the ILs as depicted in Figure 12. As a result of which it decreases the van der Waals interactions between the alkyl chain length of

ILs[42,43] and thus decrease the aggregates of IL[43] in their aqueous solution of GnCl. The breaking of the strong aggregates of [OMIM]Br[43] decrease the surface viscosity[45] of the IL mixture. Four major effects are contributing towards the viscosity of the aqueous GnCl solutions of ILs. (I) Increase in the number of particles with the increase in the compositions of GnCl; (II) effect of GnCl on the iceberg formed around the hydrophobic alkyl chain length of ILs;[42] (III) effect of GnCl on the van der Waals interactions present between the hydrophobic alkyl chain length of ILs[43] and (IV) effect of GnCl on the surface viscosity of IL mixtures.[45]

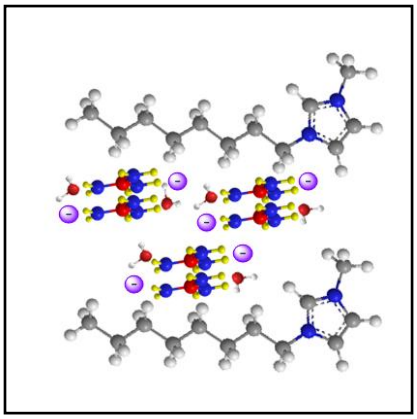

Figure 12. Proposed schematic representation of interaction of parallel stacking of Gn^+ cations of GnCl with the $–C_8H_{17}$ chain length of [OMIM]Br (Br^- ions are not shown for better representation). Red, blue and yellow represents the carbon, nitrogen and hydrogen atom of Gn^+ cation, respectively. Light violet color represents the Cl^- anion and near to that water molecules are shown with red center as the oxygen atom.

Three of them that are the (II), (III) and (IV) decrease the bulk viscosity whereas, the contribution coming out from the effect (I) enhance the bulk viscosity, η_{bulk} for aqueous GnCl solutions of [OMIM]Br. In case of higher hydrophobic $–C_8H_{17}$ group substituted [OMIM]Br, the decreasing contribution towards the η_{bulk}, coming out from the effect (II), (III) and (IV) dominates the increasing contribution towards the η_{bulk} coming out from the effect (I). Therefore the bulk viscosity, η_{bulk} of the [OMIM]Br mixture decrease with the increase in the composition of GnCl. However, in the case of lower hydrophobic alkyl group substituted ILs viz. [HMIM]Br and [BMIM]Br, the later increasing effect dominates over the former decreasing effects leads to an overall enhancement in the η_{bulk}.

6.4.1.5. Effect of Anions

The anion of a salt shows interesting effects on the viscosity of the salt solutions of ILs. Though the effect of individual salts has been already discussed in the previous section of the manuscript, however here we discuss it separately by focusing on the effects of anions on the viscosity of its aqueous solutions containing alkyl group substituted imidazolium-based ILs. Figure 13(a) represents the effects of Cl^- (LiCl) and ClO_4^- ($LiClO_4$) on the viscosity of their aqueous solutions containing alkyl group substituted imidazolium bromide based ILs. Both LiCl and $LiClO_4$ increase the viscosity of their aqueous salt solutions of lower alkyl chain length substituted ILs viz. [BMIM]Br and [HMIM]Br.

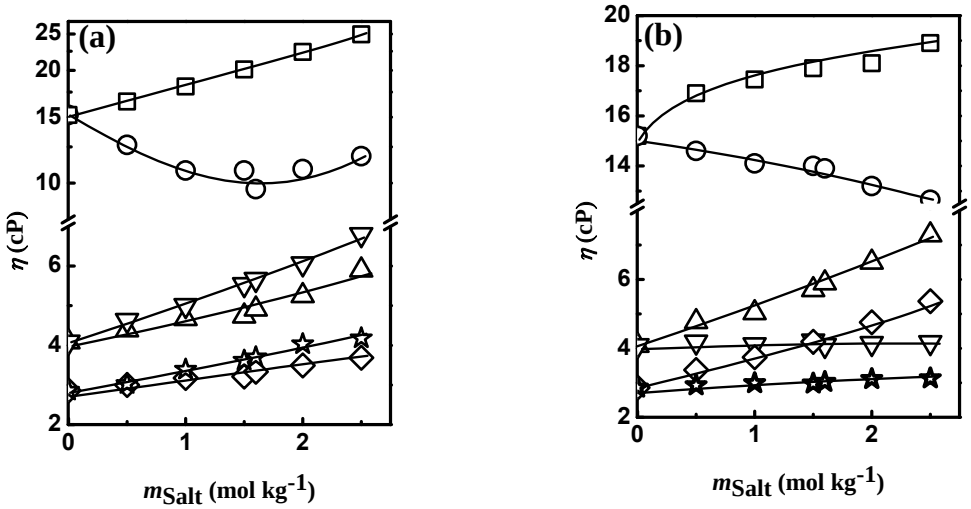

Figure 13. The η versus m_{Salt} plots for (a) [OMIM]Br with aqueous solutions of LiCl (□), $LiClO_4$ (O), [HMIM]Br with LiCl (▽), $LiClO_4$ (Δ), [BMIM]Br with LiCl (☆), $LiClO_4$ (◇), (b) [OMIM]Br with Gn_2SO_4 (□), GnCl (O), [HMIM]Br with Gn_2SO_4 (Δ), GnCl (▽), [BMIM]Br with Gn_2SO_4 (◇), GnCl (☆). In all the cases the composition of ILs are fixed as x_{IL} = 0.07.

However, the magnitude of enhancement for LiCl is more as compared to that of $LiClO_4$ and that is in accordance with the Hofmeister series. The Cl^- is present above the ClO_4^- ion in the Hofmeister series. Therefore the salting effect exerted by Cl^- is more as compared to that of ClO_4^- ion. For that reason the enhancement in η_{bulk} by Cl^- (LiCl) is

more as compared to that of ClO_4^- ($LiClO_4$). Also the effect of Cl^- and SO_4^{2-} on the viscosity of its aqueous solutions containing ILs has been studied by taking GnCl and Gn_2SO_4, respectively and the results are depicted in the Figure 13(b). Gn_2SO_4 being an anionic structure-maker (or S-O) due to its positive viscosity *B*-coefficient value for SO_4^{2-} ion (0.208 dm^3 mol^{-1}).[49] It increases the viscosity in all the studied ILs. Due to the high negative surface charge density of SO_4^{2-} ion, it attracts the dipole of water molecules strongly towards itself. Thus the water molecules required for the hydration of IL molecules are being reduced. Therefore, the cost of hydration energy of ILs are gained by the increased van der Waals interactions[43] between the hydrophobic alkyl group of ILs by minimizing their water accessible surface area[44] resulting in the formation of increased aggregated species inside the mixtures. Consequently, the viscosity of the IL mixtures increases with the increase in the compositions of Gn_2SO_4. However, GnCl is known to be a well known structure-breaker and are S-I in nature.[54,55] Both the Gn^+ and Cl^- of GnCl exert a very weak influence on the structure of water[60] and there is a possibility of a very weak interaction between the GnCl with the lower hydrophobic [BMIM]Br and [HMIM]Br due to their smaller hydrophobic surface area.[55] Therefore, we do not observe a significant change in the viscosity for [BMIM]Br and [HMIM]Br with the increase in the compositions of GnCl. However, in case of [OMIM]Br mixtures there is a possibility of strong interaction between the Gn^+ ion with the higher hydrophobic $-C_8H_{17}$ chain length.[55] As a result of which decrease aggregated species[43] are formed in the case of [OMIM]Br results into the decrease in the viscosity of the mixtures.[42,43]

Table 1. The η_{rel} ($\eta_{2.5m\ salt}/\eta_0$) values as an indication of salting behavior for different salts in aqueous salt solutions of ILs. In all the cases the composition of IL is fixed as, = 0.07 x_{IL}.

Systems x_{IL} = 0.07 + Aqueous salt solutions	η_{rel} ($\eta_{2.5m\ salt}/\eta_0$)
[BMIM]Br + LiCl	1.46
[HMIM]Br + LiCl	1.66
[OMIM]Br + LiCl	1.64
[BMIM]Br + $LiClO_4$	1.29

[HMIM]Br + $LiClO_4$	1.44
[OMIM]Br + $LiClO_4$	0.78
[BMIM]Br + GnCl	1.09
[HMIM]Br + GnCl	1.02
[OMIM]Br + GnCl	0.83
[BMIM]Br + Gn_2SO_4	1.88
[HMIM]Br + Gn_2SO_4	1.78
[OMIM]Br + Gn_2SO_4	1.24

In addition to that, the effect of these anions is also following the Hofmeister effect. The SO_4^{2-} ion is present much above in the Hofmeister series as compared to that of Cl^- ion and therefore the salting effect exerted by the former ion is more as compared to that of later Cl^- ion. For that reason SO_4^{2-} (Gn_2SO_4) show more enhancement in viscosity as compared to that of Cl^- (GnCl) ion.[8] However, the magnitude of both the S-I and S-O behavior of salts are changed with the change in the hydrophobic alkyl group substitution in ILs and can be understood by comparing the η_{rel} ($\eta_{2.5m\ salt}/\eta_0$) values; where $\eta_{2.5m\ salt}$ and η_0 represent the viscosity of 2.5 mol kg^{-1} aqueous salt solution in IL and aqueous IL without salt, respectively. The purpose of selecting 2.5 mol kg^{-1} of salt composition is for its better comparison purpose because of its maximum change in the η_{bulk} value compared to that of the pure system. It is very clear from the above Table 1 that the salting behavior of salts changes with the change in the hydrophobic alkyl group substitution in ILs as given below.

[BMIM]Br < [HMIM]Br ≈ [OMIM]Br (LiCl)

[BMIM]Br > [HMIM]Br < [OMIM]Br ($LiClO_4$)

[BMIM]Br < [HMIM]Br < [OMIM]Br (GnCl)

[BMIM]Br > [HMIM]Br > [OMIM]Br (Gn_2SO_4)

The S-I behavior of GnCl is increases with the increase in the hydrophobic alkyl group substitution in ILs. On the other hand, the S-O behavior of Gn_2SO_4 decreases with the

increase in the alkyl chain length of ILs. The S-O behavior of LiCl salt is also similar to that of Gn_2SO_4. However, the S-O behavior of LiCl is nearly same for the [HMIM]Br and [OMIM]Br. On the other hand, the S-I behavior of $LiClO_4$ in [OMIM]Br is more as compared to that of [BMIM]Br. However we are unaware about the higher S-I behavior of $LiClO_4$ in [BMIM]Br as compared to that of [HMIM]Br.

Hard and soft nature of ions can be used for the explanation of the viscosity of the aqueous salt solution of IL mixtures. According to the Pearson's HSAB concept, "hard prefers to interact with hard and soft prefers to interact with soft".[61,62]

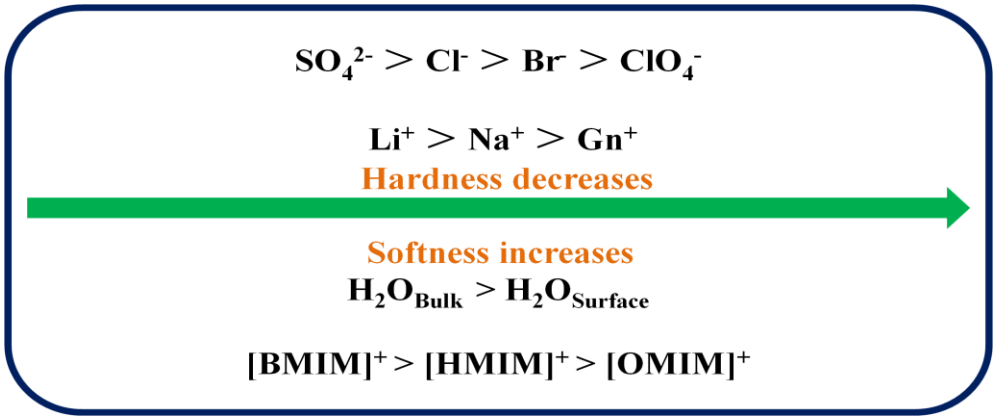

Chart 2. Increasing order of softness of salt ions, surface and bulk water molecules, and the imidazolium cation of ILs.

The salt ions used in our current study are arranged in the chart 2 in the increasing order of their softness. The water molecules present around the hydrophobic surface of alkyl chain length of IL cation (hydrophobic hydrated water molecules) are softer than that present in the bulk.[52] The IL cations are also arranged in the increasing order of their softness. $[OMIM]^+$ is more polarizable and possess diffuse electron cloud density as compared to that of $[BMIM]^+$ and hence the former is considered to be a more softer cation as compared to that of the later one. Both the Li^+ and Cl^- ions are hard in nature and preferably interact with the hard bulk water through the ion-dipole interactions. For that reason the demand of the hydration energy of the ILs increases with the increase in the composition of LiCl in the system; as more numbers of water molecules are engaged in the hydration of hard Li^+ and Cl^- ions. Consequently, aggregated species are formed

resulting into the enhancement in the viscosity of IL mixtures containing aqueous solutions of LiCl. Similarly the S-O behavior of Gn_2SO_4 can also be explained in a similar manner considering the dominating effect of hard SO_4^{2-} ion over the soft Gn^+ ion.

In the case of aqueous solutions of $LiClO_4$ and $NaClO_4$ containing ILs, both the alkali metal cations are hard and prefer to interact with the hard bulk water molecules. However, the polarizable ClO_4^- ions are soft in nature and are prefer to interact with the soft imidazolium cation of ILs.[52] In addition to this, the soft polarizable ClO_4^- ion interacts with the soft water molecules (icebergs) present around the hydrophobic alkyl chain length of ILs.[52] Consequently, it breaks the iceberg of water molecules[52] and increases the repulsion between the alkyl chain lengths resulting in the decreased aggregates of ILs. Thus, a decrease in the viscosity is observed in the case of [OMIM]Br mixtures as compared to that of lower alkyl chain length substituted ILs like [HMIM]Br and [BMIM]Br, since stronger aggregates are broken in case of former as compared to that of the later ILs.[43] As a S-I salt, the behavior of GnCl can also be explained in a similar manner like that of ClO_4^- salts.

6.4.2. CONCLUSIONS

In conclusion, the S-I and S-O behavior of salts are higher with the increase in the hydrophobicity of the IL cation. The S-O effect of Gn_2SO_4 is higher as compared to that of LiCl in lower alkyl group substituted ILs like [BMIM]Br and [HMIM]Br however, with the increase in the hydrophobic alkyl group substitution in IL cation to $–C_8H_{17}$ as in the case for [OMIM]Br, the S-O effect of LiCl is being dominated and shows more S-O behavior as compared to Gn_2SO_4. Although the chaotropic ClO_4^- salts and GnCl reduces the viscosity of higher hydrophobic [OMIM]Br mixtures however, the mechanism of reduction in viscosity is completely different in both the cases.

6.5. REFERENCES

(1) Gurney, R. W. Ionic Processes in Solution, McGraw-Hill, New York: 1953.

(2) Frank, H. S.; Wen, W.-Y. *Discuss. Faraday Soc.* **1957**, *24*, 133-140.

(3) Hofmeister, F. *Arch Exp Pathol Pharmakol* **1888**, *24*, 247-260.

(4) Lo Nostro, P.; Ninham, B. W. *Chem. Rev.* **2012**, *112*, 2286-2322.

(5) Kunz, W.; Henle, J.; Ninham, B. W. *Curr. Op.Colloid Interf. Sci.* **2004**, *9*, 19-37.

(6) Wentzel, N.; Gunton, J. D. *J. Phys. Chem. B* **2007**, *111*, 1478-1481.

(7) Collins, K. D. *Methods* **2004**, *34*, 300-311.

(8) Zhang, Y.; Furyk, S.; Bergbreiter, D. E.; Cremer, P. S. *J. Am. Chem. Soc.* **2005**, *127*, 14505-14510.

(9) Zangi, R.; Hagen, M.; Berne, B. J. *J. Am. Chem. Soc.* **2007**, *129*, 4678-4686.

(10) Tokuda, H.; Tsuzuki, S.; Susan, M. A. B. H.; Hayamizu, K.; Watanabe, M. *J. Phys. Chem. B* **2006**, *110*, 19593-19600.

(11) Smiglak, M.; Metlen, A.; Rogers, R. D. *Acc. Chem. Res.* **2007**, *40*, 1182-1192.

(12) Fujita, K.; MacFarlane, D. R.; Forsyth, M.; Yoshizawa-Fujita, M.; Murata, K.; Nakamura, N.; Ohno, H. *Biomacromolecules* **2007**, *8*, 2080-2086.

(13) Fujita, K.; Ohno, H. *Biopolymers* **2010**, *93*, 1093-1099.

(14) Gao, Y. a.; Li, N.; Zheng, L.; Zhao, X.; Zhang, S.; Han, B.; Hou, W.; Li, G. *Green Chem.* **2006**, *8*, 43-49.

(15) Moniruzzaman, M.; Kamiya, N.; Goto, M. *Langmuir* **2008**, *25*, 977-982.

(16) Takada, A.; Imaichi, K.; Kagawa, T.; Takahashi, Y. *J. Phys. Chem. B* **2008**, *112*, 9660-9662.

(17) Nicolau, B. G.; Sturlaugson, A.; Fruchey, K.; Ribeiro, M. C. C.; Fayer, M. D. *J. Phys. Chem. B* **2010**, *114*, 8350-8356.

(18) Yamaguchi, T.; Mikawa, K.-i.; Koda, S.; Serizawa, N.; Seki, S.; Fujii, K.; Umebayashi, Y. *J. Phys. Chem. B* **2012**, *116*, 7322-7327.

(19) Freire, M. G.; Neves, C. M. S. S.; Silva, A. M. S.; Santos, L. s. M.; Marrucho, I. M.; Rebelo, L. P. N.; Shah, J. K.; Maginn, E. J.; Coutinho, J. A. P. *J. Phys. Chem. B* **2010**, *114*, 2004-2014.

(20) Yamazaki, T.; Kovalenko, A.; Murashov, V. V.; Patey, G. N. *J. Phys. Chem. B* **2009**, *114*, 613-619.

(21) Funkner, S.; Havenith, M.; Schwaab, G. *J. Phys. Chem. B* **2012**, *116*, 13374-13380.

(22) von Hippel, P. H.; Wong, K.-Y. *Science* **1964**, *145*, 577-580.

(23) McKenzie, H. A.; Ralston, G. B. *Experientia* **1971**, *27*, 617-624.

(24) Weerasinghe, S.; Smith, P. E. *J. Chem. Phys.* **2003**, *118*, 5901-5910.

(25) Bennion, B. J.; Daggett, V. *Proc. Natl. Acad. Sci.* **2003**, *100*, 5142-5147.

(26) Rosgen, J.; Pettitt, B. M.; Bolen, D. W. *Biochemistry* **2004**, *43*, 14472-14484.

(27) Bonhote, P.; Dias, A.-P.; Papageorgiou, N.; Kalyanasundaram, K.; Gratzel, M. *Inorg. Chem.* **1996**, *35*, 1168-1178.

(28) Suarez, P. A. Z.; Einloft, S.; Dullius, J. E. L.; De Souza, R. F.; Dupont, J. *J. Chim. Phys.* **1998**, *95*, 1626-1639.

(29) Huddleston, J. G.; Visser, A. E.; Reichert, W. M.; Willauer, H. D.; Broker, G. A.; Rogers, R. D. *Green Chem.* **2001**, *3*, 156-164.

(30) Noda, A.; Hayamizu, K.; Watanabe, M. *J. Phys. Chem. B* **2001**, *105*, 4603-4610.

(31) Stark, A.; Behrend, P.; Braun, O.; Muller, A.; Ranke, J.; Ondruschka, B.; Jastorff, B. *Green Chem.* **2008**, *10*, 1152-1161.

(32) Seddon, K. R.; Stark, A.; Torres, M. J. *Pure Appl. Chem*. **2000**, *72*, 2275-2287.

(33) Isono, T. *J. Chem. Eng. Data* **1984**, *29*, 45-52.

(34) Zhang, Q.-G.; Xue, F.; Tong, J.; Guan, W.; Wang, B. *J. Solution Chem.* **2006**, *35*, 297-309.

(35) Jungnickel, C.; Luczak, J.; Ranke, J.; Fernandez, J. F.; Muller, A.; Thoming, J. *Colloids Surf., A Physicochem. Eng. Aspects* **2008**, *316*, 278-284.

(36) Mukerjee, P.; Ray, A. *J. Phys. Chem.* **1963**, *67*, 190-192.

(37) Carvalho, B. L.; Briganti, G.; Chen, S. H. *J. Phys. Chem.* **1989**, *93*, 4282-4286.

(38) Dias, L. G.; Florenzano, F. H.; Reed, W. F.; Baptista, M. S.; Souza, S. M. B.; Alvarez, E. B.; Chaimovich, H.; Cuccovia, I. M.; Amaral, C. L. C.; Brasil, C. R. *Langmuir* **2002**, *18*, 319-324.

(39) Schick, M. J. *J. Phys. Chem.* **1964**, *68*, 3585-3592.

(40) Rezus, Y. L. A.; Bakker, H. J. *Proc. Natl. Acad. Sci.* **2006**, *103*, 18417-18420.

(41) Marcus, Y. *Ion solvation*; Wiley-Interscience, UK, 1985.

(42) Singh, T.; Kumar, A. *J. Chem. Thermodynamics* **2011**, *43*, 958-965.

(43) Bhargava, B. L.; Klein, M. L. *Soft Matter* **2009**, *5*, 3475-3480.

(44) Chandler, D. *Nature* **2005**, *437*, 640-647.

(45) Chattopadhyay, A. K.; Ghaicha, L.; Oh, S. G.; Shah, D. O. *J. Phys. Chem.* **1992**, *96*, 6509-6513.

(46) Bowers, J.; Butts, C. P.; Martin, P. J.; Vergara-Gutierrez, M. C.; Heenan, R. K. *Langmuir* **2004**, *20*, 2191-2198.

(47) Breslow, R.; Guo, T. *Proc. Natl. Acad. Sci.* **1990**, *87*, 167-169.

(48) Breslow, R.; Rizzo, C. J. *J. Am. Chem. Soc.* **1991**, *113*, 4340-4341.

(49) Jenkins, H. D. B.; Marcus, Y. *Chem. Rev.* **1995**, *95*, 2695-2724.

(50) Nanda, R.; Kumar, A. *Ind. J. Chem.* **2013**, *52*, 1377-1382.

(51) Tsuzuki, S.; Tokuda, H.; Mikami, M. *Phys. Chem. Chem. Phys.* **2007**, *9*, 4780-4784.

(52) dos Santos, A. P.; Levin, Y. *Phys. Rev. Lett.* **2011**, *106*, 167801-167804.

(53) Lopez□Leon, T.; Ortega□Vinuesa, J. L.; Bastos□Gonzalez, D. *ChemPhysChem* **2012**, *13*, 2382-2391.

(54) Svedberg, T. *Nature* **1937**, *139*, 1051-1062.

(55) Godawat, R.; Jamadagni, S. N.; Garde, S. *J. Phys. Chem. B* **2010**, *114*, 2246-2254.

(56) Marcus, Y. *J. Chem. Thermodynamics* **2012**, *48*, 70-74.

(57) Hunger, J.; Niedermayer, S.; Buchner, R.; Hefter, G. *J. Phys. Chem. B* **2010**, *114*, 13617-13627.

(58) England, J. L.; Pande, V. S.; Haran, G. *J. Am. Chem. Soc.* **2008**, *130*, 11854-11855.

(59) Chen, L.; Xing, H.; Yan, P.; Ma, J.-M.; Xiao, J.-X. *Soft Matter* **2011**, *7*, 5365-5372.

(60) Mason, P. E.; Neilson, G. W.; Enderby, J. E.; Saboungi, M.-L.; Dempsey, C. E.; MacKerell, A. D.; Brady, J. W. *J. Am. Chem. Soc.* **2004**, *126*, 11462-11470.

(61) Pearson, R. G. *J. Am. Chem. Soc.* **1963**, *85*, 3533-3539.

(62) Parr, R. G.; Pearson, R. G. *J. Am. Chem. Soc.* **1983**, *105*, 7512-7516.

CHAPTER 7

Conclusions

In short we can deduce the following conclusions from our work.

1) From the study of the diffusional behavior of ^{1}H NMR active nuclei the following conclusions can be drawn:

(a) From the self-diffusion coefficient studies it has been shown that the diffusional motion of smaller particle diffuses faster as compared to the larger molecules. On the other hand, the translational and rotational behavior of $[IL]^{+}$ shows different behavior. Addition of salts into the IL system induces the perturbation in the nanostructural organization of ILs. In addition to this the acidity of the C2 proton has been also studied from the change in its chemical shift values and shows that LiCl increase the acidity of C2 proton more as compared to the $LiClO_4$.

(b) From the second section of the studies we conclude that the Stokes-Einstein equation strongly violates in the case of diffusional motion of water molecules. The frictional coefficient obtained from it can be used as an alternative parameter for the measurement of microviscosity experienced by each ^{1}H NMR active nuclei.

The study of these transport phenomenon and microviscosity in aqueous Li^{+} containing salt mixtures of ILs provide a better understanding of these mixtures for their potential applications.

2) From the second part of our study regarding the water in hydrophobic IL confined media we conclude that the IL can be a better replacement for the volatile organic solvents for the preparation and applications of microemulsions. Water in $[BBIM][NTf_2]$ microemulsions has been successfully studied with non-ionic TX-100 as the surfactant. NMR relaxation studies have been carried out to understand the microviscosity and pH of the aqueous IL confined media and it was found that increase in the composition of water decrease the microviscosity of the miceller core. The mole fraction of bound water and free water molecules shows inverse relationship with each other as a function of water composition. The micropolarity of the studied confined media is found to increase with the increase in the composition of water. Study of these physicochemical phenomenons in the water in IL confined media helps the scientific community in order to apply them as a medium for enzymatic reactions and material synthesis.

3) In the final section of our study regarding the effect of denaturants on the viscosity of aqueous IL mixtures with the hydrophobic alkyl group substitutions in cationic part of ILs the conclusions obtained are as follows:

The salting behavior of urea is being reversed with the increase in the hydrophobic alkyl group substitution in the imidazolium-based ILs. In addition to this, other salting-in agents substantially reduce the viscosity of the higher alkyl group substituted ILs as compared to the lower alkyl group substituted imidazolium-based ILs. Understanding of these salting phenomenons in the IL systems can contribute a significant amount of knowledge in order to understand the mixtures of ILs.

8. APPENDICES

8.1. Appendix A: NMR Spectra of Ionic Liquids

[BMIM][BF_4]

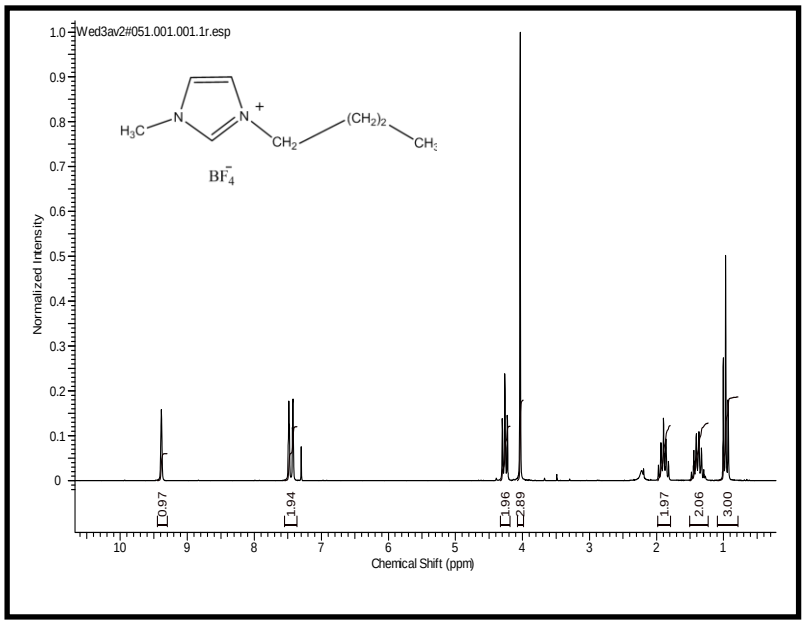

[HMIM][BF_4]

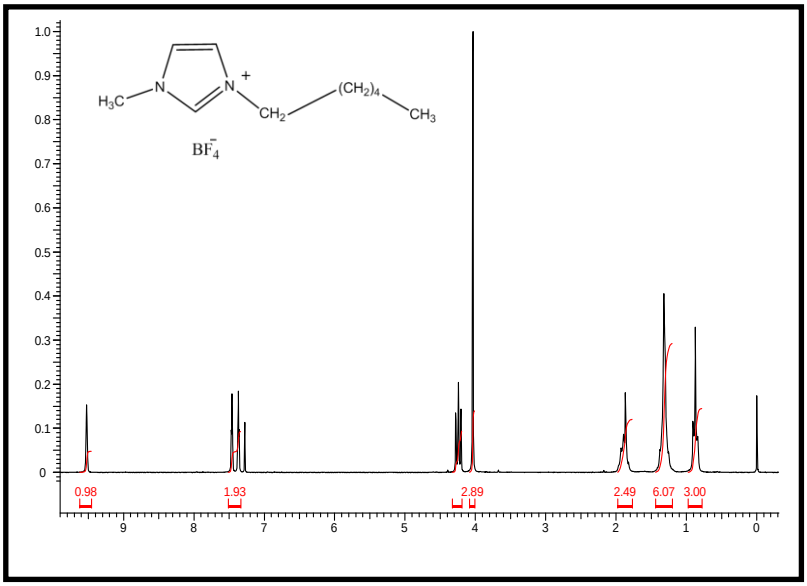

[OMIM][BF_4]

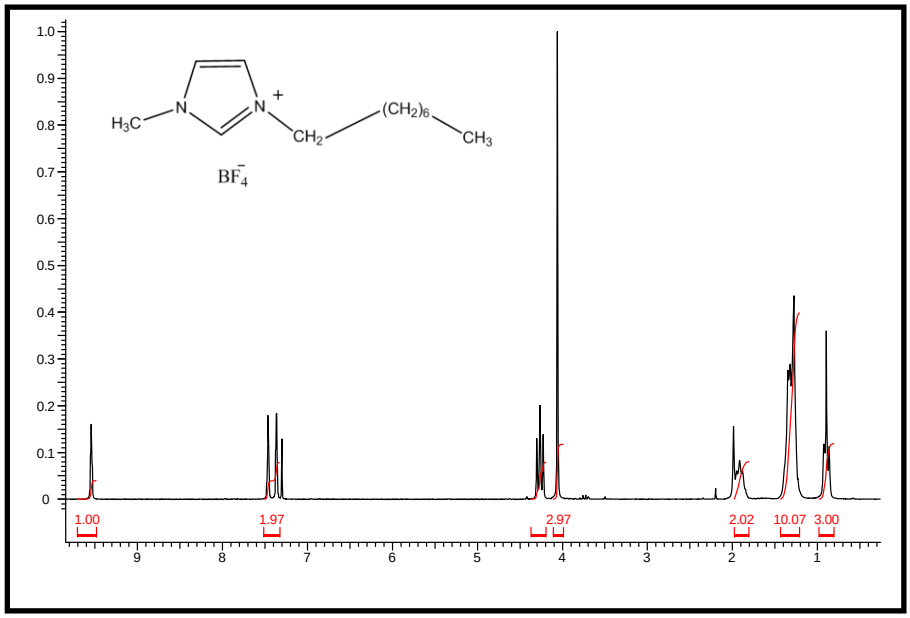

[BMIM]Br

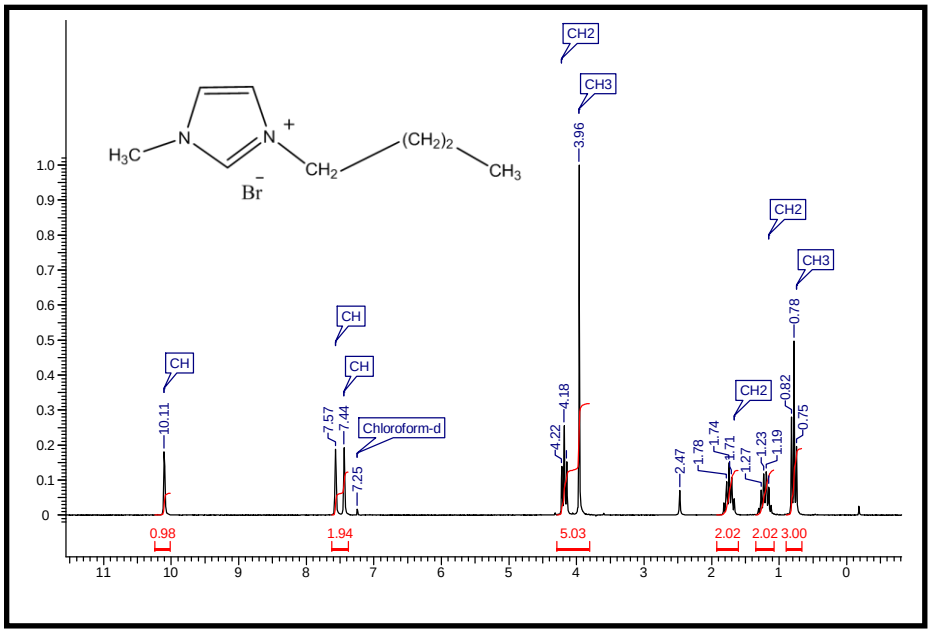

[HMIM]Br

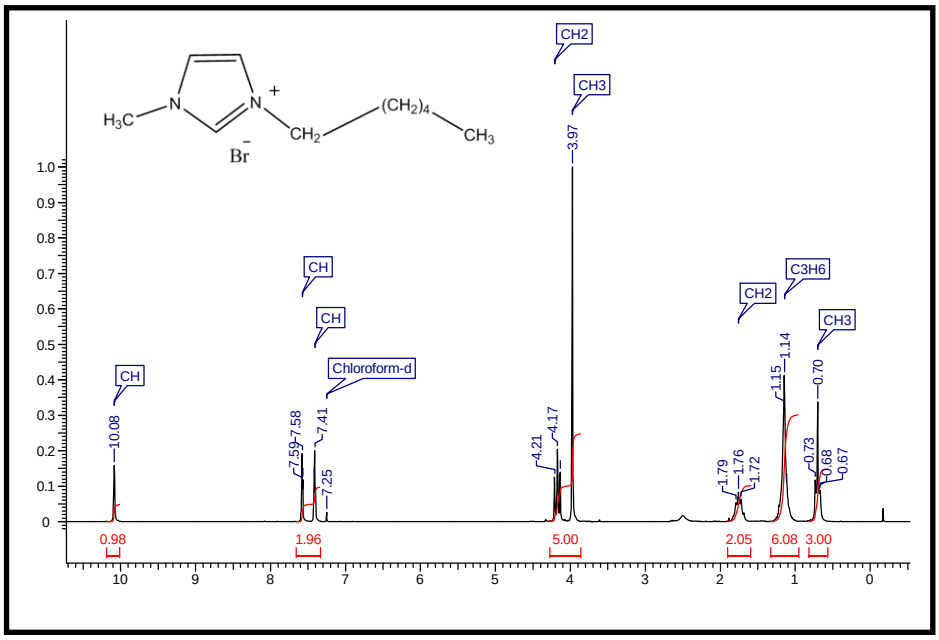

[OMIM]Br

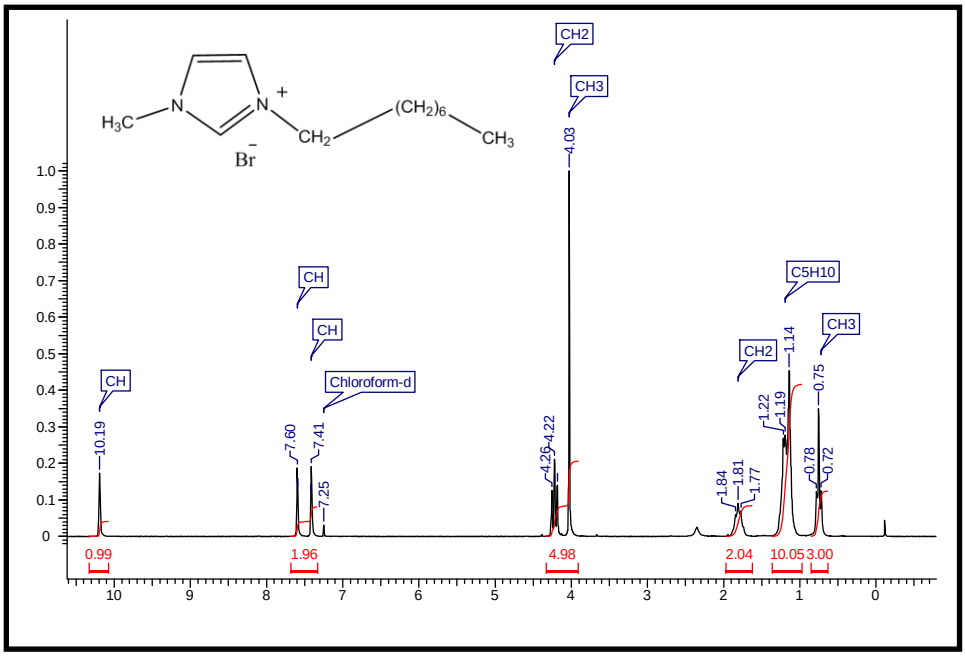

[BBIM][NTf_2]

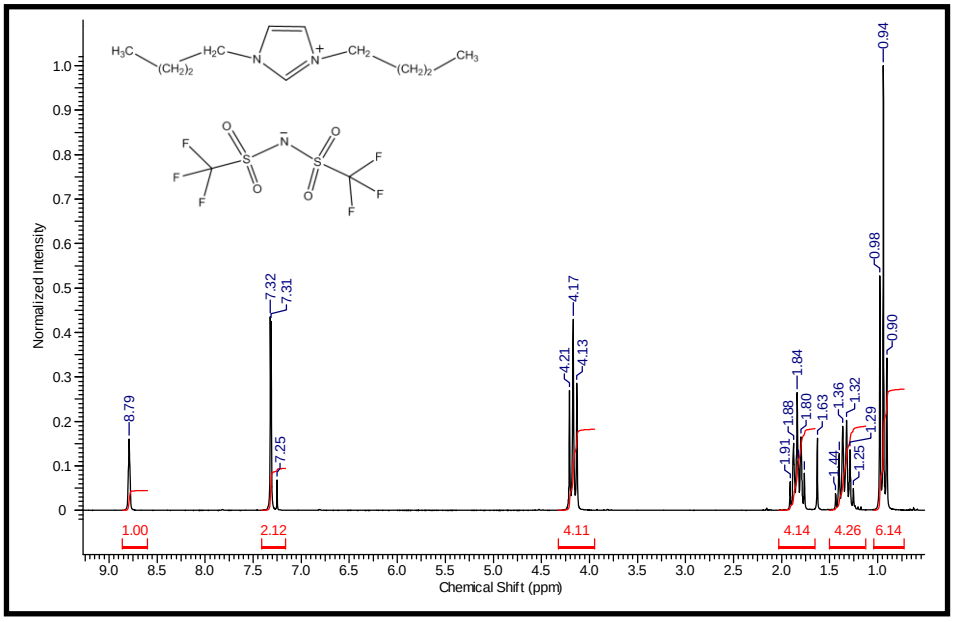
Normalized Intensity
Chemical Shift (ppm)
8.79
7.32
7.31
7.25
4.21
4.17
4.13
1.91
1.88
1.84
1.80
1.63
1.44
1.36
1.32
1.29
1.25
0.98
0.94
0.90
1.00
2.12
4.11
4.14
4.26
6.14

8.2. Appendix B: List of Publications

1. "Unusual Salting Effects in Ionic Liquid Solutions" Raju Nanda and Anil Kumar *Ind. J. Chem.* **2013,** *52A,* 1377-1382

2. "Phase Behavior, Diffusion, Structural Characteristics, and pH of Aqueous Hydrophobic Ionic Liquid Confined Media: Insights into Microviscosity and Microporsity in the [BBIM][NTf_2] + Water System" Raju Nanda and Anil Kumar *J. Phys. Chem B* **2015,** *119,* 1641-1653

3. "Interesting Viscosity Changes in the Aqueous Urea-Ionic Liquid System: Effect of Alkyl Chain Length Attached to the Cationic Ring of an Ionic Liquid" Raju Nanda, Gitanjali Rai and Anil Kumar *J. Solution Chem.* (*Accepted*)

4. "Salt Induced Weakening of Nanostructural Organization of Ionic Liquids in Water" Raju Nanda, P. R. Rajamohanan and Anil Kumar (*Manuscript under preparation*)

5. "^{1}H NMR, Self-diffusion Coefficients, Translational and Rotational Motions of Ionic Liquids and Water Molecules in Aqueous Li^{+} Containing Mixtures of Ionic Liquids" Raju Nanda, P. R. Rajamohanan and Anil Kumar (*Manuscript under preparation*)

8.3. Appendix C: Posters and Oral Presentations

1. “Characterization of some Ionic Liquids by various techniques” Poster presented on International Workshop on Ionic Liquids - Seeds for New Engineering Applications EUROTHERM Seminar 97, 2-3 February, 2012. Lisbon, Portugal.

2. "Anomalous Salt Effect on Viscosity in Ionic Liquid Solutions" Poster presented on National Science Day 2014 at CSIR - National Chemical Laboratory on 26th - 28thFebruary, 2012.

3. “Structuring and Destructuring of Water Molecules around Ionic Species: Probing Salt Effects” Poster presented on National Science Day 2013 at CSIR - National Chemical Laboratory on 26th - 28thFebruary, 2013.

4. “Water in Hydrophobic Ionic Liquid Microemulsions: Insights into Microviscosity and Microporsity of Confined Media” Poster presented on 17th CRSI National Symposium in Chemistry held on February 06-08, 2015 in NCL, Pune.

5. “Water in Hydrophobic Ionic Liquid Microemulsions: Insights into Microviscosity and Microporsity of Confined Media” Poster presented on National Science Day 2013 at CSIR - National Chemical Laboratory on 26th - 28thFebruary, 2015.